Pathology-associated expression and function of the metalloproteases meprin α and meprin β

Dissertation

zur Erlangung des Doktorgrades

der

Mathematisch-Naturwissenschaftlichen Fakultät

der

Christian-Albrechts-Universität zu Kiel

Vorgelegt von

Florian Peters

Kiel, 2019

Erster Gutachter: Prof. Dr. Christoph Becker-Pauly

Zweiter Gutachter: Prof. Dr. Thomas Roeder

Tag der mündlichen Prüfung: 10.04.2019

Zum Druck genehmigt: 10.04.2019

Preface

This dissertation was prepared partly cumulative. The data obtained in the presented work were described in detail in four publications.

1. **Ectodomain shedding of CD99 within highly conserved regions is mediated by the metalloprotease meprin β and promotes transendothelial cell migration.**
   Bedau T*, **Peters F***, Prox J*, Arnold P, Schmidt F, Finkernagel M, Köllmann S, Wichert R, Otte A, Ohler A, Stirnberg M, Lucius R, Koudelka T, Tholey A, Biasin V, Pietrzik CU, Kwapiszewska G, Becker-Pauly C.
   FASEB J. 2017 Mar;31(3):1226-1237
   *These authors contributed equally to the work.

2. **Cancer-associated mutations in the canonical cleavage site do not influence CD99 shedding by the metalloprotease meprin β but alter cell migration in vitro.**
   Bedau T, Schumacher N, **Peters F**, Prox J, Arnold P, Koudelka T, Helm O, Schmidt F, Rabe B, Jenzsch M, Rosenstiel P, Sebens S, Tholey A, Rose-John S, Becker-Pauly C.
   Oncotarget. 2017 Jul 4;8(33):54873-54888

3. **Docking of Meprin α to Heparan Sulphate Protects the Endothelium from Inflammatory Cell Extravasation.**
   Biasin V, Wygrecka M, Bärnthaler T, Jandl K, Jain PP, Bálint Z, Kovacs G, Leitinger G, Kolb-Lenz D, Kornmueller K, **Peters F**, Sinn K, Klepetko W, Heinemann A, Olschewski A, Becker-Pauly C, Kwapiszewska G.
   Thromb Haemost. 2018 Oct;118(10):1790-1802

4. **Tethering soluble meprin α in an enzyme complex to the cell surface affects IBD associated genes.**
   Peters F, Scharfenberg F, Colmorgen C, Armbrust F, Wichert R, Arnold P, Potempa B, Potempa J, Pietrzik CU, Häsler R, Rosenstiel P, Becker-Pauly C.
   FASEB J.; *in press*

In the following, most relevant results from the publications 1-4 are briefly described, while unpublished data are illustrated in detail.

Table of Contents

List of Figures

List of Tables

Abstract

By proteolysis, the enzymatic cleavage of peptide bonds, proteins undergo an irreversible posttranslational modification which is used for protein maturation, activation, signaling and cellular adhesion. The work of this thesis approaches the role of the extracellular metalloproteases meprin α and meprin β in physiological and pathological conditions, especially in skin and inflammation related diseases.

The first part of this thesis addresses the meprin expression in murine skin and their resulting role in wound healing and deposition of extracellular matrix in this organ. In contrast to human skin, meprin expression in mice was low and the lack of meprin in knock-out mice was not compensated by other astacin protease family members. Nevertheless, re-epithelialization of the epidermis in *in vivo* wound healing studies was decreased when both meprin α and meprin β were absent. Furthermore, based on previous findings that meprins are over-expressed in fibrotic and hyperkeratotic skin diseases, we employed and analyzed mouse models over-expressing meprin β in skin in order to study its contribution to the onset of disease. In a genetic mouse model, which is transgenic for the transcription factor Fra2, mice develop skin fibrosis over time and indeed over-express meprin β in skin. Interestingly, the transcribed meprin β mRNA corresponded to the meprin β' isoform, which is associated with expression in cancer cells and might be differentially translated or stabilized in comparison to the normal meprin β mRNA. Since Fra2 as part of the transcription factor complex AP-1 activates several other genes besides the meprin β gene, mouse models directly over-expressing meprin β in skin were generated. Epidermal over-expression of meprin β led to a pigmentary phenotype and hyperproliferation of keratinocytes that might derive from local inflammation and cell stress through loss of cellular adhesion. On the other hand, a dermal over-expression of meprin β did not show an obvious phenotype or development of fibrosis.

The second part is focused on proteolytic processing of the adhesion molecule CD99, which is a novel meprin β substrate. Indeed, cleavage of CD99 by meprin β was observed in *in vitro* studies and had significant effect on transendothelial migration of cancer cells. Furthermore, inhibition of meprin β increased CD99 levels in mouse lung and infiltration and migration of immune cells was delayed in an acute inflammation model upon meprin β knock-out, thereby strengthening a role for CD99 cleavage by meprin β *in vivo*.

Finally, altered localization of meprin α was investigated during pathological conditions. Increased levels of secreted meprin α were observed in plasma of patients suffering from idiopathic pulmonary arterial hypertension. Under normal conditions, soluble meprin α was observed to bind to epithelial cells via heparan sulphate, which had impact on infiltration of immune cells and epithelial barrier integrity. Moreover, covalent binding of meprin α to meprin β on the secretory pathway could also tether soluble meprin α to the plasma membrane. The meprin enzyme complex exhibited enhanced

stability and increased activity of the meprin monomers. The altered localization of meprin α also influenced gene regulation of epithelial cells and contributed to inflammatory disease progression.

Zusammenfassung

Durch Proteolyse, der enzymatischen Spaltung von Peptidbindungen, werden Proteine irreversibel posttranslational modifiziert, was für die Reifung, Aktivierung, Signalwirkung und zelluläre Adhäsion von Proteinen notwendig ist. Diese Arbeit befasste sich mit den extrazellulären Metalloproteasen Meprin α und Meprin β und ihre Rolle in physiologischen und pathologischen Bedingungen mit besonderem Fokus auf haut- und entzündungsbasierten Erkrankungen.

Der erste Teil dieser Arbeit thematisierte die Expression von Meprinen in muriner Haut, sowie ihre potentielle Beteiligung im Wundheilungsprozess und am Aufbau von extrazellulärer Matrix. Im Gegensatz zu humaner Haut war die Meprin Expression in Mäusen gering und eine Gendeletion in knock-out Mäusen wurde nicht kompensiert durch andere Mitglieder der Astacin-Proteasefamilie. Jedoch war die epidermale Reepithelialisierung in *in vivo* Wundheilungsstudien verringert, wenn Meprin α und Meprin β gleichermaßen fehlten. Vorherige Arbeiten konnten zeigen, dass Meprine überexprimiert in fibrotischen und hyperkeratotischen Hauterkrankungen vorliegen können. Daher haben wir Mausmodelle verwendet und analysiert, die Meprin β in der Haut überexprimieren, um ihre Beteiligung zur Entstehung der Krankheiten zu überprüfen. In einem genetischen Mausmodell, welches transgen für den Transkriptionsfaktor Fra2 ist, entwickeln Mäuse mit der Zeit eine Hautfibrose und zeigen eine Überexpression von Meprin β. Interessanterweise entspricht die transkribierte Meprin β mRNA der Isoform Meprin β‘, welche assoziiert ist mit Expression in Krebszellen und möglicherweise anders translatiert oder stabilisiert wird als die normale Meprin β mRNA. Da Fra2 als Teil des Transkriptionsfaktorkomplexes AP-1 weitere Gene neben dem Gen für Meprin β aktiviert, wurden Mausmodelle generiert, die auf direkter Weise Meprin β überexprimieren. Durch Überexpression von Meprin β in der Epidermis entwickelten Mäuse einen Pigmentierungsphänotyp und eine Hyperproliferation von Keratinozyten, welche möglicherweise durch lokale Entzündung und Zellstress durch Verlust von Zelladhäsion entstanden. Im Gegensatz dazu zeigte eine dermale Überexpression von Meprin β keinen offensichtlichen Phänotyp oder Entstehung von Fibrose.

Der zweite Teil beschäftigte sich mit der proteolytischen Spaltung des Adhäsionsmoleküls CD99, welches als neues Meprin β Substrat in *in vitro* Studien identifiziert wurde. Die Proteolyse von CD99 durch Meprin β hatte signifikanten Einfluss auf transendotheliale Migration von Krebszellen. Des Weiteren wurden erhöhte CD99 Level in Lungen nach Inhibition von Meprin β gezeigt, sowie eine geringere Infiltration und Migration von Immunzellen in einem akuten Entzündungsmodell mit Meprin β knock-out Mäusen. Diese Beobachtungen bekräftigen die Spaltung von CD99 durch Meprin β im lebenden Organismus.

Im dritten Teil wurde eine veränderte Lokalisation von Meprin α in pathologischen Bedingungen untersucht. Erhöhte Level von löslichem Meprin α wurden im Plasma von Patienten gefunden, die an

pulmonaler arterieller Hypertonie erkrankt waren. In normalen Bedingungen wurde beobachtet, dass sich Meprin α über Heparansulfat an Epithelzellen anlagert, was Einfluss auf Infiltration von Immunzellen und Barrierefunktion des Epithels zeigte. Des Weiteren kann Meprin α auch durch kovalente Bindung an Meprin β auf dem sekretorischen Weg an der Zelloberfläche lokalisiert sein. Dieser Meprin Enzymkomplex führte zu erhöhter Stabilität und Aktivität der einzelnen Meprin Monomere. Die veränderte Lokalisation von Meprin α hatte außerdem einen Einfluss auf Genregulation in Epithelzellen und trug zum Verlauf von Entzündungsprozessen bei.

1. Introduction

Proteases are essential regulators of various biological processes in physiological and pathophysiological conditions. Unlike other posttranslational modifications like phosphorylation and lipidation, cleavage of peptide bonds is irreversible, leading to liberation of signal molecules, activation of proteins and their degradation. Dysregulated expression and activity of a single protease can therefore lead to disturbances within the tightly regulated protease web. These disturbances include decreased or increased substrate shedding, resulting in altered signal transduction and changes in cellular morphology or tissue homeostasis. Therefore, knowledge about each protease is crucial to understand their specific role in physiological processes and progression of pathologies.

1.1 Meprin metalloproteases

Meprin metalloproteases were first discovered in 1981 as a novel metallo-endopeptidase in the brush border membrane of murine kidney (Beynon et al., 1981). Later on, an unexpected proteolytic activity in the intestine of patients after pancreas surgery revealed meprin expression in the gut (Sterchi et al., 1982). In the following years, meprin α and meprin β were identified as two individual enzymes located on different chromosomes (Gorbea et al., 1993; Jiang et al., 1993). Due to their conserved zinc-binding motif (HExxHxxGxxHxxxRxDR) and a Met-turn in close proximity to the active site cleft, which includes a tyrosine to further coordinate the zinc ion (Gomis-Rüth et al., 2012), meprins were assigned to the family of astacin proteases (Dumermuth et al., 1991). Other family members are bone morphogenetic protein 1 (BMP-1), mammalian tolloid (mTLD), tolloid 1 (Tll1), tolloid 2 (Tll2) and ovastacin, which share a similar catalytic domain but differ in their overall domain composition.

Both meprin proteases are type I transmembrane proteins, sharing an equal domain structure consisting of a N-terminal pro-peptide, an astacin-like protease domain, a MAM domain (meprin, A5-protein and receptor protein-tyrosine phosphatase μ) for dimerization of two monomers, a TRAF domain (tumor necrosis factor-receptor associated factor) as well as an EGF (epidermal growth factor)-like domain, followed by a transmembrane domain and a C-terminal cytosolic tail (Figure 1). Unlike meprin β, meprin α possess an inserted domain with a furin cleavage site. During maturation, meprin α is shed by furin in the Golgi apparatus, which makes it a secreted protease that can form large oligomers up to 6 MDa in size (Bertenshaw et al., 2003; Marchand et al., 1995). Meprin β, on the other hand, is transported to the cell surface and can be shed in its inactive form by ADAM proteases (Herzog et al., 2014; Wichert et al., 2017). Interestingly, when expressed together, both proteases form a disulfide-linked heterodimer, that tethers furin cleaved meprin α to plasma membranes and regulates its secretion through shedding of meprin β (Johnson and Hersh, 1992; Marchand et al., 1995). Both meprin proteases share a similar cleavage specificity, preferring negatively charged amino acids at the P1’ position (Becker-Pauly et al., 2011). The so far identified substrate spectrum includes adhesion molecules, growth factors and proteins of the extracellular matrix (Jefferson et al., 2013). Although

meprins share 38% amino acid homology in the human isoforms, meprins differ in expression and localization, which makes some proteins unique substrates for each meprin.

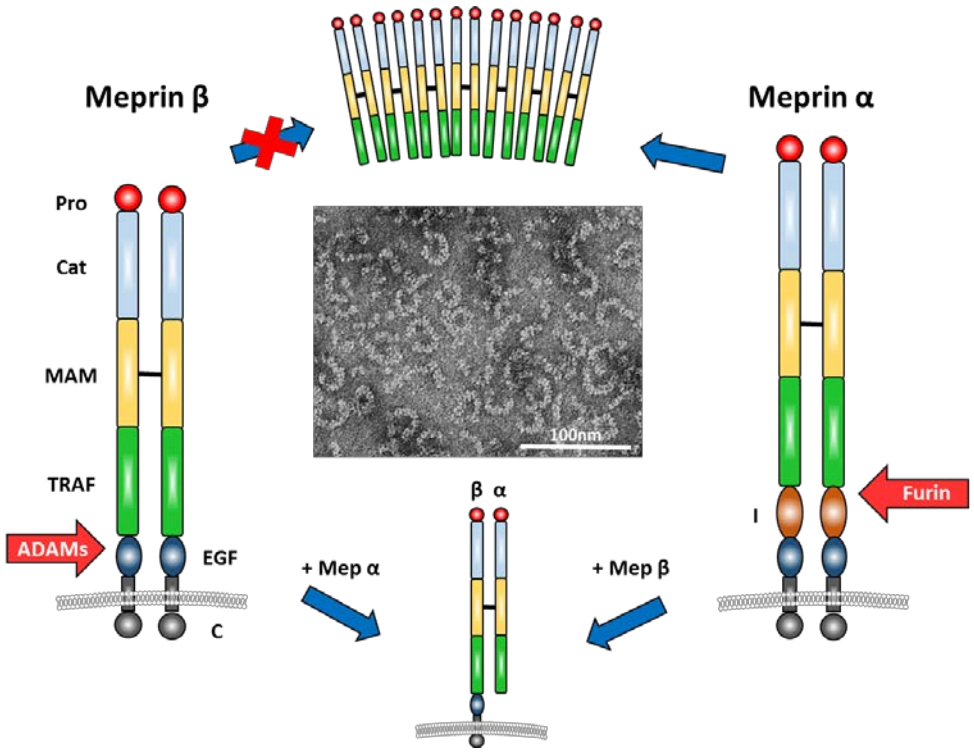

Figure 1: Domain structure and oligomerization of meprin α and meprin β.

Meprin metalloproteases are disulfide-linked type I transmembrane enzymes consisting of several domains. Upon furin cleavage within its inserted domain (I), meprin α is secreted to the extracellular space subsequently forming large oligomeric structures. Meprin β can be shed by ADAMs from the plasma membrane but cannot form oligomers larger than dimers. Being expressed together, meprin α and meprin β form heterooligomers that tether meprin α to the plasma membrane. (Adapted from (Arnold et al., 2017)).

Total gene knock-outs in mice can demonstrate the physiological role of the translated protein *in vivo*. For proteases, accumulation of non-cleaved substrates reveals necessary activities of an enzyme in a complex organism which cannot be compensated by other proteases. However, compensatory effects occur in many cases and are essential for an organism to survive and to not be dependent on one single enzyme. Meprin α and meprin β single- as well as double knock-out mice are viable and show no alterations in development (Banerjee et al., 2009; Norman et al., 2003). Nevertheless, collagen maturation and deposition in the dermis is reduced and resembles an Ehlers-Danlos syndrome-like phenotype by decreased tensile strength (Broder et al., 2013). Although meprins are able to maturate collagens, other proteases like BMP-1 or ADAMTS could promote reasonable development of skin (Kessler et al., 1996; Li et al., 2001, 1996). Furthermore, mucus detachment in the small intestine of meprin β knock-out mice is impaired which could lead to mucus accumulation and bacterial overgrowth (Schütte et al., 2014; Wichert et al., 2017). Interestingly, missing meprin activity was either shown to be beneficial or disadvantageous for an organism in different induced pathological

situations. Therefore, research on meprin proteases could be of high interest in the setting of disease initiation and progression.

1.2 Skin, wound healing, fibrosis and psoriasis

The skin is the largest organ of the body, exhibiting necessary functions like homeostasis, protection against environmental assaults, water loss and mechanical traumata. Therefore, the skin undergoes constant remodeling which requires a tightly regulated network between cells, extracellular matrix (ECM) and signaling molecules. The dermis is the lower part of the two main skin layers, which consists mainly of collagen fibers and fibroblasts and harbors the hair follicles. The epidermis represents the upper part, which is build up by keratinocytes that finally undergo a special form of cell death to build the cornified envelope. Interestingly, human epidermis is made up of several layers of differentially differentiated keratinocytes while murine epidermis is thin and composed of only 2-3 cell layers (Figure 2). Additionally, hair roots occupy the majority of the murine dermis and enlarge surface area of basal keratinocytes. Despite these anatomical differences, mouse models are widely used for research on skin physiology and pathologies in order to understand these mechanisms and the complex interplay of different cells and genes in an organism.

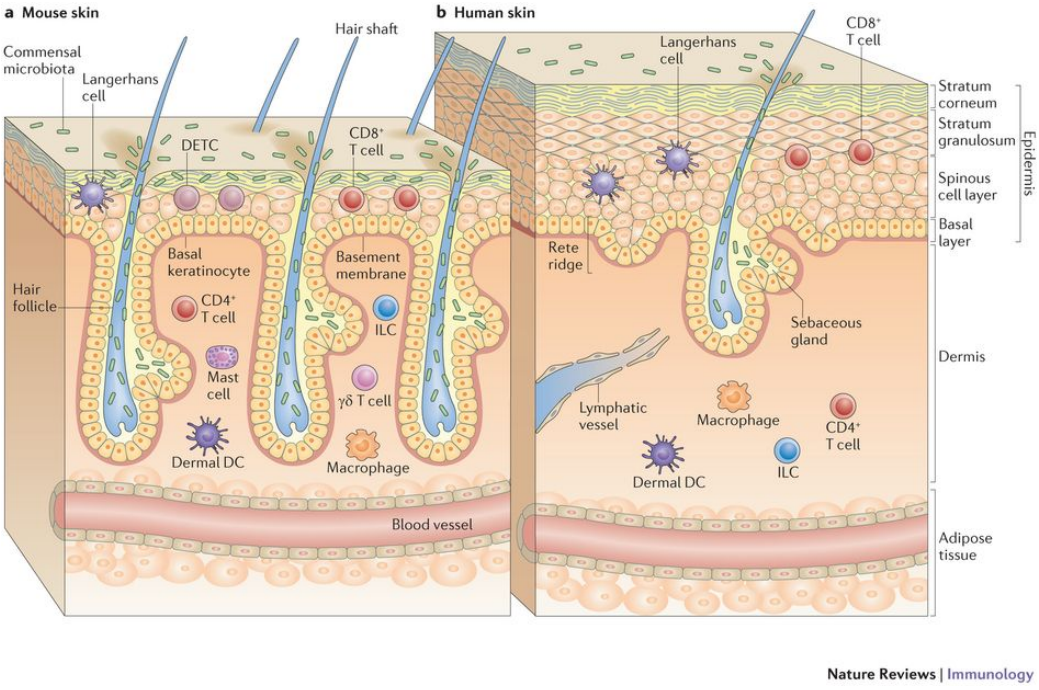

Figure 2: Structure of and cellular composition of human and murine skin.

Skin can be separated into an upper part (epidermis) and lower part (dermis) that are composed of different cells and extracellular matrix. While the epidermis of human skin (panel b) shows several layers of differentiating keratinocytes that form the cornified envelope, murine epidermis (panel a) consists only of few keratinocyte layers. Additionally, murine skin harbors more hair follicles that occupy majority of the dermal layer. (Adapted from (Pasparakis et al., 2014)).

Cutaneous wound healing is an intricate process that requires coordination of several cell types and communication via chemical, biological and physical signals. In brief, a first inflammatory process

results in deposition of new extracellular matrix by fibroblasts, wound contraction of myofibroblasts and scar formation for restoration of the injured tissue. Normal wound repair can be monitored by three overlapping phases: inflammation, tissue formation and tissue remodeling (Figure 3). Upon injury, disruption of the vascular network leads to liberation of platelets from the blood stream into damaged tissue, thereby sealing the wound by forming a fibrin clot. Platelets also secrete various growth factors and cytokines like TGFβ and PDGF that activate dermal fibroblasts and attract neutrophils to infiltrate into the wound (Moulin et al., 1998). Neutrophils themselves produce pro-inflammatory cytokines and ECM degrading enzymes to clear the wound from damaged tissue (Hübner et al., 1996; Nwomeh et al., 1998). For proper re-epithelialization, keratinocytes from the wound edge have to migrate over the provisional matrix to form a new epidermal layer. This process requires reorganization of the intracellular cytoskeleton and dissolution of desmosomal and hemidesmosomal linkages (Goliger and Paul, 1995). Furthermore, infiltrating macrophages promote neovascularization of the tissue and activated fibroblasts deposit new collagen fibrils (Okuno et al., 2011; Xue and Jackson, 2015). Lastly, under mechanical stress, fibroblasts differentiate to myofibroblasts that express smooth muscle actin for contraction and closure of the wound (Tomasek et al., 2002). Critical steps are infection and ongoing inflammation, leading to persistence of cytokines, large amounts of fibroblasts and myofibroblasts and excessive ECM deposition. The results are fibrotic lesions like keloids and hypertrophic scars that remain in the skin (Tredget et al., 1997).

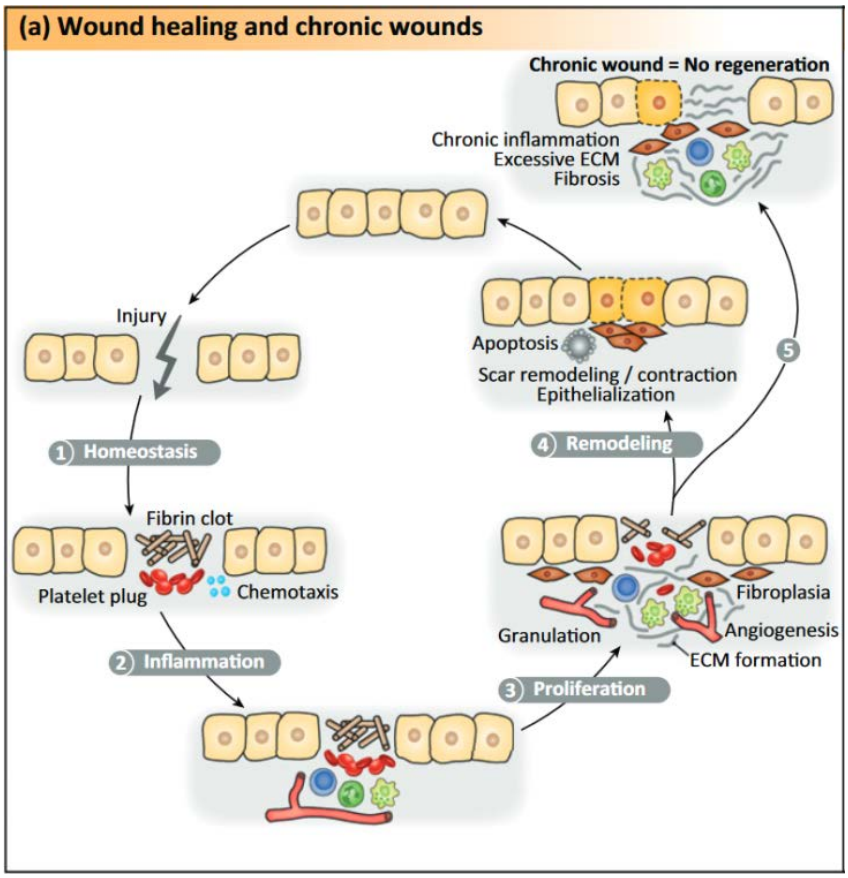

Figure 3: Wound healing cycle.

Upon injury, normal skin homeostasis is disrupted. Platelets from the blood stream are activated and seal the wound by a fibrin clot. Inflammatory cells are recruited to the wound and secrete cytokines and chemokines that promote proliferation of cells and deposition of extracellular matrix. After wound closure, inflammatory cells are removed and tissue is remodeled for scar formation. Persisting inflammation can lead to chronic wounds, excessive ECM deposition and fibrosis. (Adapted from (Shechter and Schwartz, 2013)).

Another chronic skin disease is psoriasis that represents many similarities to wound healing like keratinocyte hyperproliferation, inflammatory infiltration and neovascularization (Nickoloff et al., 2006). Mainly, psoriatic skin lesions originate from dysregulated cross-talk between innate and adaptive components of the immune system with resident skin cells (Boehncke and Schön, 2015). This includes excessive production of pro-inflammatory cytokines like TNFα and interleukins as well as growth factors and antimicrobial peptides that promote infiltration of immune cells and a chronic skin inflammation. However, the cause of psoriasis is not fully understood and cures remain elusive.

Of note, remodeling of the skin in physiological and pathological processes requires expression and activity of proteolytic enzymes that promote ECM deposition, cell proliferation and migration as well as maturation of cytokines and growth factors (Mezentsev et al., 2014). Therefore, investigation of the complex interplay of various enzymes and their role in these processes is crucial for understanding the development of pathologies from physiological mechanisms. However, transcription and regulation through activation and inhibition as well as single substrates of each protease within the proteolytic

web are not fully understood. Genetic models *in vitro* and *in vivo* could shed light on the physiological and pathological role of each enzyme.

1.3 Meprin expression in skin and fibrotic conditions

The metalloproteases meprin α and meprin β were identified to be expressed in both epidermis and dermis of human skin (Becker-Pauly et al., 2007; Kronenberg et al., 2010). Interestingly, distribution of the proteases within the epidermis is different, indicating specific functions for each meprin in keratinocyte differentiation and development. Meprin α is found in the *stratum basale*, a region of undifferentiated and proliferative keratinocytes. Therefore, meprin α might promote proliferation due to cleavage of growth factors, proteases and inhibitors or lead to detachment of basal keratinocytes from the basement membrane (Jefferson et al., 2013). Meprin β, on the other hand, is expressed in the outer part of the epidermis, the *stratum granulosum*, where keratinocytes undergo flattening and lose their nucleus to form the cornified envelope. Upon activation by kallikrein related peptidases (KLK), meprin β might process adhesion molecules like desmogleins, E-Cadherin and CD99 to promote desquamation of the keratinocytes (Bedau et al., 2017a; Huguenin et al., 2008; Jefferson et al., 2013; Ohler et al., 2010). Of note, in hyperproliferative skin diseases, such as Netherton Syndrome and psoriasis, meprin α was found to be expressed in the *stratum granulosum* and meprin β in the *stratum corneum* (Becker-Pauly et al., 2007). Additionally, upregulation of meprins in the dermis was observed in keloids, characterized by hyperproliferation of fibroblasts and excess deposition of extracellular matrix (Kronenberg et al., 2010). So far it is not known, if meprins promote the onset and progression of such skin diseases and therefore might be a good candidate for investigation of therapeutic treatment.

Transcription of the Mep1b gene is regulated by different promoter binding sites at the 5' untranslated region (Jiang et al., 2000). Besides promoter binding sites for tissue specific expression in kidney (HFH3, CREB, GATA1) and intestine (SI/cdx2 and LPH/cdx2), transcription of the Mep1b gene could also be activated by transcription factors of the AP-1 transcription factor complex (AP1/PEA3). AP-1 is a heterodimeric complex consisting of Fos (c-Fos, FosB, Fra1, Fra2) and Jun proteins (c-Jun, JunB, JunD) to regulate differentiation, proliferation, inflammation and apoptosis (Eferl et al., 2008). Downstream targets are proteins of the extracellular matrix like collagens (col1α2) (Chung et al., 1996) and collagen modifying enzymes like MMP-1 (Wang et al., 2012) and MMP-9 (Mittelstadt and Patel, 2012). Especially in skin, AP-1 plays a role in tissue regeneration and is responsible for differentiation of keratinocytes (Angel et al., 2001). AP-1 itself is activated by signal transduction of TGFβ ligands, which are potent growth factors that influence cell proliferation, differentiation, tissue homeostasis, morphogenesis and regeneration (Massagué, 2012). Hence, it regulates synthesis and deposition of extracellular matrix, bone formation, vascular remodeling and wound healing. It also switches epithelial cells into a mesenchymal migratory phenotype (EMT), necessary for gastrulation, embryonic tissue formation and regeneration. Due to this potency, TGFβ enhances also tumor invasion

and metastasis and promotes fibrosis. Recently, it has been shown that meprin β expression can be upregulated via TGFβ in isolated pulmonary arteries cells (Biasin et al., 2014) as well as A549 lung carcinoma cells (Biasin et al., 2017). During the last years, activation of meprin β through Fra2 (Fos-related antigen 2) was studied in regard to pathological conditions. Over-expression of Fra2 led to pulmonary hypertension and early death in Fra2 transgenic mice (Eferl et al., 2008). Interestingly, meprin β was identified as the most highly upregulated gene in the lungs and thought to be an important mediator of vascular remodeling and developing lung fibrosis in the animal model (Biasin et al., 2014). This was further proven by intra-tracheal administration of bleomycin in meprin knock-out mice for induction of lung fibrosis, which revealed decreased collagen deposition and tissue density in meprin β knock-out mice, highlighting a potential role of meprin β in disease progression (Biasin et al., 2017). Besides lung phenotypes, Fra2 transgenic mice develop microangiopathy and skin fibrosis by excess extracellular matrix deposition from week 12 to 16 (Maurer et al., 2009; Reich et al., 2010). However, expression and the role of meprin β for collagen maturation and the onset of fibrosis have not yet been studied in the skin of Fra2 transgenic mice.

1.4 Meprins as regulators of inflammatory processes and associated pathologies

Other pathologies and pathology developing mouse models highlighted a meprin contribution to several other inflammatory processes (Figure 4A). At their main expression sites in the gut and kidney, meprins are transported to the plasma membrane on the apical sites of epithelial cells or secreted into the lumen of gut and kidney. During cisplatin or ischemia-reperfusion induced acute kidney injury, meprins undergo redistribution to the basolateral site of proximal tubuli thereby degrading the basement membrane components like nidogen-1 (Herzog et al., 2007; Walker et al., 1998). This was further proven in meprin knock-out mice and treatment with the meprin inhibitor actinonin (Bylander et al., 2008; Herzog et al., 2015). Other basal laminar components cleaved by meprins are collagen IV and fibronectin whose cleavage fragments could either act as chemotactic agents or block immune responses (Adair-Kirk and Senior, 2008; Kaushal et al., 1994). Moreover, meprins were shown to induce the expression of pro-inflammatory cytokines IL-1β, IL-6 and IL-18 in macrophages or to directly activate IL-1β (Gao and Si, 2010; Herzog et al., 2009; Li et al., 2014). On the other hand, cytokines can also be deactivated as seen for IL-6 (Keiffer and Bond, 2014). Loss of IL-6 deactivation in a DSS-induced colitis model in meprin α knock-out mice led to significant increased IL-6 levels and higher systemic inflammation in the intestine, indicating a protective role of meprin α in inflammatory bowel disease (Banerjee et al., 2009). Furthermore, high abundance of meprin α in serum and urine represents a marker for Kawasaki disease, a systemic vasculitis with mucocutaneous inflammation that lead to severe morbidity (Kentsis et al., 2013).

Overall, these data implicate that dysregulated expression and localization of meprins could be associated with the onset and progression of inflammation and fibrotic conditions (Figure 4A, B).

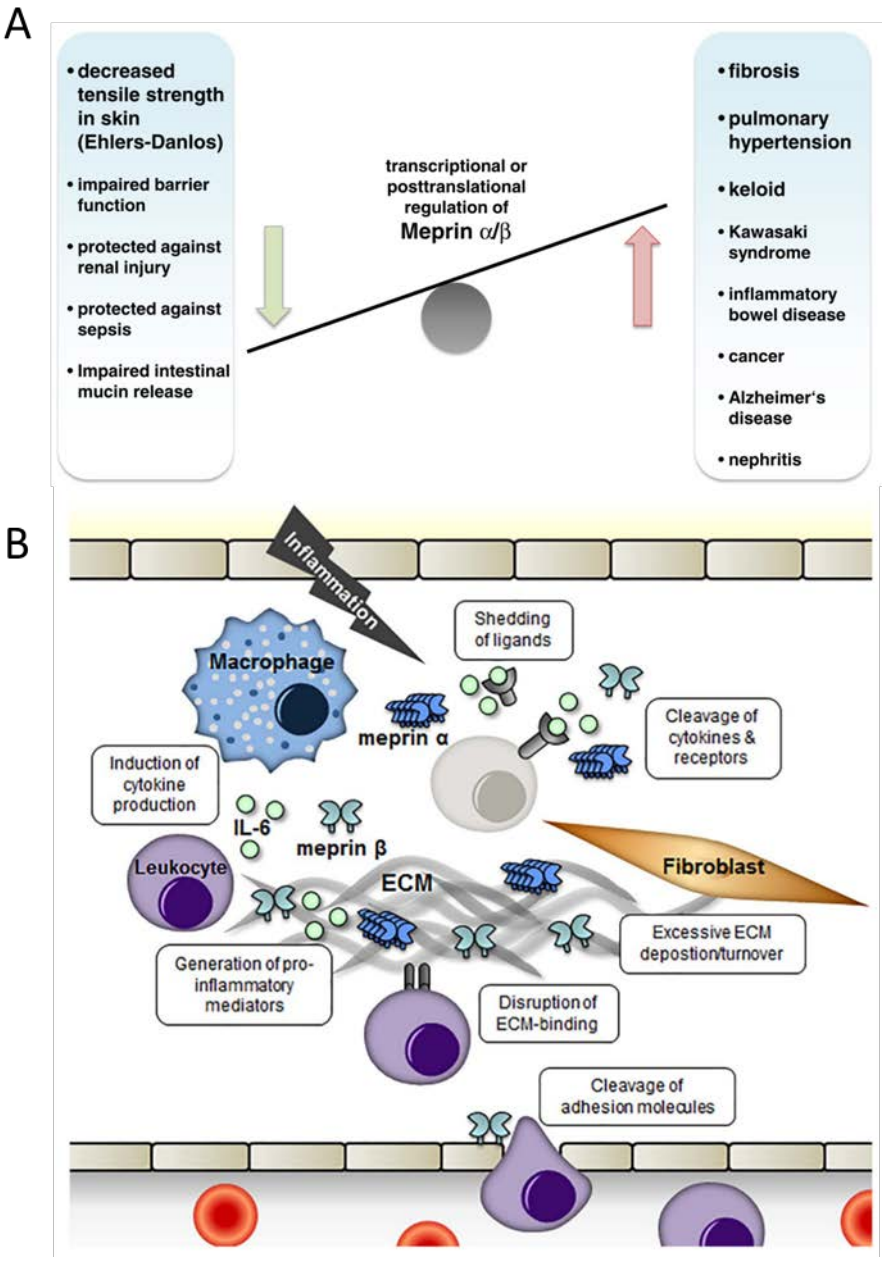

Figure 4: Contribution of meprin metalloproteases to inflammatory processes, ECM remodeling and pathologies.

(A) Up- and downregulation of meprin metalloproteases by transcription or posttranslational modifications can be associated with different (patho)physiological conditions. (Adapted from (Prox et al., 2015)). (B) Expression and localization of meprin metalloproteases can regulate inflammatory processes through induction of pro-inflammatory signals and invasion of immune cells. Furthermore, remodeling and deposition of ECM can promote development of pathologies or alter the environment of migrating and proliferating cells, e.g. cancer cells. (Adapted from (Arnold et al., 2017)).

1.5 Aim of the study

Meprin metalloproteases represent interesting enzymes because of their unique cleavage specificity and transcriptional regulation. Besides their expression in kidney and intestinal epithelial cells in normal organism physiology, various studies highlight roles of meprins in the onset and progression of pathologies. These include not only altered localization at their main expression sites but also transcription and translation in other tissues and cells like cancer cells.

Aim of the study was to further strengthen the role of meprins in the onset of pathologies with regard to transcriptional regulation, localization and substrate cleavage of the proteases by *in vitro* and *in vivo* experiments. Therefore, meprin expression should be investigated in murine skin and their role in the process of wound healing. To further elucidate the role of meprin β in the onset of skin fibrosis and other skin diseases, mouse models were examined that either express meprin β via the transcription factor Fra2 or by direct over-expression in dermis and epidermis. Moreover, cleavage of the novel meprin β substrate CD99 was analyzed and its impact on transendothelial migration of inflammatory cells and cancer cells. Lastly, localization of secreted meprin α to plasma membranes via heparan sulphate or in an enzyme complex with meprin β was investigated with regard to potential roles in epithelial barrier function and gene expression alterations.

2. Materials and Methods

Chemicals were purchased from Carl Roth if not indicated otherwise. Ultrapure water was produced by *Milli-Q® Integral water purification system* and is abbreviated with ddH2O.

2.1 Buffers

All buffers used in this study are listed in Table 1.

Table 1: Composition of buffers

Buffer	Composition
Agarose gel	1-2% (w/v) agarose, 1x TAE buffer, Ethidium bromide
Blocking solution	3% (w/v) BSA or 5% (w/v) skimmed milk, TBS
Coomassie destaining	10% (v/v) glacial acetic acid, 40% (v/v) MeOH, 50% (v/v) ddH2O
Coomassie staining	0,1% (w/v) Coomassie R250, 10% (v/v) glacial acetic acid, 40% (v/v) MeOH, 50% (v/v) ddH2O
Lysis buffer	PBS pH 7.4, 1% (v/v) Triton X-100, Complete Protease inhibitor cocktail tablet (Roche)
Lysis buffer (skin)	50 mM Tris-HCl pH 6.8, 150 mM NaCl, 1% (v/v) Triton X-100, 1% (w/v) SDS, 2 mM EDTA, Complete Protease inhibitor cocktail tablet (Roche)
PBS	135 mM NaCl, 2.7 mM KCl, 9.2 mM Na_2HPO_4, 1.8 mM KH_2PO_4, pH 7.4
Fixation buffer	4% (w/v) PFA, PBS
Sample buffer	2.5 ml Tris-HCl pH 6.8, 1 g SDS, 2.5 ml ddH2O, 0.05 g Bromophenol blue, 5 ml Glycerol, 100-200 mM DTT
SDS running buffer	25 mM Tris, 192 mM glycine, 0.1% (w/v) SDS, pH 8.3
Resolving gel buffer	1.5 M Tris, 0.4% (w/v) SDS, pH 8.8
Stacking gel buffer	0.5 M Tris, 0.4% (w/v) SDS, pH 6.8
TAE buffer	40 mM Tris, 20 mM acetic acid, 1 mM EDTA, pH 8.0
Tank blot buffer	25 mM Tris, 200 mM Glycin, 20% (v/v) methanol, pH 8.3
TBS	20 mM Tris, 137 mM NaCl, pH 7.5

2.2 Cell culture

HaCaT keratinocyte cell line and isolated murine skin fibroblasts were cultured in DMEM + GlutaMAX (Gibco, Thermo Fisher Scientific), supplemented with 10% heat-inactivated FCS, 100 units/ml penicillin, 100 µg/ml streptomycin (Gibco, Thermo Fisher Scientific) and 5 µg/ml gentamycin (Carl Roth). Isolated murine keratinocytes were cultured in CnT-57 (CellnTec),

supplemented with 100 units/ml penicillin, 100 µg/ml streptomycin (Gibco, Thermo Fisher Scientific) and 5 µg/ml gentamycin (Carl Roth). Culture conditions were under a humidified atmosphere (5% CO_2) at 37°C.

2.3 Isolation of primary murine keratinocytes and fibroblasts

Mice were sacrificed and the tail was dissected and disinfected for 5 min in povidone iodine (Betaisodona, Mundipharma) followed by 3 washes in 70% ethanol. Under the laminar flow hood, the skin was cut with a sterile scalpel and forceps, removed from the bone and divided into three pieces. Facing the dermis downwards, the skin was placed on sterile filter paper and incubated with 1% trypsin/DMEM at 37°C for 1 h. In the meantime, 10 cm culture dishes were coated with 5 µg/cm² Collagen I from rat tail (Gibco, Thermo Fisher Scientific). Collagen I was diluted in 20 mM acetic acid and transferred into culture dishes. The dishes were incubated for 1 h at room temperature, washed three times with DPBS to remove the acid and directly used or stored at 4°C. After trypsin incubation, the epidermis was removed from the dermis by forceps, rinsed with 10% FCS/PBS and grinded through a 40 µm cell strainer for 5 min. The cell suspension was centrifuged at 200 x g for 5 min, the cell pellet dissolved in CnT-57 and seeded into 10 cm collagen-coated culture dishes. After 48 h, keratinocytes were washed with DPBS and raised to 90% confluency in CnT-57.

For fibroblast isolation, the remaining dermis was rinsed with 10% FCS/PBS, cut into small pieces and transferred into a microcentrifuge tube with 1 ml Collagenase I (500 U/ml) in 1x HBSS (Thermo Fisher Scientific). The tissue was incubated at 37°C for 1-2 h by gentle shaking and centrifuged at 500 x g for 10 min. The tissue/cell-pellet was dissolved in DMEM with 10% FCS and placed in 10 cm culture dishes. After 48-72 h, the detached cells were washed with DPBS and raised to total confluency. For longer cultivation, cells were immortalized by transfection of SV-40 plasmid to avoid senescence and differentiation to myofibroblasts.

2.4 Skin lysate preparation

Mice were sacrificed, the skin shaved and dissected. The skin was snap frozen in liquid nitrogen or directly pulverized in a nitrogen cooled mortar. Skin lysis buffer was added to the skin powder and incubated for 24 h at 4°C under rolling conditions. Skin lysates were centrifuged at 13.000 rpm, 4°C for 30 min and transferred into new microcentrifuge tubes. Total protein concentration was measured by BCA assay and 50 µg of denatured skin lysates used for SDS-PAGE and Western Blot analysis.

2.5 Cell lysis, SDS-PAGE and Western blot analysis

Cells were transfected and incubated for 24 h, harvested and lysed in lysis buffer containing 1% Triton x-100/PBS and protease inhibitor tablet with EDTA (Roche). Protein concentration was measured using BCA assay (Thermo Fisher Scientific). 30 µg total protein cell lysate or 50 µg tissue lysate were separated by SDS-PAGE and transferred by tank-blotting onto nitrocellulose membranes (GE

Healthcare) with constant current of 800 mA (4 membranes) or 250 mA (2 membranes). Membranes were blocked with 5% milk in Tris-buffered saline (TBS) for 1h at room temperature, incubated overnight with primary antibody in milk at 4°C, washed 3x with TBS and incubated with horseradish peroxidase-conjugated secondary antibodies in TBS at RT for 1h. After further washes, protein signals were detected with SuperSignal West Femto (Thermo Fisher Scientific) in a chemiluminescence detection system (LAS-3000, Fujifilm).

Table 2: Primary antibodies for Western blot analysis

Primary Antibody	Species	Dilution	Supplier
HA-Tag	Rabbit	1:1000	Cell Signaling Technology
Mepβ Tier 2	Rabbit	1:1000	Pineda Antibody Service
LF-68 (Col I, C-telopeptide)	Rabbit	1:1000	Larry W. Fisher
LF-42 (Col I, C-pro-peptide)	Rabbit	1:1000	Larry W. Fisher
α-SMA	Mouse	1:1000	Dako
Cytokeratin 14 (ab7800)	Mouse	1:100 (2 µg/ml)	Abcam
Cytokeratin 5 (ab52635)	Rabbit	1:10000	Abcam
E-Cadherin	Rabbit	1:1000	Abcam
CD99, murine	Goat	1:500	Dietmar Vestweber, Max Planck Institute of Molecular Biomedicine, Münster, Germany
β1 integrin	Rabbit	1:5000	Prof. Reinhard Fässler, Max Planck Institute of Biochemistry, Munich, Germany
Desmoglein 1 (ab124798)	Rabbit	1:1000	Abcam
Desmoglein 3 (ab14416)	Mouse	1:200	Abcam

Table 3: Secondary antibodies for Western blot analysis

Secondary Antibody	Species	Dilution	Supplier
α Rabbit IgG-HRP	Goat	1:20000	Jackson ImmunoResearch
α Mouse IgG-HRP	Sheep	1:20000	Jackson ImmunoResearch
α Goat IgG-HRP (sc-2020)	Donkey	1:10000	Santa Cruz Biotechnology

2.6 RNA isolation from murine skin and primary cells

RNA was isolated using NucleoSpin® RNA Isolation Kit (Macherey-Nagel) with additional lysation steps for murine skin. Mice were sacrificed, dorsal skin was excised and grinded to powder in a liquid nitrogen cooled mortar. Skin powder was transferred into a microcentrifuge tube with 350 µl Buffer RA1 supplemented with 1% Triton-X-100 and 3.5 µl β-mercaptoethanol. 590 µl RNase-free water and 10 µl Proteinase K were added, mixed by pipetting and incubated at RT for 10 min followed by 55°C for 10 min. Tissue lysates were centrifuged for 3 min at 10,000 x g and the supernatant transferred into a new microcentrifuge tube. 475 µl 99% ethanol were added, lysates mixed by vortexing and transferred into an RNA binding column (blue ring). After centrifugation at 8.000 x g for 30 s, sample preparation was continued as described in the manufacturer's protocol. RNA was stored at -80°C.

2.7 cDNA synthesis from RNA samples

Isolated RNA was transcribed into stable cDNA by using RevertAid First Strand cDNA Synthesis Kit (Thermo Fisher Scientific). 1 µg total RNA was incubated with 1 µl Oligo $(dT)_{18}$ primer in 12 µl total volume for 5 min at 65°C. Samples were chilled on ice and treated with 4 µl 5X Reaction Buffer, 1 µl RiboLock RNase Inhibitor (20 U/µl), 10 mM dNTP Mix and 1 µl RevertAid M-MuLV RT (200 U/µl). After an incubation of 60 min at 42°C, reaction was terminated by heating at 70°C for 5 min. cDNA samples were stored at -80°C or used for RT-PCR.

mRNA levels can be detected and quantified using semi-quantitative or quantitative RT-PCR with specific primer pairs for genes of interests.

2.8 Semi-quantitative RT-PCR from murine and human RNA samples

For semi-quantitative RT-PCR, cDNA is amplified in a PCR machine and analyzed via agarose gel electrophoresis. Gene specificity is ensured by specific primer pairs that target intron spanning regions of genes and produce PCR products of a specific length. Amplification of a house keeping gene, e.g. GAPDH or β-actin, can be used to estimate total amounts of the gene of interest.

Table 4: Pipetting scheme for semi-quantitative RT-PCR

Reagent	**Volume in µl**
Template cDNA	1
Forward primer (10 µM)	1
Reverse primer (10 µM)	1
dNTP Mix (2 mM)	2
10x DreamTaq Buffer	2
DreamTaq Polymerase	0.5
ddH_2O	12.5

Table 5: Primer pairs used for semi-quantitative RT-PCR

Primer	Sequence
mMepA Frag2 For	5'-GCC CAG AGG CCT CCT TCT G-3'
mMepA Frag2 Rev	5'-AGA TCA AGC CAG CGA TGC-3'
mMepB Frag2 For	5'-CAG TCC TCC ATT TTA TTC TTC-3'
mMepB Frag2 Rev	5'-GTT CCG TTA GGG AAA ACA TCC-3'
mGAPDH For	5'-CAT TGA CCT CAA CTA CAT GG-3'
mGAPDH Rev	5'-AAT GCC AAA GTT GTC ATG GA-3'
mBMP1 For	5'-AGC CTG AGC CAG TCC TGG CT-3'
mBMP1 Rev	5'-TGG AAC TTC ACC AGG ACA GA-3'
mTll1 For	5'-TAT GTG GCA GCA AGA TAC CA-3'
mTll1 Rev	5'-GCC ACA TCT CCA ATT GAA TAG A-3'
mTll2 For	5'-GCT CCC GTG CAG TAC CGC AT-3'
mTll2 Rev	5'-CCT CTG CAC TGC TGA TCT TG-3'
mMepB UTR For	5'-TTG CAG CTT TCG TCT GGA-3'
mMepB' Exon3 For	5'-GAC GGG ATG TAC ATG ATG-3'
mMepB Exon6 Rev	5'-TGA ACA CTG AGA TAT AGT-3'

Table 6: PCR program for semi-quantitative RT-PCR

Step	Temperature	Time
Initial denaturation	95°C	5 min
Denaturation	94°C	60 sec
Annealing	55°C	30 sec
Elongation	72°C	60 sec
Final elongation	72°C	10 min
Cooling	4°C	hold

30 cycles

6x DNA Loading Dye (Thermo Fisher Scientific) was added and samples loaded on a 1.5% agarose gel containing ethidium bromide for detection. Gel electrophoresis was performed at constant voltage of 100 V for 35 min and DNA fragments were visualized at a UV-transilluminator (Intas Science Imaging).

2.9 Quantitative RT-PCR (qPCR) from murine and human RNA samples

For qPCR analysis, cDNA was amplified in the LightCycler®480 II Real-Time PCR System (Roche Applied Science) according to the manufacturer's instructions. In order to ensure specificity for target

gene amplification, primer pairs were generated using *Universal ProbeLibrary Assay Design Center* (http://qpcr.probefinder.com/roche3.html). During amplification, specific UPL probes bind to intron spanning regions of the gene of interest. Degradation of the UPL probes by the DNA polymerase leads to release of fluorescent dyes from quenchers, which is measured by the PCR machine. Relative amounts of the target gene were normalized to the house keeping gene GAPDH.

Table 7: Pipetting scheme for qPCR

20x Assay	**Volume in µl**
Forward Primer (100 µM)	1.2
Reverse primer (100 µM)	1.2
UPL Probe	4
ddH_2O	13.6

Table 8: Primer pairs used for qPCR

Primer	**UPL probe**	**Sequence**
mMepB #97 For	#97	5'-AGA CCC AAC GAT GAC CAG TG-3'
mMepB #97 Rev		5'-GTT CCG TTA GGG AAA ACA TCC-3'
mMepA #107 For	#107	5'-GGC ACC TGT GTG AAC GTA AA-3'
mMepA #107 Rev		5'-AGA TCA AGC CAG CGA TGC-3'
mACTA2 #58 For	#58	5'-CTC TCT TCC AGC CAT CTT TCA T-3'
mACTA2 #58 Rev		5'-TAT AGG TGG TTT CGT GGA TGC-3'
mCol1a2 #71 For	#71	5'-CAA GCA TGT CTG GTT AGG AGA G-3'
mCol1a2 #71 Rev		5'-AGG ACA CCC CTT CTA CGT TGT-3'
mTYR #46 For	#46	5'-CAC CAT GCT TTT GTG GAC AG-3'
mTYR #46 Rev		5'-GGC TTC TGG GTA AAC TTC CAA-3'
mKRT5 #22 For	#22	5'-CAG AGC TGA GGA ACA TGC AG-3'
mKRT5 #22 Rev		5'-CAT TCT CAG CCG TGG TAC G-3'
mKRT14 #22 For	#22	5'-CCT CTG GCT CTC AGT CAT CC-3'
mKRT14 #22 Rev		5'-GAG ACC ACC TTG CCA TCG-3'
mKRT10 #9 For	#9	5'-CGA AGA GCT GGC CTA CCT AA-3'
mKRT10 #9 Rev		5'-GCA GCG TTC ATT TCC ACA-3'
mTgfb1 #72 For	#72	5'-TGG AGC AAC ATG TGG AAC TC-3'
mTgfb1 #72 Rev		5'-GTC AGC AGC CGG TTC CCA-3'
mDSG1 #18 For	#18	5'-GCT CAT CAT GGG GTT CCT AGT-3'
mDSG1 #18 Rev		5'-CCC CTC CAC AAT CAC AGC-3'

mDSG3 #82 For	#82	5'-GAT GAG GAC ACG GGT AAA GC-3'
mDSG3 #82 Rev		5'-ACC ATC ATT ACG ACC CAG GA-3'
mCD207 #74 For	#74	5'-TGT CCT CAG AAT CGG AAC AA-3'
mCD207 #74 Rev		5'-TTG GTA AGT CCA ATC CAG TGT G-3'
mIL6 #6 For	#6	5'-GCT ACC AAA CTG GAT ATA ATC AGG A-3'
mIL6 #6 Rev		5'-CCA GGT AGC TAT GGT ACT CCA GAA-3'
mAdgre1 #42 For	#42	5'-GGA GGA CTT CTC CAA GCC TAT T-3'
mAdgre1 #42 Rev		5'-AGG CCT CTC AGA CTT CTG CTT-3'
mIL18 #46 For	#46	5'-CAA ACC TTC CAA ATC ACT TCC T-3'
mIL18 #46 Rev		5'-TCC TTG AAG TTG ACG CAA GA-3'
mIL1b #38 For	#38	5'-AGT TGA CGG ACC CCA AAA G-3'
mIL1b #38 Rev		5'-AGC TGG ATG CTC TCA TCA GG-3'

20x assay was prepared for gene specific amplification, diluted in ddH_2O and transferred in 384 well plate. 0.5 µl of transcribed cDNA were mixed with 2x Probes Master (Roche Diagnostics) and added to the specific assay sample. qPCR war performed using LightCycler®480 II (Roche Applied Science). Relative amounts of target genes were normalized to the housekeeping gene GAPDH.

2.10 Scratch wound healing assay

1.5 x 10^5 HaCaT cells were seeded into 24-wells and grown 48 h to total confluence. Cells were washed with PBS and serum starved in DMEM overnight. On the next day, a cross-shaped scratch was inflicted to the monolayer. After another washing step for removal of detached cells, 500 µl serum-free DMEM were added supplemented with indicated inhibitors or recombinant protease. Images of the scratch were taken at 0 h and 24 h with Leica DMi8 microscope. Wound areas were analyzed using ImageJ MRI_Wound_Healing_Tool.

For primary murine keratinocytes, 1.5 x 10^5 cells were seeded into 24-wells and grown overnight to total confluence in basal keratinocyte medium (CnT-57, CellnTec). A cross-shaped scratch was inflicted to the monolayer and detached cells were removed by PBS washing. 500 µl of CnT-57 were added and images taken at 0 h, 24 h and 48 h with Leica DMi8 microscope. Wound areas were analyzed using ImageJ MRI_Wound_Healing_Tool.

2.11 Meprin β activity assay

Meprin β activity in cell supernatant of isolated primary keratinocytes was measured by fluorogenic peptide cleavage assay using a specific meprin β peptide substrate (mca-EDEDED-K-ε-dnp; Genosphere Biotechnologies) in a final concentration of 10 µM. The peptide consists of a fluorophore (7-methyloxycoumarin-4-yl (mca)), a substrate peptide for meprin β (EDEDED) and a quencher (K-ε-

2,4-dinitrophenyl (dnp)). 200 µl cell supernatant were incubated with 10 µg/ml trypsin at 37°C, 30 min for meprin β activation. 1 µM F2 inhibitor were added after 20 min for meprin β inhibition. After addition of the fluorogenic peptide, changes in fluorescence intensity were measured every 30 s at 37°C for 120 min using a fluorescent spectrometer Infinite F200 PRO (Tecan) with excitation at 320 nm and emission at 405 nm. Slope of activity from 3 biological replicates was plotted and used for statistical analysis.

2.12 Experimental animals

Mice were kept in constant environmental conditions (12h light-dark cycles, temperature) and in an IVC (Individually Ventilated Cages) system with food and drinking water *ad libitum* in accordance with the ethical standards set by the National Animal Care Committee of Germany. C57Bl/6N wildtype, meprin α-deficient (MepA KO, (Banerjee et al., 2009)), meprin β-deficient (MepB KO, (Norman et al., 2003)), meprin α/β double deficient (MepAB) and Fra2 transgenic mice (Fra2 tg, (Eferl et al., 2008)) were sacrificed, organs were removed and either snap frozen in liquid nitrogen or used for cell isolation.

2.13 Generation of meprin β knock-in mice

Meprin β knock-in mice were produced in collaboration with Dr. Ronald Naumann and Dr. Michael Haase from Max Planck Institute of Molecular Cell Biology and Genetics in Dresden as described before (Karimova et al., 2018). In brief, murine meprin β cDNA was cloned into CAG-cre-IRES-Rosa26 vector and inserted into Rosa26 locus of C57Bl/6N mice by homologous recombination. Homozygous meprin β knock-in (MB-KI) mice were crossed to tamoxifen inducible KRT5tm1.1-CreERT2 or Col1a2-CreERT2-ALPP mice. For excision of the Stop cassette, mice were either treated with tamoxifen-citrate food or normal chow for 4 weeks after genotyping, following treatment with normal chow. Tamoxifen-citrate food contained 400 mg/kg and was purchased from Envigo. Mice were sacrificed 4 weeks or 8 weeks after the tamoxifen treatment at the age of 12 or 16 weeks, respectively. The animal experiment was permitted by corresponding authorities of Schleswig-Holstein, Germany, (V 242 - 12659/2018 (30-4/18); 22.02.2018).

2.14 Genotyping of meprin knock-in mice in Rosa26 locus

For genotyping of meprin knock-in mice, primers were designed for generation of PCR products spanning the natural Rosa26 locus or the inserted CAG promoter region. Genomic DNA from mice was isolated by digestion of tail biopsies with DirectPCR-Tail (Peqlab Biotechnology GmbH) and Proteinase K (0.2 mg/ml, Thermo Fisher Scientific) o/n at 55°C and constant agitation. Proteinase K was heat inactivated at 85°C for 1h and samples used as templates for genotyping PCR.

Table 9: Primers used for genotyping of Rosa26 locus

Primer	Sequence
Rosa26 For	5‘-AAA GTC GCT CTG AGT TGT TAT C-3’
Rosa26 WT Rev	5‘-GAT ATG AAG TAC TGG GCT CTT-3’
Rosa26 TG Rev	5‘-TGT CGC AAA TTA ACT GTG AAT C-3’

Table 10: Pipetting scheme for Rosa26 genotyping PCR

Reagent	Volume in µl
Template DNA	2
Forward primer (10 µM)	1
Reverse primer WT (10 µM)	1
Reverse primer TG (10 µM)	1
dNTP Mix (10 mM)	0.4
10x DreamTaq Buffer	2,5
DreamTaq Polymerase	0.5
ddH_2O	16.6

Table 11: Rosa26 genotyping PCR program

Step	Temperature	Time
Initial denaturation	95°C	3 min
Denaturation	95°C	30 sec
Annealing	56°C	30 sec
Elongation	72°C	50 sec
Final elongation	72°C	10 min
Cooling	4°C	hold

35 cycles

6x DNA Loading Dye (Thermo Fisher Scientific) was added and samples loaded on a 1.5% agarose gel containing ethidium bromide for detection. Gel electrophoresis was performed at constant voltage of 100 V for 35 min and DNA fragments were visualized at a UV-transilluminator (Intas Science Imaging). Expected band sizes of the PCR products were 570 bp for the wildtype allele and 380 bp for the transgenic allele.

2.15 Genotyping of KRT5- and Col1a2-Cre mice

Insertion of the tamoxifen-inducible Cre-recombinase in either KRT5- or Col1a2-gene was determined via genotyping PCR.

Table 12: Primers used for genotyping of Cre recombinase

Primer	Sequence
Col1a2_Cre_for	5'-CAG GAG GTT TCG ACT AAG TTG G-3'
Col1a2_Cre_rev	5'-CAT GTC CAT CAG GTT CTT GC-3'
Cre general for (KRT5)	5'-GGT TCG CAA GAA CCT GAT GGA CAT-3'
Cre general rev (KRT5)	5'-GCT AGA GCC TGT TTT GCA CGT TCA-3'

Table 13: Pipetting scheme for genotyping of Cre recombinase

Reagent	Col1a2-Cre PCR Volume in µl	Cre general PCR Volume in µl
Template DNA	2	2
Forward primer (10 µM)	1	1
Reverse primer (10 µM)	1	1
dNTP Mix (10 mM)	0.4	0.4
10x DreamTaq Buffer	2.5	2.5
DreamTaq Polymerase	0.5	0.5
ddH_2O	17.6	17.6

Table 14: Specific PCR program for genotyping of Col1a2-Cre

Step	Temperature	Time	
Initial denaturation	94°C	2 min	
Denaturation	94°C	20 sec	10 cycles, -0.5°C per cycle
Annealing	65°C	15 sec	
Elongation	68°C	10 sec	
Denaturation	94°C	15 sec	28 cycles
Annealing	60°C	15 sec	
Elongation	72°C	10 sec	
Final elongation	72°C	2 min	
Cooling	4°C	hold	

Table 15: PCR program for genotyping of Cre recombinase

Step	Temperature	Time
Initial denaturation	95°C	5 min
Denaturation	95°C	30 sec
Annealing	56°C	30 sec
Elongation	72°C	15 sec
Final elongation	72°C	10 min
Cooling	4°C	hold

30 cycles

6x DNA Loading Dye (Thermo Fisher Scientific) was added and samples loaded on a 2% agarose gel containing ethidium bromide for detection. Gel electrophoresis was performed at constant voltage of 100 V for 30 min and DNA fragments were visualized at a UV-transilluminator (Intas Science Imaging). Expected band sizes of the Col1a2-Cre PCR products were 186 bp and 342 bp for the general Cre PCR.

2.16 Validation of Cre recombinase activity

Excision of the stop cassette by tissue specific Cre recombinase was determined by PCR from genomic DNA of tissue biopsies.

Table 16: Primers used for validation of Cre recombinase activity

Primer	Sequence
LoxP For	5'-GGA CAA ACT CTT CGC GGT CT-3'
mMep in Rosa26 For	5'-TAG AGA TCA TAA TCA GCC-3'
mMepB in Rosa26 Rev	5'-CTC TGT CCC GTT CTG GAA-3'

Table 17: Pipetting scheme for PCR of Cre recombinase activity

Reagent	Volume in µl
Template DNA	2
Forward primer LoxP For (10 µM)	1
Forward primer mMep in Rosa26 For (10 µM)	1
Reverse primer mMepB in Rosa26 Rev (10 µM)	1
dNTP Mix (2 mM)	2
10x DreamTaq Buffer	2
DreamTaq Polymerase	0.5
ddH_2O	11.5

Table 18: PCR program for validation of Cre recombinase activity

Step	Temperature	Time
Initial denaturation	95°C	5 min
Denaturation	94°C	60 sec
Annealing	56°C	30 sec
Elongation	72°C	90 sec
Final elongation	72°C	10 min
Cooling	4°C	hold

30 cycles

6x DNA Loading Dye (Thermo Fisher Scientific) was added and samples loaded on a 1% agarose gel containing ethidium bromide for detection. Gel electrophoresis was performed at constant voltage of 110 V for 30 min and DNA fragments were visualized at a UV-transilluminator (Intas Science Imaging). Expected band sizes of the excised stop cassette and uncleaved DNA segment were 720 bp and 980 bp, respectively.

2.17 *In vivo* wound healing experiment with meprin knock-out mice

In vivo wound healing experiments of meprin knock-out mice was performed by Daniel Kruppa, University of Freiburg, Germany. Meprin knock-out mice and corresponding wildtype littermates were treated with 4 µg/g Carprofen narcotized by isoflurane. For wounding, skin was shaved and excised by two skin punch biopsies of 6 mm diameter on dorsal site. Wound size was measured until full healing on day 11. For histological analyses, wound area was excised, fixed in 4% PFA/PBS and paraffin embedded. The animal experiment was permitted by corresponding authorities of Baden-Württemberg, Germany.

2.18 Histological analyses

Biopsies of dorsal and ventral skin as well as ears were excised and fixed 24h at 4°C in 4% PFA/PBS. Paraffin embedding, sectioning and subsequent azan trichrome and haematoxylin and eosin staining was performed by Katrin Neblung-Masuhr (Anatomical Institute, University of Kiel). Fontana-Masson staining was performed as described in manufacturer's protocol (Sigma-Aldrich). Tissue sections were analyzed by light microscopy (Leica DMi8 microscope). Thickness of epidermis was measured with Leica Application Suite X and mean was calculated from ten different measurements.

2.19 Immunofluorescence staining of murine tissue

Paraffin embedded tissue sections were rehydrated, boiled in 10 mM citric buffer (pH 5.5) and blocked with 5% FCS/PBS. Primary antibody was diluted in 5% FCS/PBS and applied overnight at 4°C in a dark, humid chamber. Tissue sections were washed 3 times in PBS for 5 min and incubated with secondary antibody for 2 h at room temperature. Excessive secondary antibody was removed by 3

washes in PBS. Nuclear staining was performed by 5 min incubation with 1 µg/ml DAPI/PBS, followed by 3 washes with PBS for 5 min. Stained tissue was mounted with Faramount Aqueous Mounting Medium (Dako).

Table 19: Primary antibodies used for immunofluorescence staining

Primary antibody	Species	Dilution	Supplier
HA-Tag (C29F4)	Rabbit	1:1000	Cell Signaling Technology
mMepβ	Goat	1:500	R&D Systems
α-SMA	Mouse	1:100	Dako
LF-68 (Col I, C-telopeptide)	Rabbit	1:1000	Larry W. Fisher
Melan-A (sc-20032)	Mouse	1:50	Santa Cruz Biotechnology
F4/80 (MCA497R)	Rat	1:100	Biorad
Desmoglein 1 (ab124798)	Rabbit	1:250	Abcam
Desmoglein 3 (ab14416)	Mouse	1:500	Abcam
Cytokeratin 14 (ab7800)	Mouse	1:200	Abcam
E-Cadherin	Rabbit	1:500	Abcam

Table 20: Secondary antibodies used for immunofluorescence staining

Secondary antibody	Species	Dilution	Supplier
α Rabbit IgG Alexa Fluor® 488	Donkey	1:300	Thermo Fisher Scientific
α Mouse IgG Alexa Fluor® 594	Donkey	1:300	Thermo Fisher Scientific
α Goat IgG Alexa Fluor® 488	Donkey	1:300	Thermo Fisher Scientific
α Rabbit IgG Alexa Fluor® 594	Donkey	1:300	Thermo Fisher Scientific
α Rat IgG Alexa Fluor® 594	Goat	1:300	Thermo Fisher Scientific

Images were acquired with a confocal laser scanning microscope (FV1000, Olympus).

2.20 Cytokine array

Cytokine content in murine skin was identified by Proteome Profiler Mouse XL Cytokine Array (R&D Systems). Array was incubated with 200 µg skin protein lysate of two Cre-pos + TAM mice and two control mice and further performed as described in the manufacturer's protocol. Array blots were analyzed with Analyze Particles Tool in ImageJ.

2.21 Statistical analysis

All statistical analyses were performed with GraphPad Prism 5 software for one-way ANOVA followed by Tukey post-test or two-way ANOVA followed by Bonferroni post-test. Values are expressed as mean ± SD. The null hypothesis was rejected at $P < 0.05$.

3. Results

3.1 Expression and regulation of meprin α and meprin β in murine skin

Besides kidney and intestinal epithelial cells, the metalloproteases meprin α and meprin β were found to be expressed in human epidermis as well as in the dermis of fibrotic skin (Becker-Pauly et al., 2007; Kronenberg et al., 2010). However, expression of meprins in murine skin is also crucial to investigate the role of the proteases *in vivo* in different genetic models. To date, only total meprin knock-out animals are described in literature and characterized. In these mouse models, loss of both meprin α and meprin β lead to a less thickened dermis with reduced tensile strength, mimicking an Ehlers-Danlos syndrome-like phenotype (Broder et al., 2013).

Murine skin of either meprin α-, meprin β- or double knock-out mice was excised and analyzed via RT-PCR for meprin expression on RNA level (Figure 5). Faint bands were detected in all genotypes with heterogeneous distribution. Signals were also obtained in the knock-out samples since transcription from DNA to RNA is not inhibited by addition of the knock-out cassette to gain deletion of the translated protein. In order to investigate if other members of the astacin family compensate for the loss of meprins, RT-PCR was also performed for BMP-1, Tll1 and Tll2. While BMP-1 and Tll1 expression was the strongest in the wildtype mice, no signals were detected for Tll2.

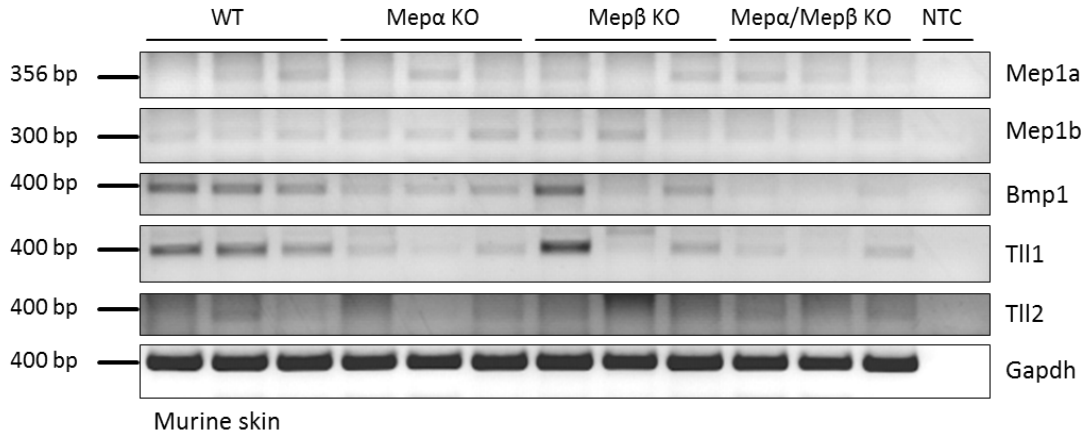

Figure 5: Expression of astacin-like proteases in murine skin.

mRNA was isolated from dorsal skin of meprin knock-out mice and wildtype littermates and transcribed to cDNA. Total amounts of astacin-like proteases gene transcripts were specifically amplified by RT-PCR and visualized by agarose gel electrophoresis. The housekeeping gene GAPDH served as loading control. NTC = non template control.

The skin consists mainly of dermal fibroblasts in the dermis and keratinocytes in the epidermis. To differentiate between these two cell types and get detailed ideas of meprin expression, cell cultures of isolated primary cells were established. RT-PCR for the astacin protease expression in dermal fibroblasts revealed stronger signals for meprin α RNA than in whole skin samples with heterogeneous distribution in all genotypes (Figure 6A). Interestingly, meprin β RNA showed highest expression in

meprin β knock-out conditions, indicating a possible feedback loop between translated protein and gene transcription. BMP-1 RNA was transcribed heterogeneously while Tll1 expression showed strong signals in all samples. Expression of Tll2 could not be observed in dermal fibroblasts. In cultured primary keratinocytes, equal results were obtained for BMP-1, Tll1 and Tll2 as in the fibroblasts (Figure 6B). Of note, RT-PCR for meprin α revealed undetectable expression of meprin α RNA in keratinocytes. Meprin β, on the other hand, was detected in the knock-out conditions and not in wildtype cells, comparable to the fibroblasts.

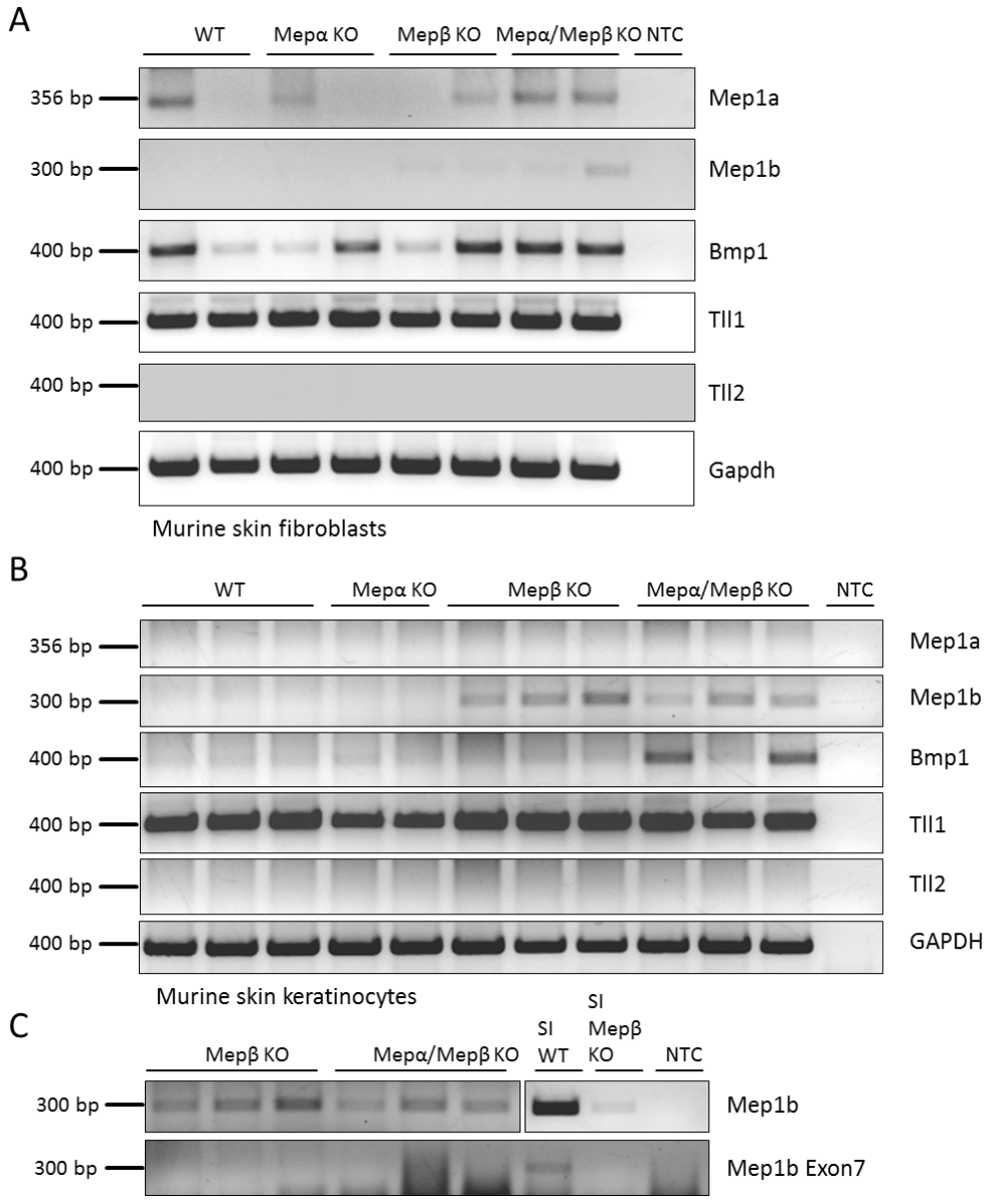

Figure 6: Expression of astacin-like proteases in primary murine skin fibroblasts and keratinocytes.

mRNA was isolated from primary murine skin fibroblasts (A) and keratinocytes (B, C) and transcribed to cDNA. Total amounts of astacin-like proteases gene transcripts were specifically amplified by RT-PCR and visualized by agarose gel electrophoresis. The housekeeping gene GAPDH served as loading control. (C) RT-PCR of meprin β deficient keratinocytes and small intestine (SI) samples using primer that flank the neomycin cassette containing exon 7 of meprin β. NTC = non template control; SI = small intestine.

To generate meprin β knock-out mice, a stop cassette was integrated into exon 7 of meprin β in the genome of mice (Norman et al., 2003). The stop cassette terminates translation of the meprin mRNA at ribosomes and leads to a shorter, incomplete protein and the gene knock-out. However, transcription of the genes and mRNA production is unaffected, leading to signals of knock-out genes in RT-PCR as observed for meprin α and meprin β in the cultured primary cells. Primer pairs were generated, spanning the exon 7 of meprin β, to exclude transcribed signals in the knock-out conditions. Indeed, only in wildtype small intestine and not in the knock-out intestine or keratinocytes, a predicted 300 bp signal was obtained (Figure 6C).

In conclusion, unlike in human skin samples, only a slight expression of meprins and BMP-1 on RNA level was detected in murine skin homeostasis while other astacin members did not compensate for loss of meprins in knock-out mice.

3.2 Meprins in wound healing and re-epithelialization *in vivo* and *in vitro*

In normal skin homeostasis, the ECM of the dermis remains in a steady state with quiescent fibroblasts and vanishingly low ECM turnover. Since meprins are able to maturate pro-collagen and other ECM related proteins and loss of meprins leads to reduced ECM deposition during skin development, they could play a role in skin wound healing. After induction of a wound, damaged tissue needs to be removed and new matrix has to be deposited by activated fibroblasts and proteases. Moreover, keratinocytes have to migrate from the wound edge to restore the epidermal barrier function, recognizable as migrating tongue.

Meprin α-, meprin β- and meprin double knock-out mice and their corresponding wildtype littermates were wounded by skin punch biopsies (performed in collaboration with Daniel Kruppa and Dr. Alexander Nyström, University of Freiburg). Wound areas were measured every second day and revealed no significant changes between all genotypes (Figure 7A). However, meprin α deficient mice showed a slight reduction in wound closure until day 5. Furthermore, day 3 wounds were cut out and analyzed in detail by histology and immunofluorescence. Staining for keratin 14, a marker of basal keratinocytes, visualized the beginning migration of keratinocytes from the wound edge to the inside of the wound (Figure 7B, C). The length of the migrating tongue was measured in all genotypes and showed reduced re-epithelialization in meprin double deficient mice (Figure 7D). Interestingly, loss of either meprin α or meprin β did not alter re-epithelialization compared to wildtype littermates, indicating a possible compensatory effect of the retained meprin during wound healing.

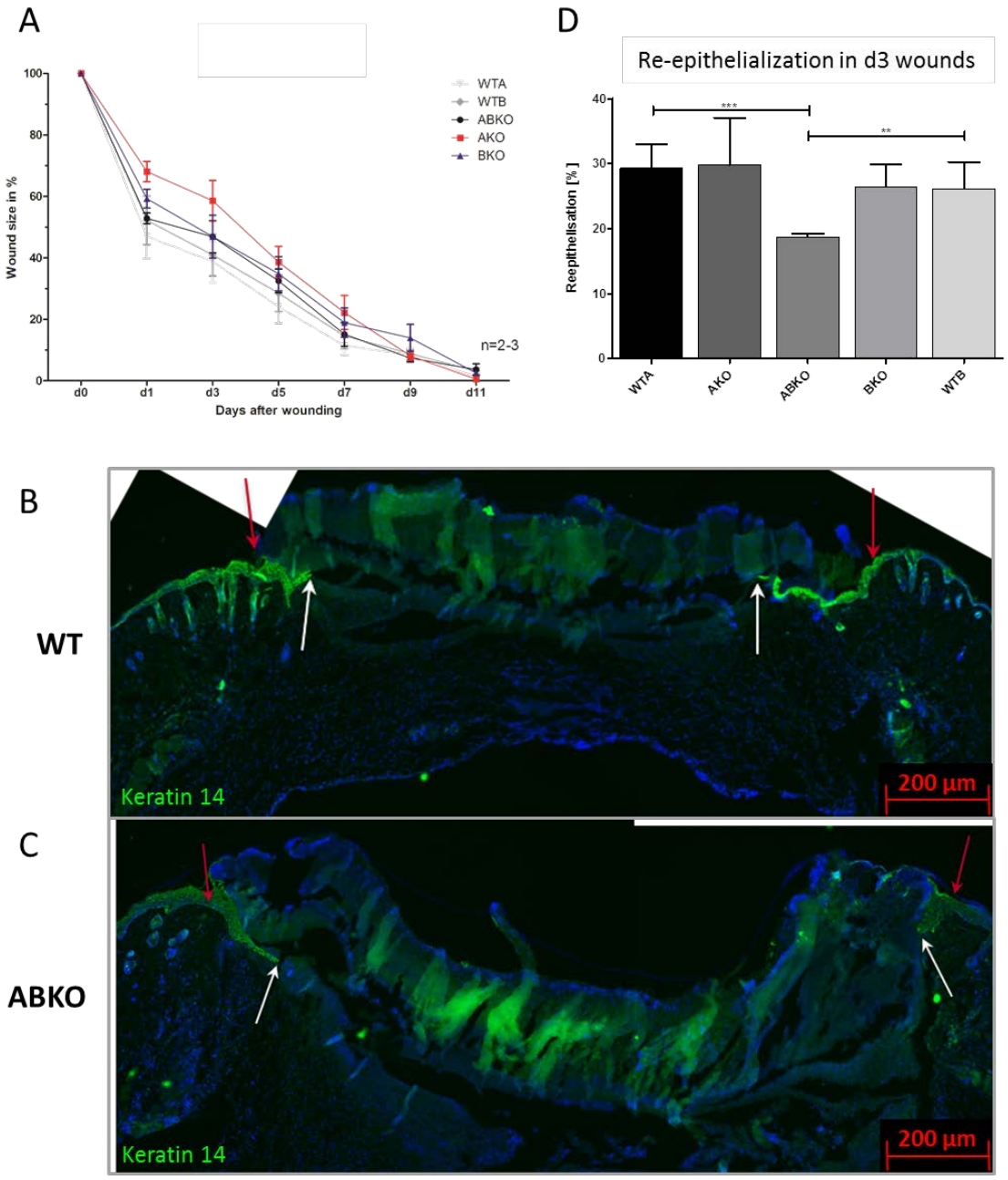

Figure 7: *In vivo* wound healing of meprin deficient mice.

Meprin α-, meprin β-, meprin double knock-out mice and corresponding littermates were wounded by punch skin biopsy. (A) Wound area of 2-3 mice per genotype was measured every second day until complete wound healing. No differences between all genotypes in wound closure properties were obtained. (B, C) Immunofluorescence staining of keratin 14 in day 3 wounds of wildtype (B) and meprin double knock-out mice (C). Red arrows indicate the wound edge and white arrows mark the migrating tongue of basal keratinocytes from the wound edge. (D) Quantification of re-epithelialization in day 3 wounds of all genotypes, indicating significantly reduced migration of keratinocytes in meprin double deficient mice (n = 3-6). WTA/B = wildtype littermates of meprin α/meprin β mice; AKO = meprin α knock-out; BKO = meprin β knock-out; ABKO = meprin double knock-out.

Since altered re-epithelialization was observed in *in vivo* wound healing studies of meprin KO mice, the role of keratinocytes in wound closure was further analyzed. Therefore, scratch assays with a keratinocyte cell line and primary keratinocytes were performed in cell culture.

First, the human keratinocyte cell line HaCaT was used in an assay supplemented with the meprin inhibitor actinonin (Figure 8A, B). After overnight serum starvation, a cross-shaped scratch was inflicted to a confluent monolayer. Cells were treated either with actinonin or DMSO control followed by microscopic imaging of the scratched areas after 0 h and 24 h. A significant change of cell migration and wound healing was obtained in actinonin-treated samples compared to the DMSO control (Figure 8B). As actinonin mainly inhibits meprin α and to a lower extent meprin β, the scratch assay was repeated using the meprin β specific inhibitor F2 (Figure 8C). Interestingly, no change in wound area closure after 24 h was observed implicating that meprin α activity might promote keratinocyte migration. As a proof of concept, HaCaT cells were treated with recombinant active meprins in different concentrations in another approach (Figure 8D, E). Addition of active meprin α decelerated cell migration in a dose dependent manner, which was significant from a concentration of 100 pM recombinant protein. Activity could be blocked by actinonin, although not to the same level as in the control samples. For active meprin β, 1 nM protein decelerated cell migration significantly which could be blocked by addition of F2 inhibitor. Here, inhibition of recombinant meprin β by F2 accelerated cell migration in comparison to the control. In conclusion, inhibition of endogenous meprins in HaCaT cells showed retarded cell migration. However, addition of recombinant active proteases had the same effects, implicating different functions of meprins in their soluble or membrane-bound form.

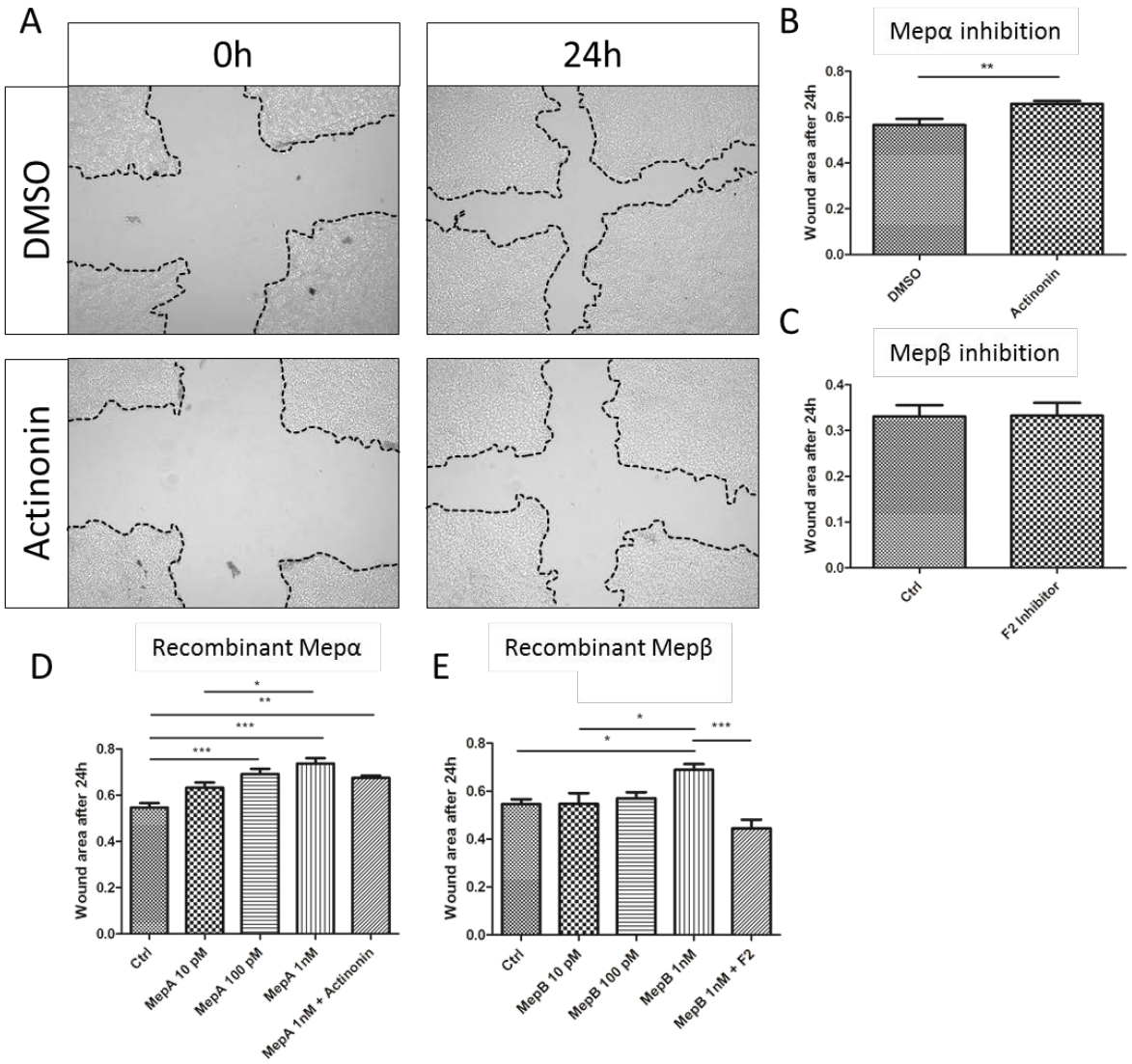

Figure 8: Scratch wound healing assay of HaCaT keratinocytes.

(A) HaCaT cells were grown to a confluent monolayer and 24 h serum starved. A cross-shaped scratch was inflicted and microscopic images were taken at 0 h and 24 h. Cells were treated with actinonin or DMSO control. (B) HaCaT cells treated with 10 µM actinonin showed significant reduced migration properties compared to DMSO-treated cells (n = 12). (C) Meprin β inhibition by addition of 100 nM F2 inhibitor showed no altered wound healing properties compared to untreated cells (n = 12). (D) HaCaT cells showed significantly reduced wound healing properties after treatment with recombinant active meprin α in a dose dependent manner. Inhibition with 10 µM actinonin reverted the effect (n = 6). (E) HaCaT cells showed significantly reduced wound healing properties when treated with 1 nM recombinant active meprin β. Inhibition with 100 nM F2 inhibitor reverted the effect (n = 6).

In order to compare the results obtained from the HaCaT cells to those of the *in vivo* wound healing, murine keratinocytes were isolated from mouse tail of each meprin knock-out model. Keratinocytes were grown to a confluent monolayer in basal keratinocyte medium, a cross-shaped scratch was inflicted and microscopic images were taken every 24 h. Interestingly, both meprin α and meprin β single knock-out keratinocytes did not show significant changes in wound healing properties compared to wildtype cells (Figure 9A, B). The double knock-out cells showed a tendency to

increased migration and proliferation in first place, however, the wound area was comparable to wildtype cells after 72 h (Figure 9C).

Conclusively, loss of either meprin α or meprin β had no obvious effect on wound closure. However, inhibition of both meprins by the inhibitor actinonin or by genetic knock-out slightly decelerate re-epithelialization and migration of keratinocytes.

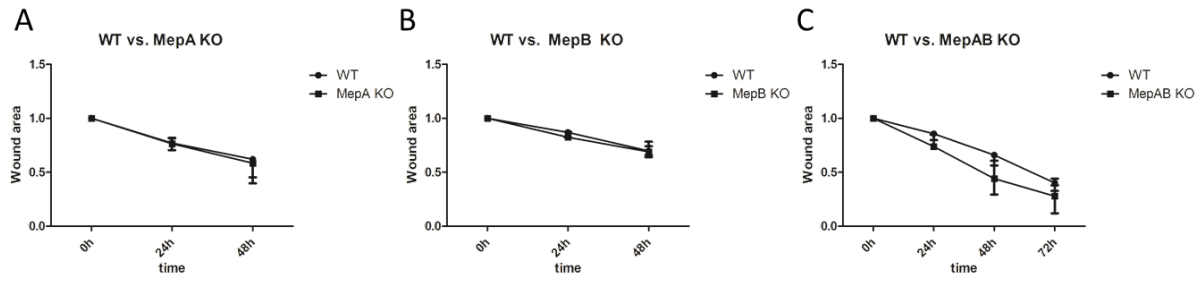

Figure 9: Scratch wound healing assay of primary skin keratinocytes from meprin deficient mice.

(A-C) A cross shaped scratch was inflicted to a monolayer of primary skin keratinocytes from (A) meprin α-, (B) meprin β-, (C) meprin double knock-out mice and corresponding wildtype mice. Wound area was measured every 24 h by bright field microscopy and analyzed using ImageJ MRI_Wound_Healing_Tool. No difference in wound healing properties was observed through the different genotypes. Data are represented as mean from 3 biological replicates with 6 technical replicates.

3.3 Meprin expression and regulation in meprin β over-expressing mouse models

Meprins were identified to be upregulated or alternatively distributed in various skin diseases like Netherton Syndrome, psoriasis and keloids (Becker-Pauly et al., 2007; Kronenberg et al., 2010). However, it is not known if meprin over-expression is a result of the disease progression or if meprin itself contributes to the onset of the disease. Therefore, mouse models with altered meprin regulation and expression could elucidate the role in pathologic conditions *in vivo*.

3.3.1 Meprin β over-expression in the Fra2 transgenic mouse model

The Fra2 transgenic mouse model was described to develop lung fibroses during a short period of time leading to pulmonary hypertension and an early death of mice (Eferl et al., 2008). Of note, Fra2 is a transcription factor of meprin β, which was identified as most highly upregulated gene in lung tissue of Fra2 transgenic mice (Biasin et al., 2014). Besides the lung phenotype, microangiopathy and skin fibrosis develop from week 12 to 16 in Fra2 tg mice resulting in systemic sclerosis (Maurer et al., 2009; Reich et al., 2010). Meprin β expression in Fra2 tg skin has not yet been investigated or associated to the developing skin pathology.

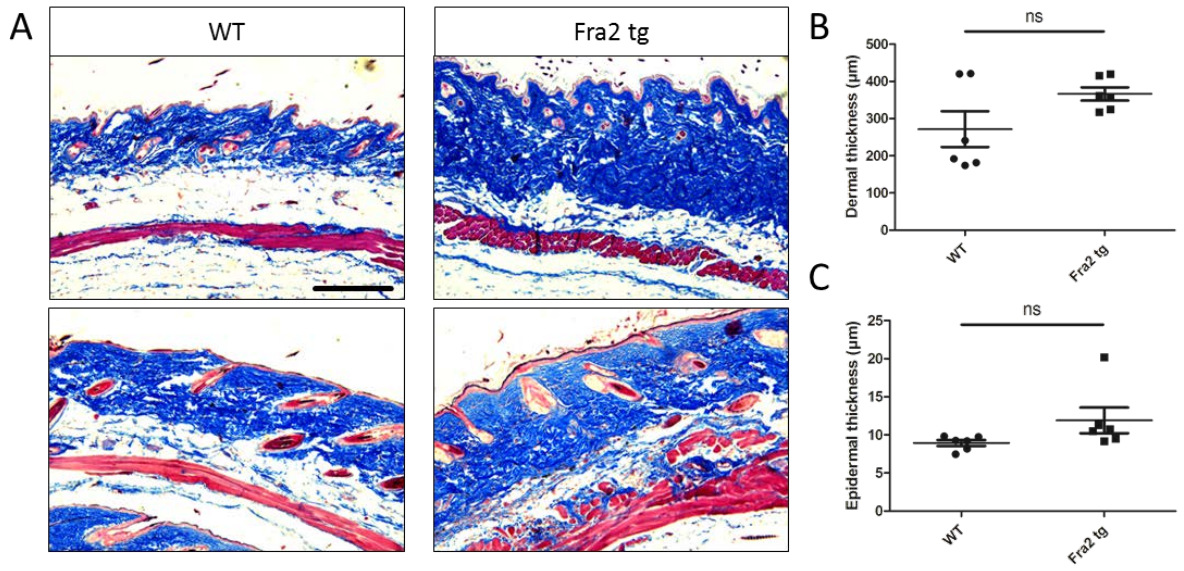

Figure 10: Developing fibrosis in dorsal skin of 15 weeks old Fra2 tg mice.

(A) Azan stained tissue sections of dorsal skin from Fra2 tg mice and wildtype littermates (scale bar = 250 µm). (B) Dermal thickness measurements of wildtype and Fra2 tg mice showed increased collagen deposition in Fra2 tg mice (n = 6 with mean of 10 measurements per tissue section). (C) Epidermal thickness measurements of wildtype and Fra2 tg mice showed enlarged epidermal layer in Fra2 tg mice (n = 6 with mean of 10 measurements per tissue section).

Dorsal skin of 15 weeks old Fra2 tg and littermate wildtype mice was excised, sectioned and stained with azan or hematoxylin and eosin (Figure 10A). Measurements of the dermis and epidermis revealed a slight increased thickness in Fra2 tg mice compared to wildtype mice, indicating a developing skin fibrosis (Figure 10B, C). Furthermore, RNA was isolated from whole skin specimens. Subsequent qPCR revealed significant over-expression of meprin β in Fra2 tg skin to up to 22000 fold compared to wildtype mice (Figure 11A). Signals for meprin α could not be observed or were out of range. The marker gene for fibrosis progression ACTA2, coding for α-smooth muscle actin (α-SMA), tended to be upregulated, and Col1a2, coding for collagen1 α2, was significantly increased (Figure 11B, C). Overall, high variability in gene expression of Fra2 tg mice was observed through all individual mice. To exclude interference of other cell types than fibroblasts in skin, murine fibroblasts were isolated from mouse tail and raised in cell culture. RNA isolation and qPCR for meprins and fibrosis marker genes were repeated. Here, meprin β reached up to 600 fold upregulation in Fra2 tg fibroblasts compared to wildtype cells (Figure 11D). Meprin α gene expression was not altered in Fra2 tg cells but showed a tendency to be downregulated (Figure 11E). On the other hand, fibrosis marker genes ACTA2, Col1a2 and TGFb1 were upregulated as observed in whole skin (Figure 11F, G, H).

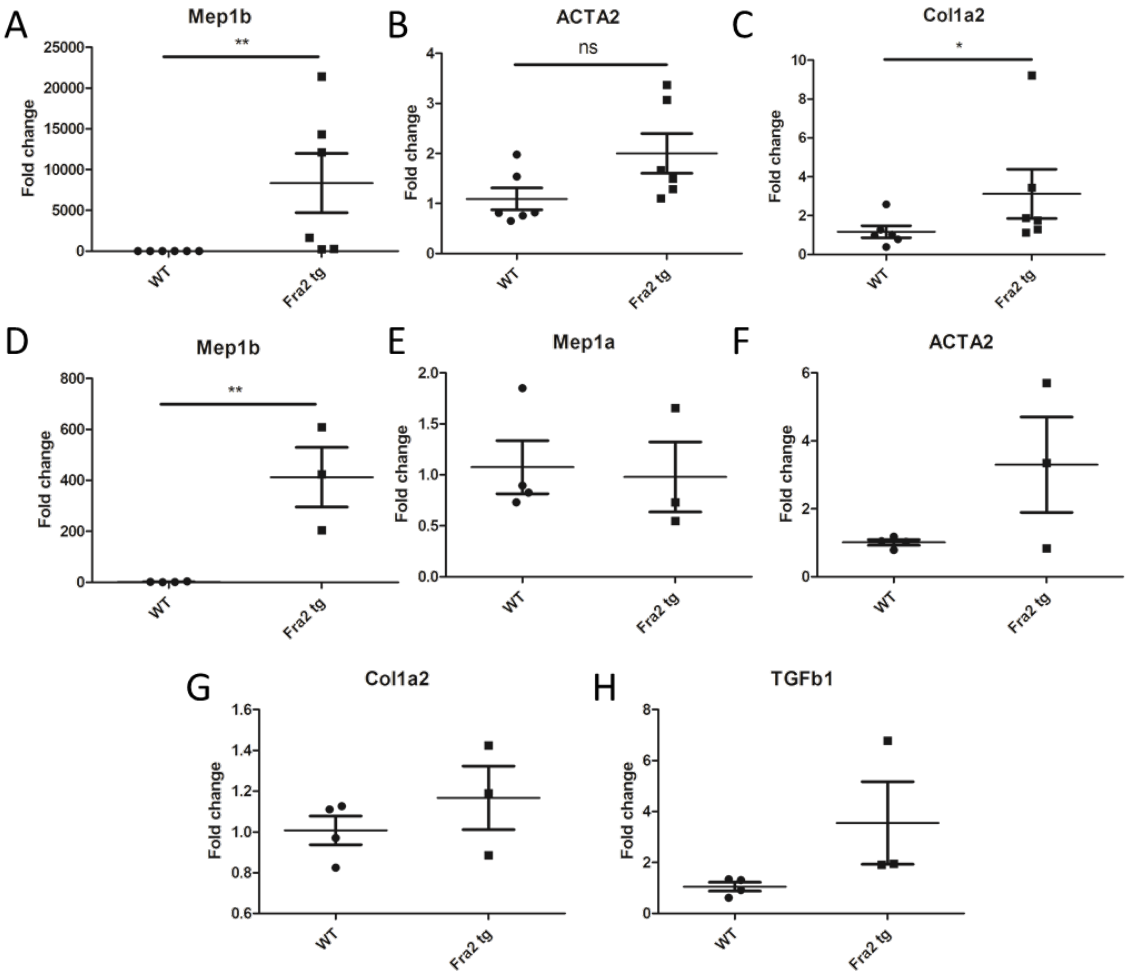

Figure 11: Relative gene expression in wildtype and Fra2 tg skin and isolated skin fibroblasts.

(A – C) Relative changes in gene expression of (A) Mep1b, (B) ACTA2 and (C) Col1a2 in dorsal skin of wildtype and Fra2 tg mice showed upregulation of Mep1b and the fibrosis marker genes ACTA2 and Col1a2 in 15 weeks old Fra2 tg mice (n = 6). (D – H) Relative changes in gene expression of (D) Mep1b, (E) Mep1a, (F) ACTA2, (G) Col1a2 and (H) TGFb1 in isolated dermal fibroblasts from wildtype and Fra2 tg mice. Mep1b, ACTA2 and Col1a2 showed upregulation in Fra2 tg cells while Mep1a expression levels were not altered (n = 3-4).

Besides Fra2, other transcription factors could regulate meprin β gene expression. For example, tissue specific transcription factors lead to transcription of meprin β in epithelial cells of the intestine and kidney. Interestingly, two different meprin β transcripts were identified, depending on tissue or cell type (Dietrich et al., 1996; Jiang et al., 2000; Matters and Bond, 1999). A larger meprin β transcript variant, meprin β', was identified in murine and human cancer cells, whose expression could be stimulated using retinoic acid or phorbol myristal acetate (PMA). The sequence of meprin β' has an elongated 5' end but differs between mouse and man. Transcription of the human form starts few base pairs upstream, resulting in a larger 5' untranslated region with no changes in protein sequence. The murine meprin β' RNA is a product of alternative splicing, having 3 unique exons that are not present in the normal meprin β transcript (Figure 12A). The translated protein has a different signal peptide and altered start of the pro-peptide. The physiological consequences with regard to stability, cellular

transport and proteolytic activity of meprin β' have not yet been investigated. Fra2 is a part of the AP-1 transcription factor complex and AP-1 transcription factor binding sites were also identified in the promoter region of meprin β. Hence, this finding raised the question, which type of meprin β transcript originates from AP-1/Fra2 promoter binding.

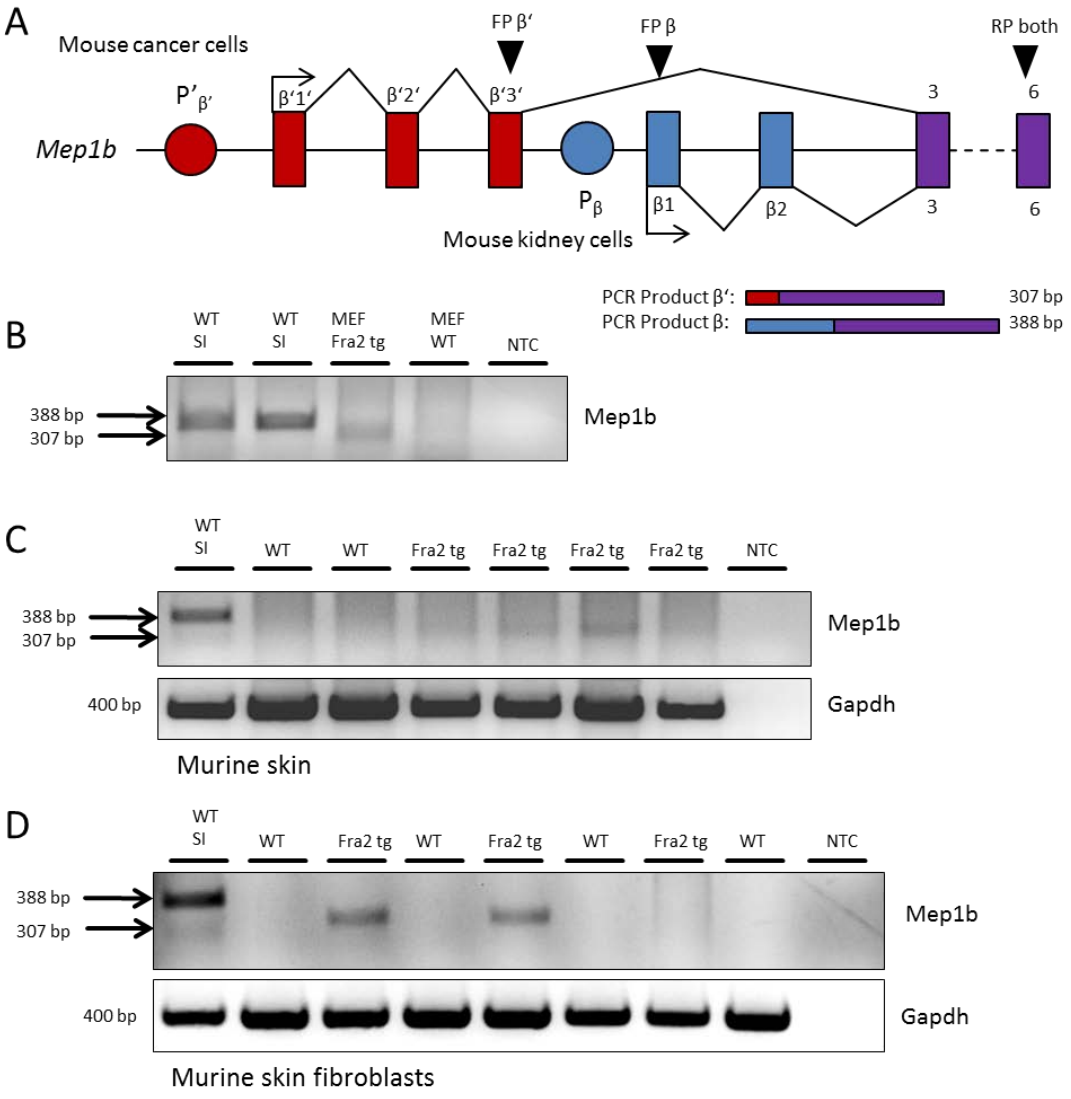

Figure 12: Alternative splicing of murine meprin β in Fra2 tg mice.

(A) Proposed mechanism of alternative splicing of murine Mep1b in mouse cancer cells and mouse kidney cells. Exons (β and β') are indicated as boxes, promoter binding sites (P and P') as circle. Binding sites of primers are marked with arrow heads. FP = forward primer, RP = reverse primer. Adapted from (Jiang et al., 2000). (B) RT-PCR for Mep1b splice variants revealed alternative splicing in Fra2 tg MEFs and normal meprin β mRNA in small intestine samples. SI = small intestine. (C) RT-PCR for Mep1b splice variants revealed production of meprin β' mRNA in skin of Fra2 tg mice. (D) RT-PCR for Mep1b splice variants showed alternative spliced meprin β' mRNA in Fra2 tg skin fibroblasts.

Total RNA was isolated from wildtype murine small intestine and Fra2 tg and wildtype murine endothelial fibroblasts (MEF). RT-PCR for meprin β and meprin β' was performed using 3 primers as indicated in Figure 12A to discriminate between both transcript variants. In murine small intestine, a

PCR product of 388 bp occurred on the gel which corresponded to the expected meprin β transcript (Figure 12B). In Fra2 tg MEFs, the PCR product of meprin β' was detected as 307 bp band while no signal was obtained in wildtype MEFs. Furthermore, RT-PCR was repeated using total RNA from Fra2 tg and wildtype skin (Figure 12C). Here, faint bands of the meprin β' transcript were detected in three Fra2 tg mice. To exclude interference of other cell types in the skin, RNA from murine fibroblasts was also determined (Figure 12D). Again, two of three Fra2 tg fibroblasts showed signals of the meprin β' transcript. Interestingly, a faint band of the 307 bp PCR product was also present in small intestine sample. In conclusion, Fra2 promoter binding leads to transcription of meprin β' in murine skin, MEFs and murine dermal fibroblasts.

3.3.2 Meprin β over-expression in KRT5 expressing cells (KRT5-Cre MB-KI)

Since over-expression of Fra2 in the Fra2 tg mouse model is not limited to certain cells and organs and Fra2 affects many other genes besides meprin β, a new mouse model was established over-expressing only murine meprin β. For this, murine meprin β cDNA was fused to a 2x HA-tag and cloned into CAGs ROSA Ires vector. Upstream of meprin β, a loxP-site flanked stop cassette prevents translation of the protein. Homologous recombination led to insertion of the meprin β construct into the Rosa26 locus of C57Bl/6N mice, which is highly accessible for transcription, leading to generation of meprin β knock-in mice (MB-KI). Meprin β knock-in mice were crossed to KRT5-Cre mice, which express a Cre recombinase upon tamoxifen treatment in keratin 5 transcribing cells (KRT5-Cre MB-KI mice). An active Cre recombinase is able to excise the stop cassette and causes subsequent meprin β translation and over-expression (Figure 13A).

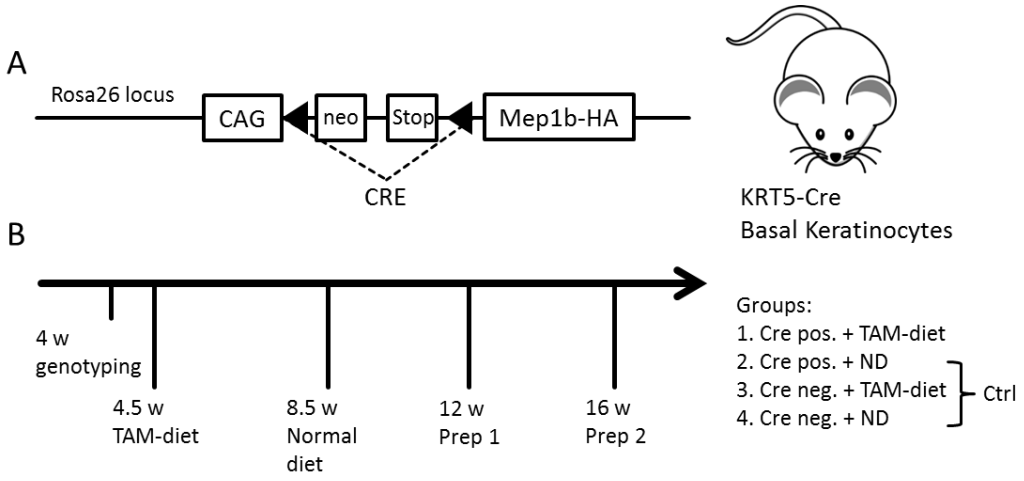

Figure 13: Cloning and integration of Mep1b in Cre mice and scheme of tamoxifen treatment.

(A) Integration of CAG-Stop-Mep1b-HA cDNA into Rosa26 locus of C57Bl/6 mice. Meprin β knock-in mice were crossed to KRT5-Cre mice for epidermis specific expression of Cre recombinase and excision of the Stop cassette. (B) Time scheme of tamoxifen treatment and preparation of mice. Mice were divided into four groups by genetic background and feeding.

KRT5-Cre positive and negative meprin β knock-in mice were genotyped and either fed a tamoxifen diet or normal diet from 4.5 weeks to 8.5 weeks of age. Mice were then sacrificed at the age of 12 or 16 weeks (Figure 13B). To validate cleavage of the stop cassette and tissue specificity of the Cre recombinase, DNA was isolated from skin, lung, heart, liver and stomach of a tamoxifen-treated and normal fed Cre positive mouse. A PCR was designed using primer that target the CAG promoter region, the meprin β inserted region and a region within the stop cassette (Figure 14A). Analysis of the PCR products revealed excision of the stop cassette only in skin of the Cre positive and tamoxifen-treated mice (Figure 14B).

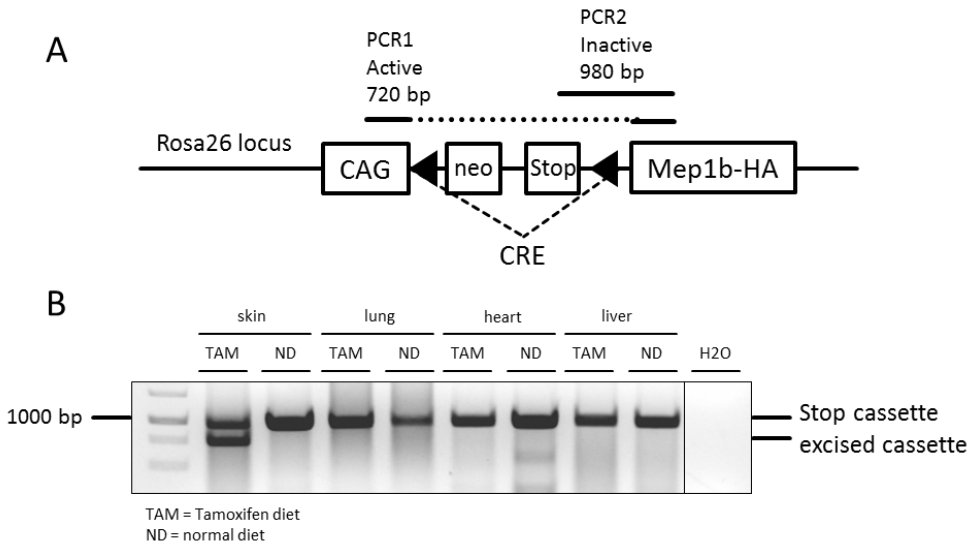

Figure 14: Activation of meprin β over-expression in skin of KRT5-Cre MB-KI mice.

(A) RT-PCR scheme for excision of the Stop cassette was performed using primers that bind in the CAG promoter, within the Stop cassette and in Mep1b. Cre activity leads to excision of the Stop cassette and amplification of a 720 bp PCR product, while an intact Stop cassette would amplify a 980 bp PCR product. (B) RT-PCR for excision of the Stop cassette in different tissues of tamoxifen- and normal chow-treated KRT5-Cre MB-KI mice. Deletion of the Stop cassette was only obtained in skin of tamoxifen-treated mice. TAM = tamoxifen diet; ND = normal diet.

After two weeks of tamoxifen diet treatment, Cre positive mice developed a reticulate pigmentation in the ears, got a darker tail and lost hair at the ventral site (Figure 15A-E). At later ages, mice lost also hair at the dorsal site, developed the reticulate pigmentation and the skin appeared scaly. Interestingly, the dermal sheet of Cre positive and tamoxifen fed mouse tails showed also an untypical reticulate pigmentation, indicating a possible pigmentary incontinence (Figure 15F). No obvious differences were observed between female and male mice.

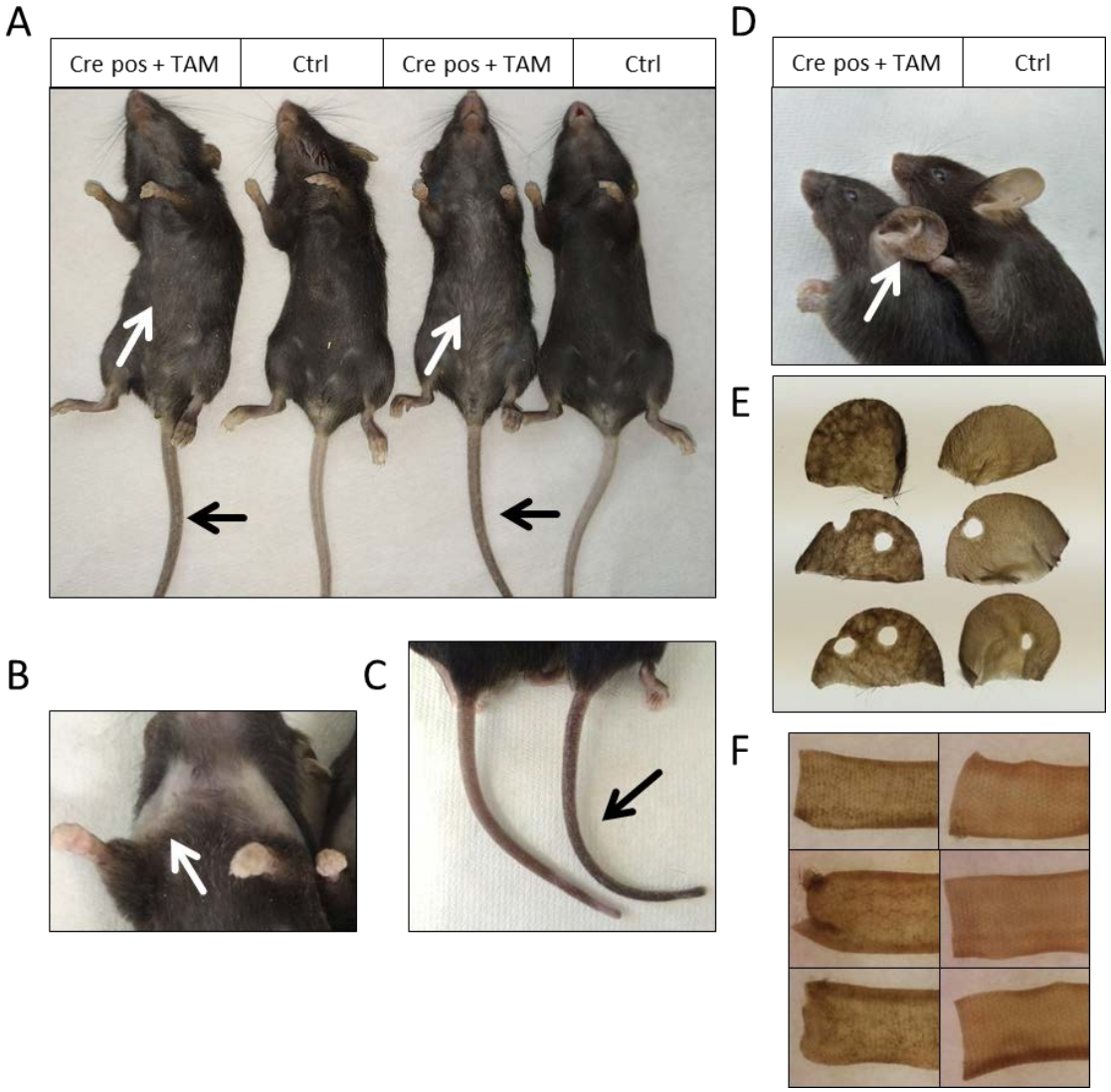

Figure 15: Pigmentary phenotype of tamoxifen-treated KRT5-Cre MB-KI mice.

(A, B) KRT5-Cre positive, tamoxifen-treated mice developed non scarring hair loss (noncicatricial alopecia) (A) on the complete ventral site or (B) on chest height (marked with white arrows). (A, C) Darker tail pigmentation was observed in KRT5-Cre positive, tamoxifen-treated mice (marked with black arrow). (D, E) KRT5-Cre positive, tamoxifen-treated mice developed a reticulate or mottled pigmentation in the ear (marked with white arrow). (F) Dermal sheet of KRT5-Cre positive, tamoxifen-treated mouse tail showed unusual reticulate pigmentation.

To further investigate the alterations in skin pigmentation, tissue sections of the ears were stained for the HA-tag of meprin β (green) and Melan-A (red), a protein involved in biogenesis of melanosomes in melanocytes (Figure 16A). Interestingly, meprin β signals were obtained sectional and were not distributed throughout the whole epidermis, possibly correlating with the reticulate pigmentation. Melanocytes were mainly observed in the dermis of the murine skin. However, the number of melanocytes appeared unaltered in all genotypes. In order to investigate whether the hyperpigmentation originated from increased melanosome biogenesis, qPCR for tyrosinase mRNA was performed, which is an enzyme that catalyzes the melanin production from tyrosine in

melanocytes. TYR tended to be slightly upregulated in tamoxifen-treated KRT5-Cre positive MB-KI mice (Figure 16B). Moreover, serial sections of dorsal skin and ears revealed elevated melanin staining in basal and cornified epidermis, which occurred both in meprin β containing and meprin β absent sites (Figure 16C, highlighted by arrow heads). F4/80 staining showed no signals for macrophages at those sites, indicating that melanosomes were transported and stored directly in keratinocytes and not in macrophages as reported for cases of pigmentary incontinence.

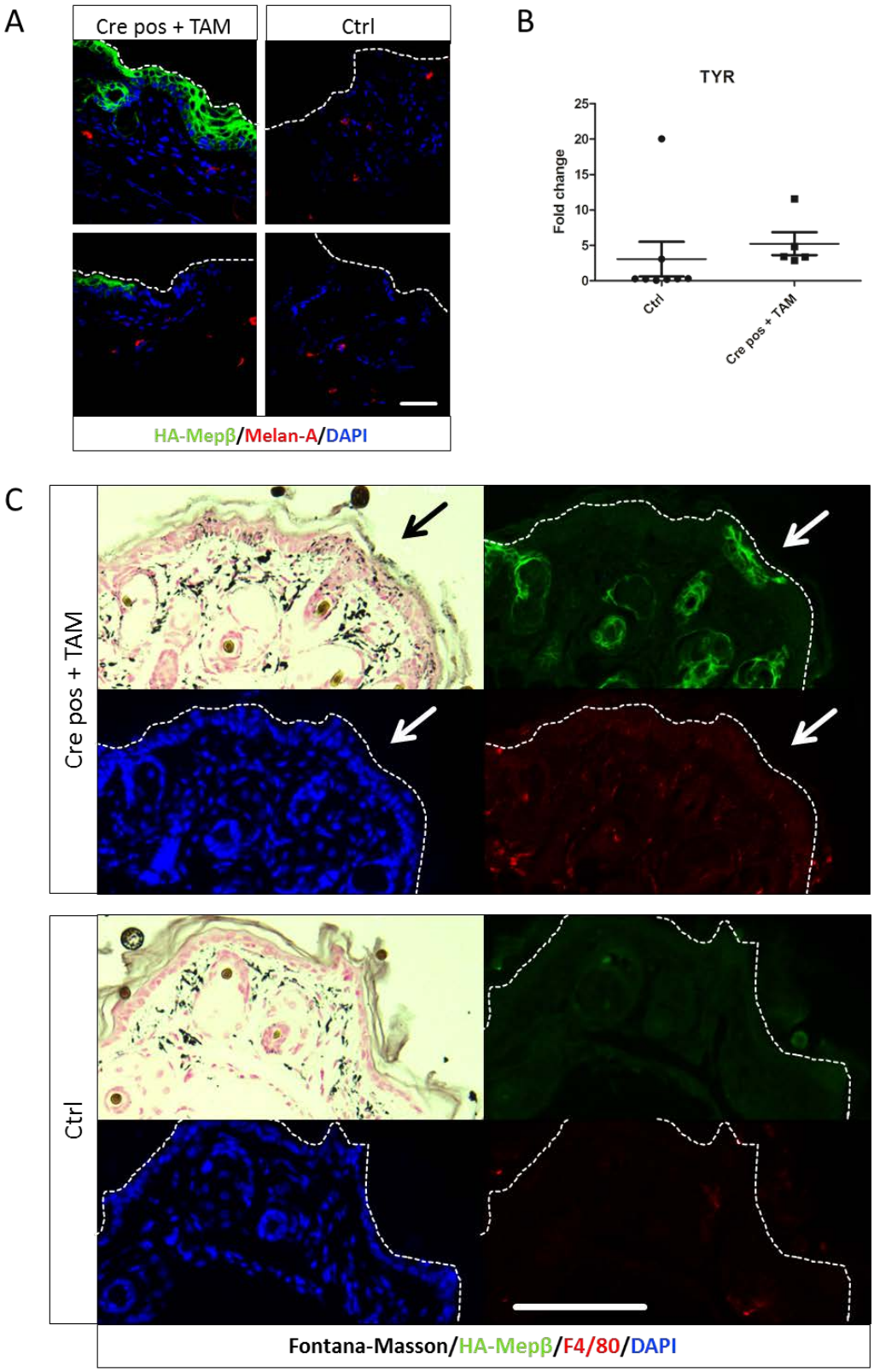

Figure 16: Elevated melanin deposition in epidermis at meprin β expressing sites.

(A) Immunofluorescence staining for HA-Tag meprin β (green) and Melan-A (red) in KRT5-Cre MB-KI ears (scale bar = 40 µm). (B) qPCR for TYR from dorsal skin revealed no difference between Cre positive and tamoxifen-treated mice. (C) Serial section of KRT5-Cre MB-KI ear stained for melanin by Fontana-Masson staining and immunofluorescence for meprin β (green) and F4/80 (red). Arrow heads highlight co-localization of melanin and meprin β (scale bar = 100 µm).

Primary keratinocytes were isolated from mouse tails for further experiments. Interestingly, less keratinocytes from Cre positive, tamoxifen-treated mice were able to adhere to the bottom of the culture dish in comparison to control cells in the first place (Figure 17A). However, subsequent cultivation of the cells revealed no difference in proliferation or adhesion. Of note, primary Cre positive cells showed a darker pigmentation compared to control cells, which was lost over few passages of cultivation, confirming the enhanced pigmentation of keratinocytes as observed in tissue sections (Figure 17B). In order to validate meprin β expression and enzymatic activity, supernatants from cultured keratinocytes were analyzed employing a specific meprin β activity assay (Figure 17C). Supernatant samples were either untreated or incubated with trypsin, to activate meprin β. Keratinocytes from Cre positive, tamoxifen-treated mice showed significant meprin β activity after trypsin activation, which could be inhibited by the meprin β specific inhibitor F2. Only little meprin β activity was observed in samples without trypsin activation, indicating low concentrations of meprin β activators in cell culture.

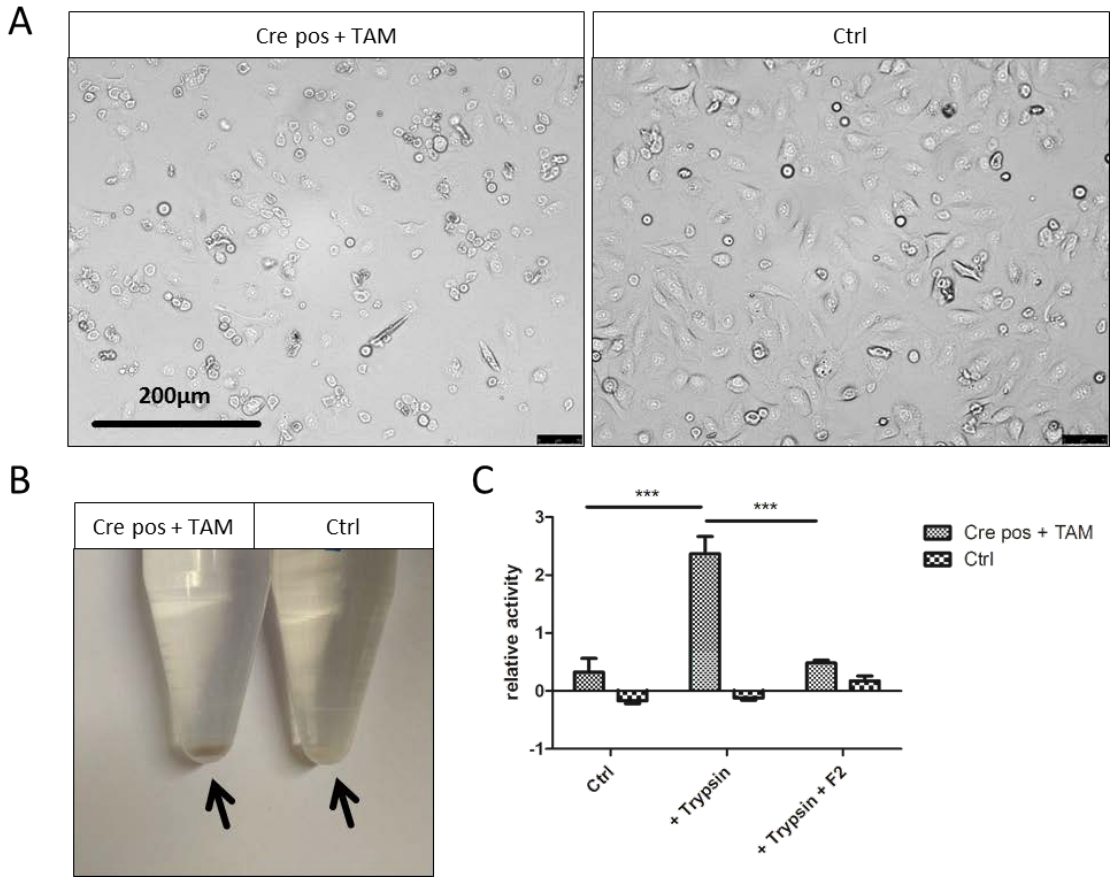

Figure 17: Morphology and meprin β activity of isolated KRT5-Cre MB-KI tail keratinocytes.

(A) Isolated tail keratinocytes from Cre positive, tamoxifen-treated mice show less viability and adhesion to collagen coated dishes compared to control cells. (B) Cell pellets from passage 1 cultivated tail keratinocytes. Cells from Cre positive, tamoxifen-treated mice appeared showed pigmentation. (C) Meprin β activity was measured in cell supernatants of Cre positive, tamoxifen-treated keratinocytes after trypsin activation and inhibited by the meprin β inhibitor F2 (n = 3).

In order to elucidate a role of meprin β in progression of hyperproliferation of keratinocytes, epidermal thickness of dorsal and ventral skin as well as in mouse ears was analyzed. Interestingly, significant thickening of the epidermis and hyperproliferation was observed in Cre positive and tamoxifen-treated mice in comparison to all control groups (Figure 18A-D). Consistent with the thickening of the epidermis, increased gene expression of cytokeratins 5, 10 and 14 could be observed, demonstrating an overall higher amount of keratinocytes in whole skin specimens (Figure 18E-G). In order to validate also increased expression of cytokeratins on protein level, Western blot analysis from whole dorsal skin was performed. Indeed, cytokeratin 14 levels showed increased expression in meprin β over-expression samples in the full length form and an additional 20 kDa C-terminal fragment appeared (Figure 18H). The signals for cytokeratin 5 were heterogeneous in all samples, with no detectable differences between the genotypes.

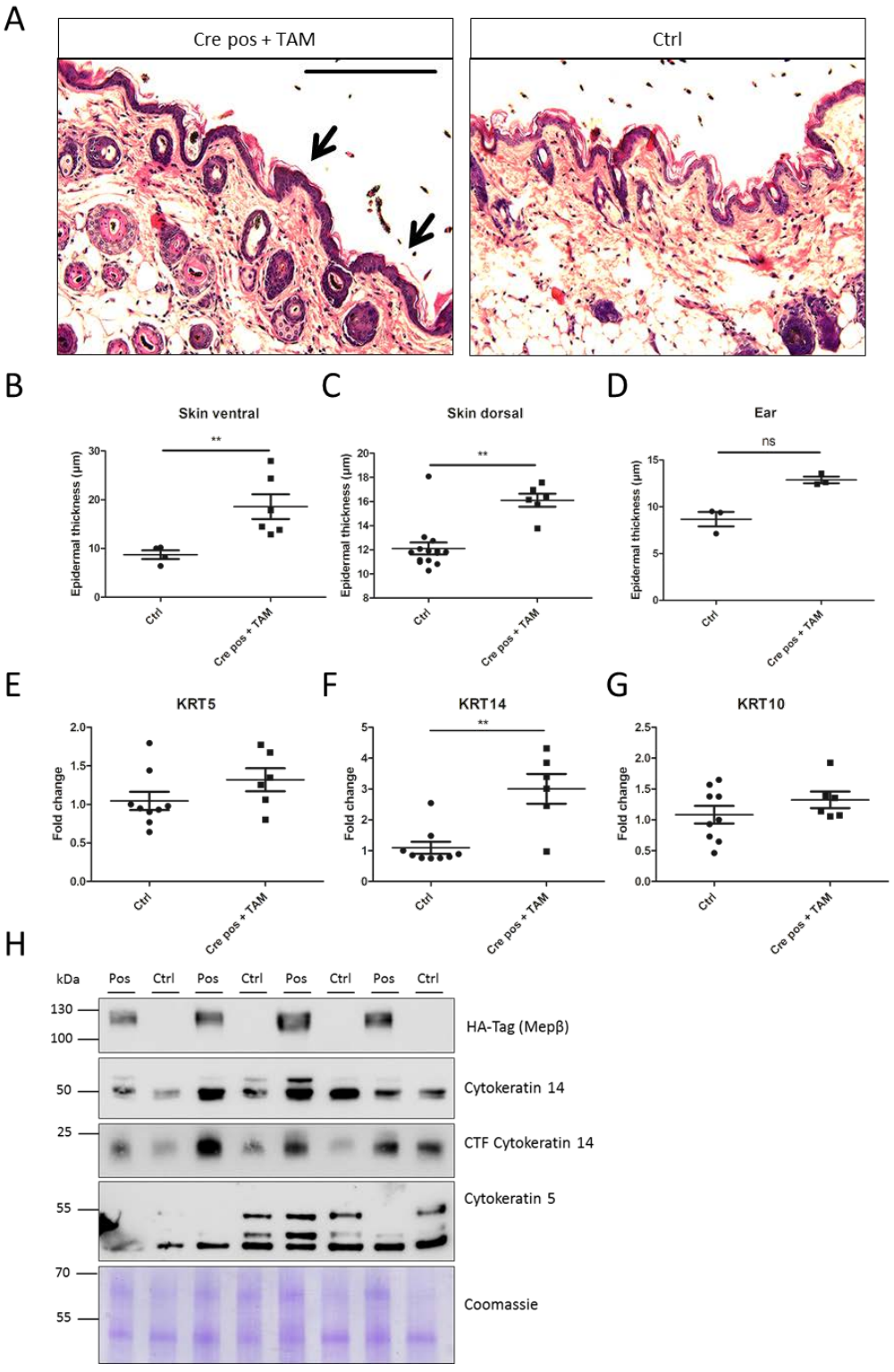

Figure 18: Meprin β over-expression in epidermis leads to hyperproliferation of keratinocytes.

(A) H&E stained dorsal skin of Cre-positive, tamoxifen-treated KRT5-Cre MB-KI mice showed thickening of the epidermis in comparison to control mice (scale bar = 200 µm). (B – D) Measurements of epidermal thickness of (B) ventral skin, (C) dorsal skin and (D) ear revealed significant thickening of the epidermal layer (each data point represents mean of 10 measurements of one biological replicate). (E – F) Relative changes in gene expression of (E) KRT5, (F) KRT14 and (G) KRT10. Expression of KRT14 was significantly increased in Cre-positive, tamoxifen-treated KRT5-Cre MB-KI mice (n = 6-9). (H) Western blot analysis of dorsal skin lysates for meprin β- and cytokeratin expression.

Adhesion molecules play a major role in anchorage of basal keratinocytes to the basal lamina as well as for their differentiation, to detach and to form the cornified envelope. Therefore, qPCR was performed to analyze gene expression of desmogleins, components of intercellular desmosome junctions. Interestingly, desmogleins 1 and 3 showed increased expression in dorsal skin of Cre positive, tamoxifen-treated mice compared to control littermates (Figure 19A, B). Of note, meprin β was shown to cleave desmogleins *in vitro* but cleavage of these adhesion molecules for keratinocyte differentiation *in vivo* remained elusive (Jefferson et al., 2013). Western blot analysis of skin lysates revealed protein levels of full length desmoglein 1 only in control samples and for desmoglein 3, a 20 kDa fragment could be observed in Cre positive, tamoxifen-treated mice, indicating possible proteolytic processes (Figure 19C). Furthermore, immunofluorescence staining for desmogleins in dorsal skin confirmed their expression in the epidermis (Figure 19D). Stronger signals for desmoglein 1 (green, upper panel) were observed in control mice as seen in the Western blot. However, co-localization of desmoglein 3 (red, middle panel) and meprin β (green, middle panel) was not visible in dorsal skin. Besides desmogleins, expression levels of other adhesion molecules and possible meprin β substrates were analyzed. E-Cadherin and meprin β showed high co-localization in hair follicles and hair shafts and increased E-cadherin expression was obtained in Cre positive, tamoxifen-treated mice by Western blot (Figure 19C, D). Of note, the *in vitro* characterized 97 kDa E-cadherin cleavage fragment produced by meprin β was more pronounced in meprin β over-expressing skin (Huguenin et al., 2008). Furthermore, staining for β1 integrin and CD99 was performed. Signals for β1 integrin increased and less cleavage fragments were observed in presence of meprin β. For CD99, the full length protein was expressed heterogeneously and no fragments of lower molecular weights occurred in Western blot (Figure 19C).

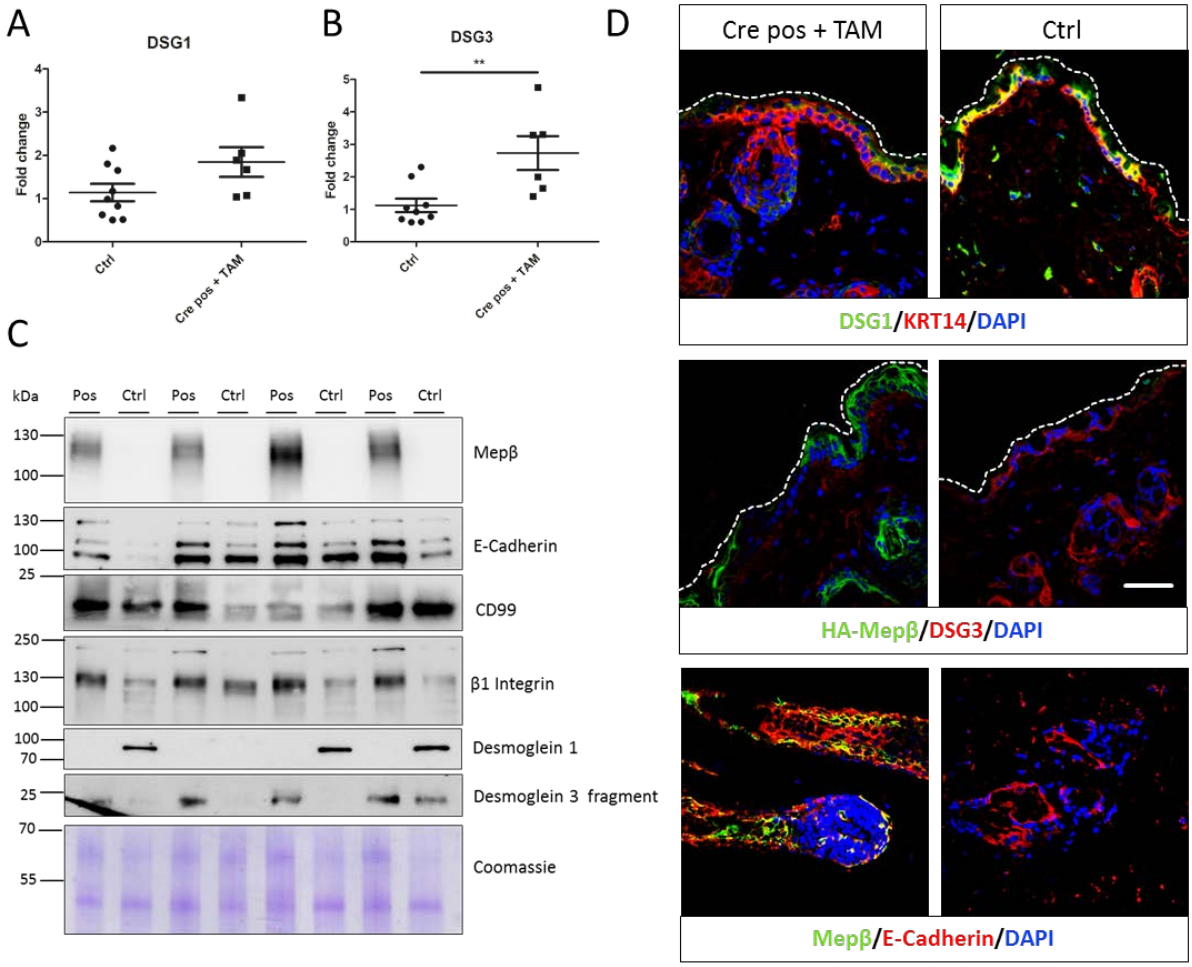

Figure 19: Meprin β over-expression in epidermis leads to increased expression of adhesion molecules.

(A, B) Relative changes in gene expression of (A) DSG1 and (B) DSG3 showed production of desmoglein mRNA in skin of Cre-positive, tamoxifen-treated KRT5-Cre MB-KI mice (n = 6-9). (C) Western blot analysis of dorsal skin lysates for meprin β- and adhesion molecule expression. (D) Immunofluorescence staining for desmoglein 1 and 3, meprin β, E-Cadherin and cytokeratin 14 (scale bar = 40 µm).

Inflammation was shown to result in hyperproliferation of keratinocytes and promotes onset of psoriasis (Nickoloff et al., 2007). Therefore, expression of inflammation related genes was analyzed from skin samples. The Langerhans cell marker CD207 as well as macrophage marker Adgre1 (F4/80) showed increased mRNA expression in dorsal skin of meprin β over-expressing mice (Figure 20A, B). This is further supported by more F4/80 positive macrophages observed in skin tissue sections (Figure 20C), associated with the upregulation of the proliferation inducer TGFβ1 and pro-inflammatory cytokines IL-18, IL-6 and IL1b (Figure 20D-G). In order to validate increasing amounts of pro-inflammatory cytokines on protein level, a proteome profiler cytokine array was performed, analyzing 111 murine cytokines simultaneously. Astonishingly, total cytokine amounts from two control and two meprin β over-expressing mice appeared rather equal (Figure 20H). Nevertheless, some proteins differed between both genotypes that were chemoattractants for inflammatory cells (CCL22, CCL11,

CCL6), proliferation stimulator of T- and B-cells (CD40) or inhibitors of angiogenesis (endostatin) and apoptosis (osteoprotegerin) (Figure 20I).

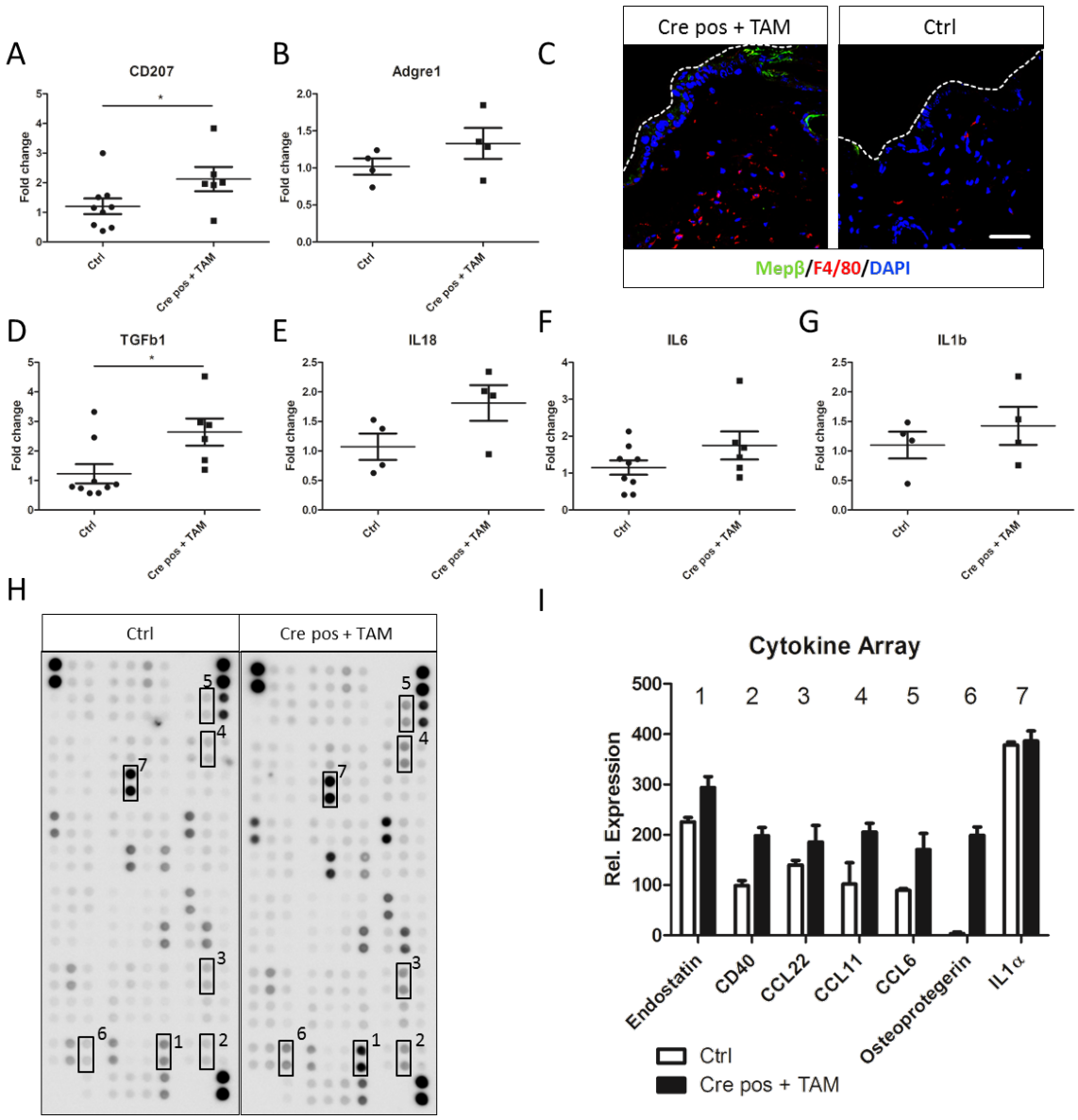

Figure 20: Regulation of inflammation related markers in KRT5-Cre MB-KI mice.

(A, B) Relative changes in gene expression of (A) CD207 and (B) Adgre1 showed increased expression of Langerhans cell and macrophage markers in skin of Cre-positive, tamoxifen-treated KRT5-Cre MB-KI mice (n = 4-9). (C) Immunofluorescence staining of dorsal skin revealed enhanced amount of F4/80 positive macrophages in meprin β over-expressing skin. (D-G) Relative changes in gene expression of (D) TGFβ1, (E) IL18, (F) IL6 and (G) IL1β showed increased expression in skin of Cre-positive, tamoxifen-treated KRT5-Cre MB-KI mice (n = 4-9). (H) Cytokine array blots incubated with skin lysate of one control and one Cre pos + TAM mouse. Selected genes for further analysis are highlighted with numbers and boxes. (I) Relative expression of selected genes from cytokine array of two control and two Cre pos + TAM mice. Numbers can be linked to boxes in (H) (n = 2).

In conclusion, meprin β was specifically over-expressed in epidermis and hair follicle of KRT5-Cre positive mice leading to hyperproliferation of keratinocytes and a pigmentation phenotype. However,

meprin β expression appeared only partially, which influenced pigmentation, adhesion molecule cleavage and probably inflammation at particular sites in the skin. The obtained phenotype probably resembles the rare syndromes Dermatopathia Pigmentosa Reticularis (DPR) and Epidermolysis bullosa simplex with mottled pigmentation and noncicatricial alopecia (MP-EBS) that originate from cytokeratin 5 and 14 loss-of-function mutations (Belligni et al., 2011; Nagai et al., 2016).

3.3.3 Meprin β over-expression in Col1a2 expressing cells (Col1a2-Cre MB-KI)

Dermal expression of meprin β was only detectable in human fibrotic skin and not in normal skin homeostasis (Kronenberg et al., 2010). Additionally, being highly expressed in fibrotic skin of Fra2 mice, meprin β might contribute to progression or initiation of dermal fibrosis. To overcome side effects and dysregulation of other genes in the Fra2 mouse model, direct over-expression of meprin β was induced as described in 3.3.2. Meprin β over-expressing mice were crossed to Col1a2-Cre mice, which express a Cre recombinase after tamoxifen treatment in collagen1α2 transcribing cells (Figure 21A). Therefore, direct over-expression of meprin β in murine dermis could be studied with regard to altered ECM deposition and fibrosis development *in vivo*.

Col1a2-Cre positive and negative meprin β knock-in mice were genotyped and either fed a tamoxifen diet or normal diet from 4.5 weeks to 8.5 weeks of age. At the age of 12 weeks, mice were sacrificed and activity of the Cre recombinase analyzed in different tissues by using PCR for excision of the Stop cassette (Figure 14A). Faint bands of the excised Stop cassette were observed in skin and stomach of Cre positive and tamoxifen-treated mice (Figure 21B). However, low PCR efficiency was obtained from some biopsies. Further validation of skin samples of six different mice revealed Stop cassette excision only in Cre positive mice (Figure 21C).

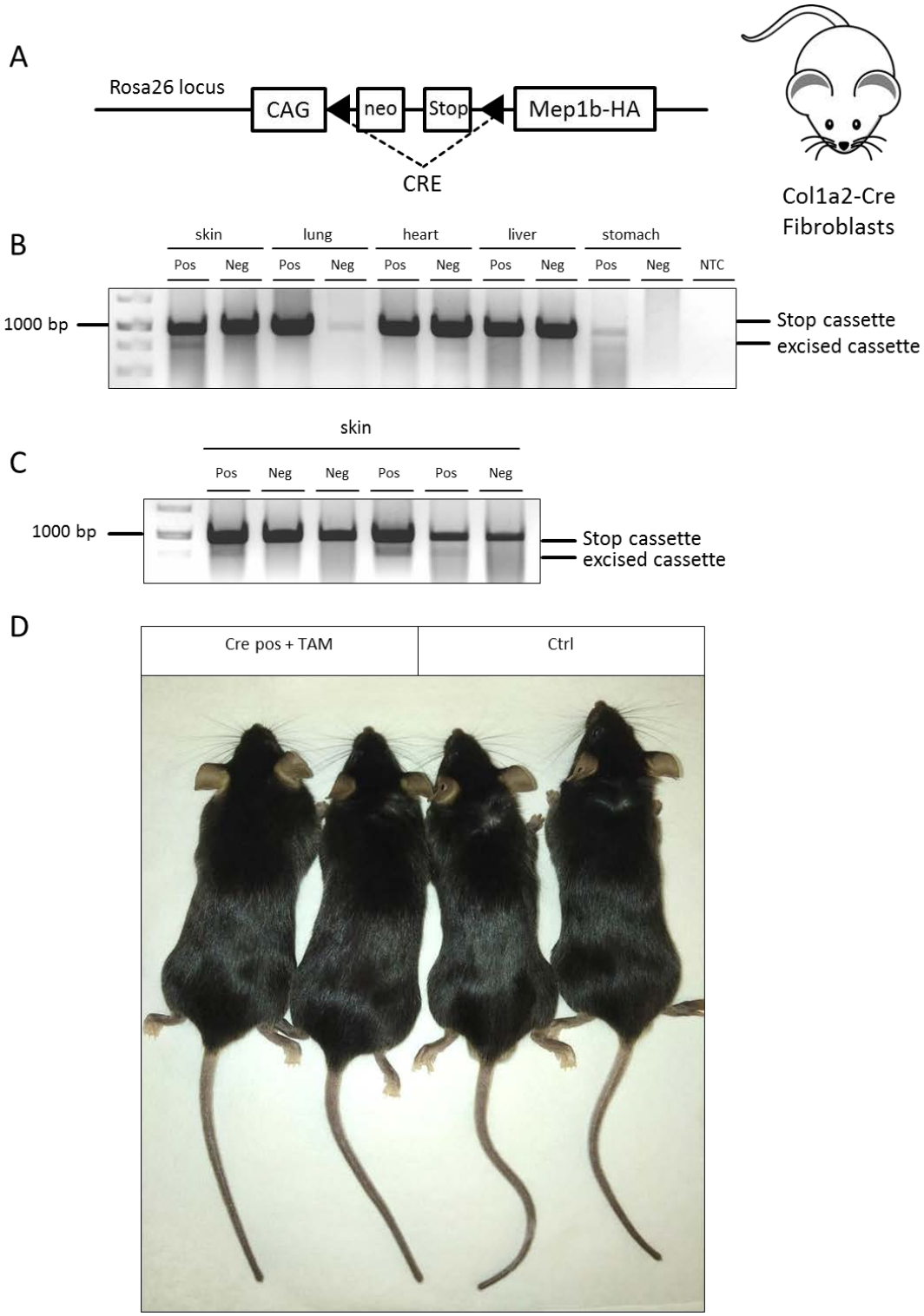

Figure 21: Activation and phenotype of meprin β over-expression in Col1a2-Cre MB-KI mice.

(A) Integration of CAG-Stop-Mep1b-HA cDNA into Rosa26 locus of C57Bl/6 mice. Meprin β knock-in mice were crossed to Col1a2-Cre mice for dermis specific expression of Cre recombinase and excision of the Stop cassette. (B) RT-PCR for excision of the Stop cassette in different tissues of tamoxifen-treated Col1a2-Cre positive and negative MB-KI mice. Deletion of the Stop cassette was only obtained in skin of Cre positive and tamoxifen-treated mice. Pos = Cre positive; Neg = Cre negative. (C) RT-PCR in skin of Col1a2-Cre positive and negative MB-KI mice revealed PCR fragments of excised Stop cassette in Cre positive mice. (D) No obvious phenotype differences were observed in 12 weeks old, tamoxifen-treated Col1a2-Cre MB-KI mice.

In comparison to KRT5-Cre MB-KI mice, Col1a2-Cre MB-KI did not show an obvious phenotype during and after tamoxifen treatment. At 12 weeks of age, fur and pigmentation of sacrificed mice appeared normal and no difference in skin thickness was observed (Figure 21D). Dorsal skin was excised and analyzed via Azan and H&E staining. Thickness and density of the collagen layer showed no apparent variation between Cre positive, tamoxifen-treated mice and the control groups (Figure 22A). In order to validate over-expression of meprin β on protein level, immunofluorescence staining of skin was performed. Indeed, meprin β could be detected in the dermis via its C-terminal HA-tag and via a specific antibody, however in a lower amount (Figure 22B, C). Co-localization with collagen1 and the fibrosis marker α-smooth muscle actin (α-SMA) was not detectable and their amount in the skin biopsies appeared unaltered. For better quantification of protein amounts, dorsal skin was grinded in a mortar, lysed and analyzed by immunoblot. Meprin β was detectable with an HA-Tag antibody and specific meprin β antibody in Cre positive, tamoxifen-treated mouse samples as 125 kDa band (Figure 22D). Immunoblot staining for collagen1α1 C-telopeptide resulted in equal amounts of maturated collagen I in the skin of all mice, however, less collagen was present in female samples. The same effect was seen with an antibody against the C-pro-peptide of collagen I where equal amounts of cleaved pro-peptide were present within the genders. Staining for α-SMA appeared only in few samples with heterogeneous expression through all individual samples, consistent with the immunofluorescence staining of tissue sections.

Conclusively, meprin β was specifically over-expressed in the dermis of Col1a2-Cre positive mice. However, obvious changes towards a developing skin fibrosis were not observed in 12 weeks old mice.

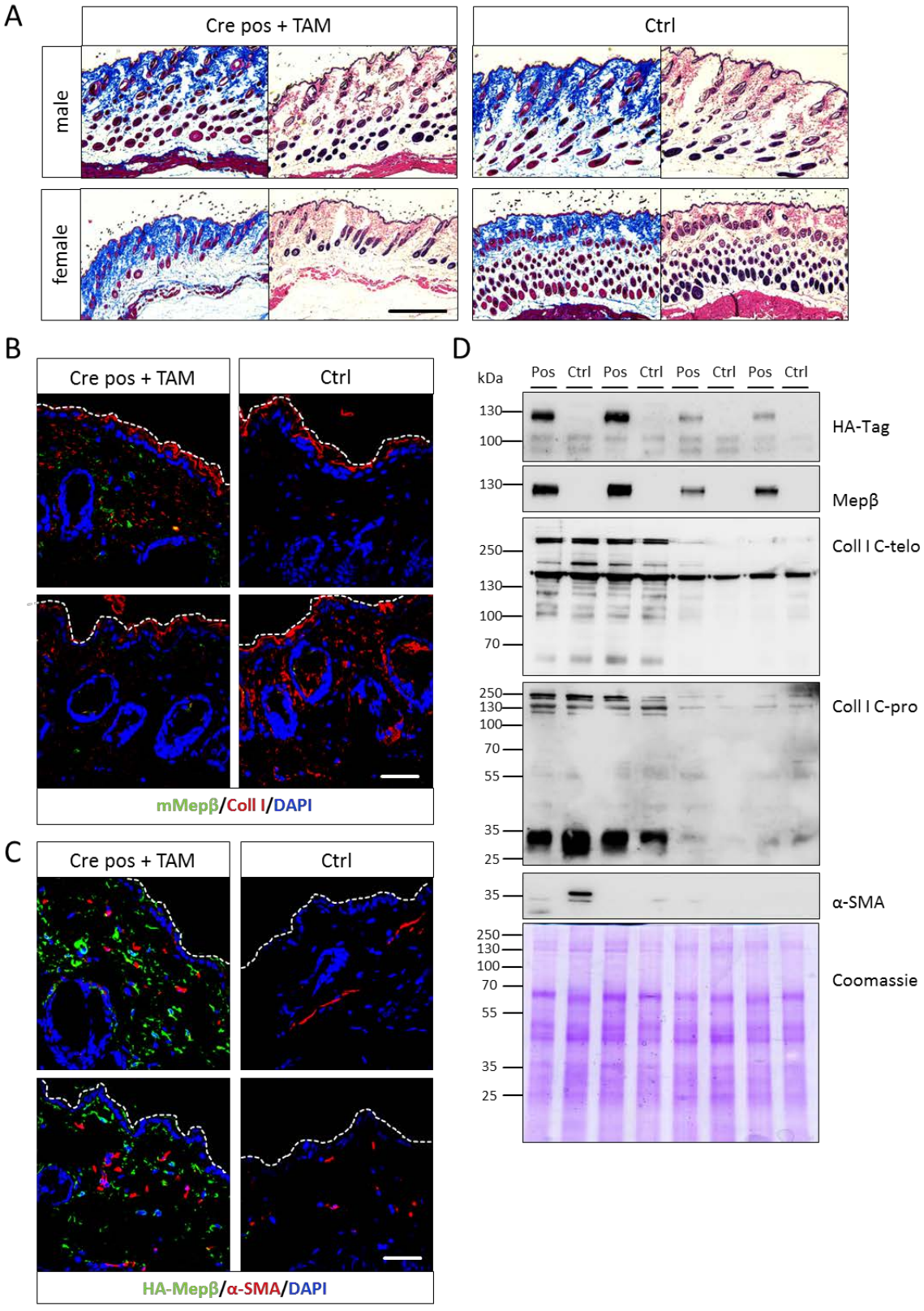

Figure 22: Analysis of skin sections and lysates of Col1a2-Cre MB-KI mice.

(A) Azan (left panel) and hematoxylin and eosin staining (right panel) of dorsal skin sections from 12 weeks old Col1a2-Cre MB-KI mice and control littermates. (B) Immunofluorescence staining for meprin β (green) and collagen I C-telopeptide (red) in dorsal skin sections of Col1a2-Cre MB-KI mice. Expression of meprin β was obtained in Cre positive mice and signals for collagen I were heterogeneously distributed. (C) Immunofluorescence staining for HA-meprin β (green) and α-

SMA (red) in dorsal skin sections of Col1a2-Cre MB-KI mice. Strong meprin β expression was observed in dermal fibroblasts that did not co-localized with α-SMA containing myofibroblasts. (D) Western blot analysis from dorsal skin lysates of Col1a2-Cre MB-KI mice. Meprin β over-expression was obtained in Cre positive samples. Total amounts of collagen I and cleaved C-pro-peptide were unaltered between the genotypes, however reduced in samples of female mice.

3.4 Cleavage of CD99 by meprin β mediates cell migration of inflammatory cells and cancer cells

Migration of immune cells is crucial in order to reach all regions of a tissue and to get excess to potential inflammatory sites. Immune cells circulate in the vascular system and have to overcome the endothelial barrier. Adhesion molecules and their shedding from cell surfaces by proteases play a major role for the process of transendothelial migration (TEM). The adhesion molecule CD99 was identified as potential meprin β substrate in a proteomics approach, namely terminal amine isotopic labeling of substrates (TAILS) (Jefferson et al., 2013). The type I transmembrane protein CD99 is expressed on both endothelial cells and cells of the hematopoietic system and forms homophilic interactions between both cell types during TEM. Hence, cleavage of CD99 by meprin β might promote extravasation of migrating cells into tissue.

First, a potential processing of CD99 by meprin β was analyzed by incubation of recombinant CD99 with active recombinant meprin β. Subsequent mass spectrometry analysis revealed that meprin β was able to cleave CD99 at several sites within highly conserved regions of acidic amino acids, accordantly to the preference of meprin β for negatively charged amino acid residues. Furthermore, co-expression of meprin β and CD99 in HeLa cells confirmed cleavage of CD99 at the cell surface, resulting in two C-terminal fragments that were further processed by the γ-secretase within the transmembrane region (Figure 23A, B). Interestingly, meprin α was not able to shed CD99 from the cell surface, both in single transfection and expressed in the meprin enzyme complex (Figure 23C). In order to investigate the potential influence on cell migration, an *in vitro* TEM assay was performed. Endothelial bEnd.3 cell were seeded onto transwells to form a confluent monolayer. Afterwards, migration of CFSE labelled Lewis lung carcinoma cells (LLC) was measured in presence or absence of recombinant active meprin β. Meprin β was able to induce permeability of the endothelial monolayer and promoted transmigration of LLCs. To further prove the *in vivo* relevance of CD99 shedding by meprin β, CD99 expression was investigated by histology and Western blot in lungs of wt and meprin β knock-out mice. Interestingly, meprin β deficient mice exhibited increased levels of CD99. As a proof of concept, wt mice showed accumulated CD99 in lungs after daily injection of the meprin inhibitor actinonin for one week, indicating processing of CD99 by meprin β *in vivo*.

Conclusively, CD99 was confirmed as substrate of meprin β *in vitro* and *in vivo*. Shedding of CD99 resulted in two C-terminal cleavage fragments that were further processed by the γ-secretase, producing a smaller fragment that might have intracellular regulatory functions. Furthermore, cleavage of homophilic CD99 interaction diminished cell adhesion and promoted TEM (Figure 23D; this was published in (Bedau et al., 2017a) and is attached as appendix 1).

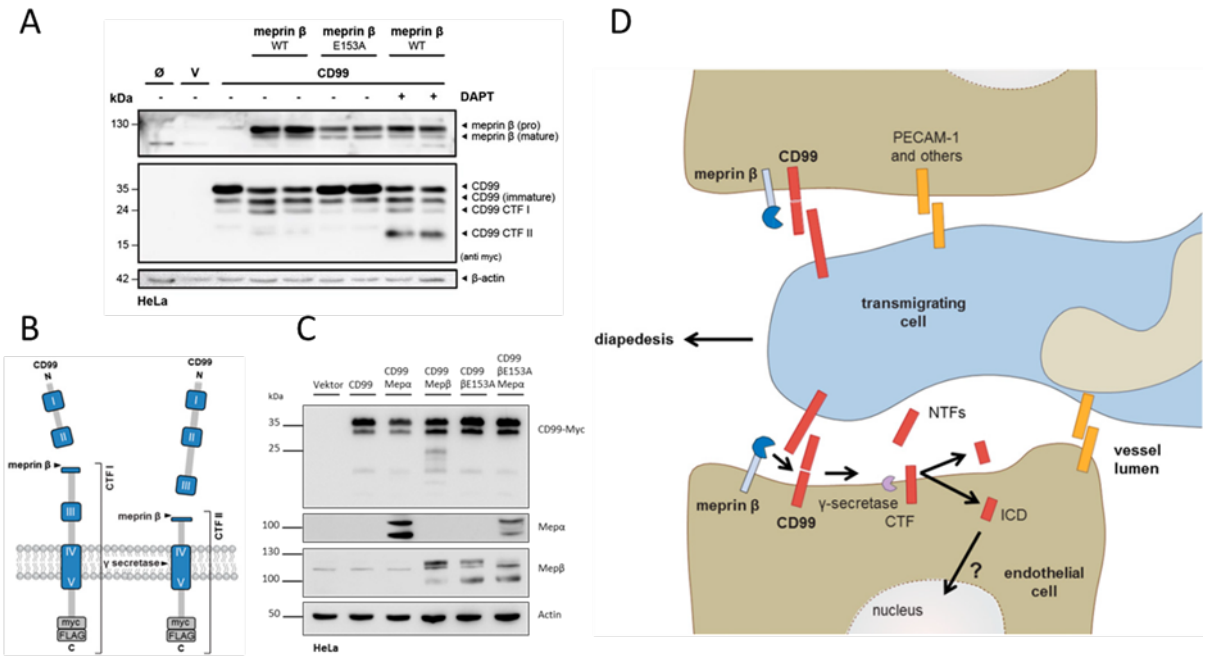

Figure 23: Cleavage of CD99 by meprin β diminishes cell adhesion and promotes transendothelial cell migration.

(A) Co-transfection of meprin β and CD99 in HeLa cells showed processing of CD99 and production of two CTFs that were further cleaved by the γ-secretase complex. (B) Schematic representation of the C-terminally tagged CD99 within the plasma membrane. Arrowheads indicate cleavage sites of meprin β and γ-secretase that lead to production of CTF I and CTF II. (C) Co-transfection of CD99 with meprin α did not lead to cleavage of CD99 and CTF generation. (D) Schematic model of CD99 cleavage by meprin β and γ-secretase on endothelial cells, promoting transendothelial migration. (A, B, D) Adapted from (Bedau et al., 2017a), appendix 1. (C) Adapted from (Peters et al., *in press*) appendix 4.

The role of CD99 shedding by meprin β *in vivo* was further analyzed by an acute inflammation model (air pouch) in meprin β knock-out and wildtype mice. Inflammation was induced by a dorsal air pouch followed by injection of carrageenan (Figure 24A). Interestingly, meprin β deficiency led to decreased inflammatory cell number in the pouch lavage in comparison to the control group, demonstrating a crucial role for meprin β in cell extravasation (Figure 24B).

Besides inflammatory cells, CD99 could also be found on cancer cells. High CD99 expression is a hallmark of certain cancer cells like Ewings sarcoma (Ambros et al., 1991; Fellinger et al., 1991). Additionally, meprin β expression could be found in primary and metastatic sites of pancreatic neuroendocrine tumors and might promote metastasis of cancer cells through cleavage of CD99 (Carr et al., 2013; Maitra et al., 2003). Two databank annotated CD99 mutations of lung squamous cell carcinoma (p.D92H) and lung adenocarcinoma (p.D92Y) were analyzed with regard to meprin β cleavage and cell migration. Of note, the mutated Asp92 is located at the P1' position within the meprin β cleavage site, leading to generation of the CTF II. Loss of CD99 cleavage by meprin β might alter cell migration ability and therefore be disadvantageous for the tumor cell. The mutated CD99 variants were co-transfected with meprin β in HeLa cells. Western blot analysis revealed cleavage of

CD99 by meprin β and production of the CTF II in all CD99 variants (Figure 24C). Subsequent mass spectrometry analysis identified a shift of the cleavage site to Asp94, two amino acids C-terminal of the mutated site at Asp92. Additionally, the D92H variant of CD99 showed significantly increased cell migratory potential compared to wildtype form. In order to investigate downstream signaling of CD99 shedding by meprin β, phosphorylation of Src kinase was analyzed via Western blot. The full-length isoform of CD99 was described to inhibit Src phosphorylation and thereby decrease anchorage-independent growth, migration and metastasis of tumor cells (Scotlandi et al., 2007). Interestingly, transfection of each CD99 variant did not alter Src phosphorylation in osteosarcoma U2-OS cells (Figure 24D). However, treatment of these cells with recombinant active meprin β increased pSrc levels independently from CD99.

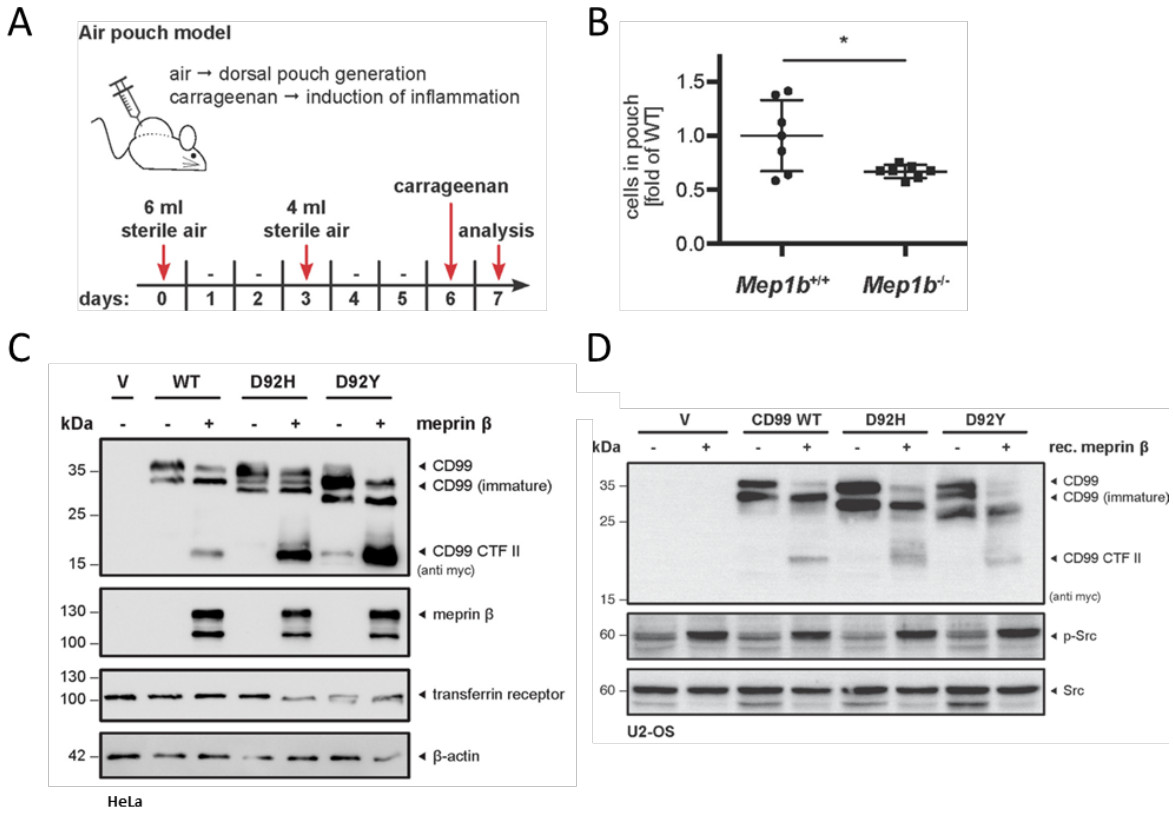

Figure 24: Meprin β mediates inflammatory cell migration *in vivo* and enhances Src phosphorylation.

(A) Air pouch model for induction of acute inflammation in meprin β deficient mice and wildtype littermates. Six days after subcutaneous injection of sterile air, administration of carrageenan into the dorsal air pouch induces immune cell infiltration. Pouch lavage was isolated 24 h later. (B) Total cells in pouch lavage were counted and normalized to wildtype. Cell infiltration was significantly reduced in meprin β deficient mice. (C) Cancer-associated mutations in the meprin β cleavage site of CD99 do not alter generation of CTF II. (D) Treatment of U2-OS cells with recombinant meprin β enhances phosphorylation of Src kinase. Adapted from (Bedau et al., 2017b), appendix 2.

Overall, extravasation of inflammatory cells was shown to be dependent on meprin β presence in an *in vivo* acute inflammation model. Moreover, cancer-associated mutated variants of CD99 could still be cleaved by meprin β by a shifted cleavage site and D92H variant exhibited increased migratory

potential. Phosphorylation of Src kinase was not altered after over-expression of CD99 in cell culture, as reported before (Scotlandi et al., 2007). Interestingly, presence of meprin β increased pSrc, thereby potentially promoting pro-tumorigenic activity of malignant cells (this was published (Bedau et al., 2017b) and is attached as appendix 2).

3.5 Expression and localization of meprins can change in certain pathological conditions and alters cell migration and gene expression

The localization of proteins is strictly regulated by their signal peptide or localization sequences within the amino acid sequence, which guides the translated protein to its place of destination. Proteins with a transmembrane domain mainly remain in membrane compartments, while soluble proteins are secreted, cytosolic or stay in cellular organelles. Cellular polarization and sorting of proteins to either apical or basolateral sites of a cell is of high scientific interest because missorting could promote or arise from developing pathologies. Meprin proteases are mainly found at apical sites of cells, e.g. in the luminal part of kidney or intestinal epithelial cells. However, missorting of meprins to the basolateral site was observed during acute renal ischemia reperfusion (Trachtman et al., 1995), glomerulonephritis (Oneda et al., 2008) and in tumor stroma (Lottaz et al., 1999), demonstrating a switch from physiological to pathological activity of meprins. Due to its inserted domain, meprin α is shed by furin on the secretory pathway and secreted into the extracellular space (Marchand et al., 1995). Interestingly, meprin α could also be found on cell surfaces of epithelial cells, indicating possible interactions of soluble meprin α with membrane resident proteins that could alter function of the protease.

Apical localization of meprin α was observed in lung epithelial cells and pulmonary arteries of donors and idiopathic pulmonary arterial hypertension (IPAH) patients. However, increasing amount of circulating soluble meprin α was measured in the plasma of IPAH patients (Figure 25A). In *in vitro* binding experiments, recombinant meprin α was able to bind to isolated donor human pulmonary artery endothelial cells (hPAEC) in a concentration dependent manner, which could be reduced by treatment with heparinase I (Figure 25B) or was impaired in CHO cells deficient for glycosaminoglycan (GAG) or heparan sulphate. Moreover, confocal microscopy of lung sections confirmed a co-localization of meprin α and heparan sulphate on the extracellular-luminal site (Figure 25C) and less expression levels of heparan sulphate could be observed in pPAECs of IPAH patients that showed reduced absorption of recombinant meprin α (Figure 25D). In order to unravel the role of membrane localized meprin α in epithelial cells, epithelial barrier function of hPAECs was investigated in presence or absence of meprin α. hPAEC monolayer was activated with LPS and treated with active meprin α. After subsequent addition of isolated neutrophils from the blood of healthy donors, changes in electrical impedance were measured. While LPS treatment decreased epithelial barrier function and led to invasion of neutrophils, meprin α significantly impaired migration

of neutrophils (Figure 25E). As a proof of concept, hPAECs were pre-treated with heparinases to remove heparan sulphate and to prevent meprin α binding to the cell surface. Indeed, neutrophil migration was slightly abolished in a short time interval, demonstrating a role for membrane bound meprin α in immune cell invasion through endothelial barriers (this was published in (Biasin et al., 2018) and is attached as appendix 3).

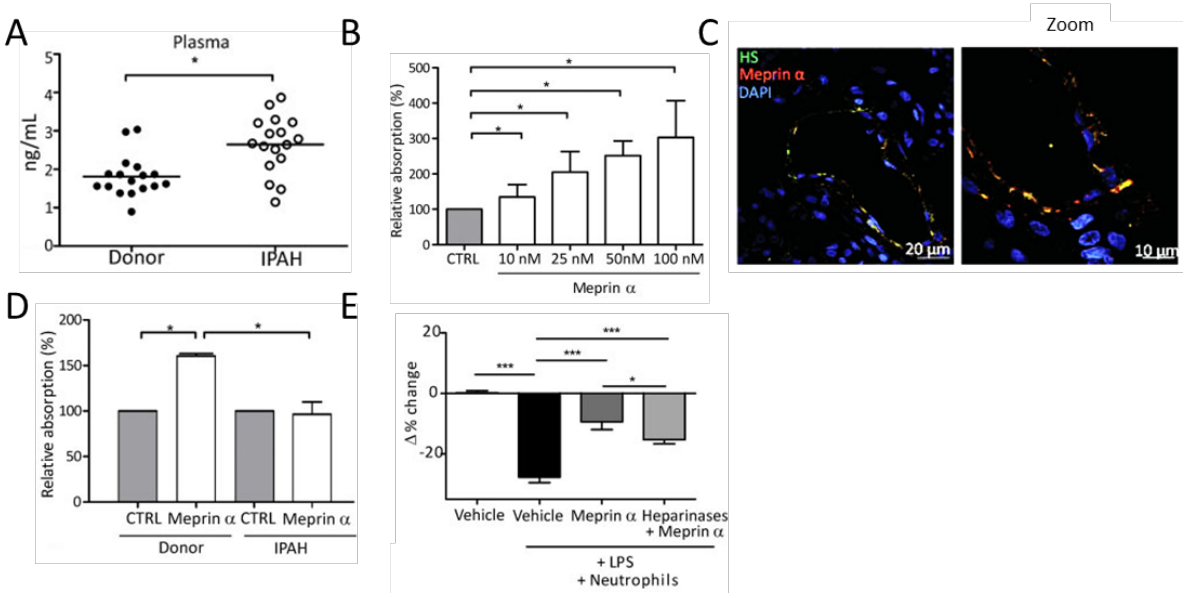

Figure 25: Meprin α binds to heparan sulphate in pulmonary artery epithelial cells and mediates immune cell migration.

(A) Significantly elevated levels of soluble meprin α were measured in plasma of IPAH patients. (B) Recombinant meprin α was able to bind to hPAECs in a dose dependent manner (n = 6, data are shown as mean ± SD). (C) Immunofluorescence staining for meprin α (red) and heparan sulphate (green) of a donor lung section revealed co-localization of both proteins. (D) Significant binding of 100 nM recombinant meprin α to donor and not IPAH hPAECs (n = 3, data are shown as mean ± SD). (E) Addition of meprin α to LPS activated hPAECs reduced neutrophil invasion by increased electrical resistance compared to vehicle. Pre-treatment of hPAECs prevented meprin α binding and promoted neutrophil invasion (n = 3). Adapted from (Biasin et al., 2018), appendix 3.

Besides heparan sulphate, meprin α can also bind to meprin β. Shortly after discovery of meprins, it became evident that meprin α and meprin β can form a heterodimer in mice and rat when co-expressed in the same tissue (Johnson and Hersh, 1992; Marchand et al., 1995). This is important to investigate, since formation of a meprin enzyme complex might have impact on meprin β shedding and activation on the cell surface. For instance, membrane bound meprin α might be able to be activated and could cleave substrates on the cell surface, which are not accessible in its soluble form.

In order to elucidate the interaction of human meprin α and meprin β, both proteases were expressed in HeLa cells. An additional meprin α fragment of 100 kDa was observed in lysates of co-transfected cells (Figure 26A, marked with an asterisk) and the mature, fully glycosylated meprin β fragment showed reduced molecular weight in presence of meprin α. Immunoprecipitation of one of the

proteases from cell lysates confirmed a direct interaction of human meprins as reported for the rodent isoforms. By mutagenesis of the intermolecular disulfide-bridge forming cysteine C305 (meprin β) and C308 (meprin α) to a serine in the MAM domain of both proteases, dimerization of meprins could be prevented. Based on the solved crystal structure of human meprin β homodimer (PDB code 4gwm) (Arolas et al., 2012), a homology model of the meprin enzyme complex was generated (Figure 26B). Of note, all interaction sites of the meprin β homodimer were also found in the heterodimer. Furthermore, an additional salt-bridge could be formed between R578 (meprin α) and E270 (meprin β) and a hydrogen bond between D201 (meprin α) and S257 (meprin β), indicating potentially increased stability of the enzyme complex compared to the homodimers. Next, localization and assembly of the meprin enzyme complex were further analyzed. Biotinylation experiments revealed an interaction on the cell surface that tethered the soluble 100 kDa meprin α fragment to the plasma membrane. However, connection of the proteases occurred already in the ER, which could be observed by treatment of cells with Brefeldin A, a potent inhibitor for the transport from the ER to the Golgi apparatus. To shed light on the previously observed shift of the mature meprin β within the enzyme complex, protein deglycosylation was performed. Removement of attached sugar residues revealed that the shift was a product of altered glycosylation and not of proteolysis at the N- or C-terminus of meprin β. Interestingly, the shift was also present in co-transfection with the cysteine variants and might not result from enzyme complex formation (Figure 26A). In order to investigate if glycosylation itself had an impact on heterodimer formation, transfected HeLa cells were treated with glycosylation inhibitors that prevent maturation of sugar trees in the ER (Kifunensine) and in the Golgi apparatus (Swainsonine). Immunoprecipitation of meprins showed differentially glycosylated proteases that still formed a heterodimer. Human meprin β possesses 8 potential N-linked and 4 O-linked glycosylation sites. Two N-linked glycosylation sites were mutated by disruption of the Asn-X-Ser/Thr consensus sequence at position N370, T372, N547 and T549. Of note, loss of the attached sugar residue at position N547 resulted in inappropriate folding of the enzyme and therefore had crucial function for the stability of meprin β (Figure 26C). In contrast, loss of the sugar residue at position N370 had no effect on meprin β maturation. However, molecular shifts appeared both in the ER- and maturated form. Next, the functional properties of each meprin within the heteromeric complex were analyzed. Both meprin proteases can be activated by tryptic proteases on the cell surface or in the extracellular space by cleaving off the inhibitory pro-peptide (Grünberg et al., 1993; Johnson and Bond, 1997; Ohler et al., 2010). It was questionable whether the heterodimer might have an impact on the activation of each monomer. Therefore, meprin activity was measured on cell surfaces and in cell supernatants using specific fluorogenic peptides for meprin α or meprin β. While activation of meprin β by the bacterial protease RgpB on the cell surface was not altered in presence of meprin α, membrane bound meprin α itself could also be activated by RgpB on the plasma membrane which could lead to cleavage of so far unknown membrane bound substrates (Figure 26D). However, cleavage of the amyloid precursor protein (APP) and the adhesion molecule CD99, both well

described substrates of meprin β, did not occur by membrane bound meprin α. Although both meprins have a common preference for negatively charged amino acids around the scissile bond (Becker-Pauly et al., 2011), substrates might differ between both proteases within the enzyme complex. Noteworthy, both meprin α and meprin β activities increased within the heterodimer in the cell supernatant while neither expression nor shedding of the complex was increased (Figure 26E). Finally, the biological relevance of the meprin heterodimer should be elucidated *in vivo*. The absence of meprin α on the apical site of intestinal epithelial cells could be observed in meprin β deficient mice (Figure 26F). Additionally, intestine lysates showed the glycosylation shift of meprin β and an altered fragment pattern of meprin α, in accordance with the previous human *in vitro* data. In human and murine gut, absence of meprin α was associated with a higher risk for inflammatory bowel disease (IBD) progression (Banerjee et al., 2009; Häsler et al., 2017). Therefore, the potential role of altered meprin α localization on gene regulation with regard to IBD should be investigated. Comparison of transcriptome analyses of wildtype, meprin α- and meprin β knock-out mice revealed changes in regulation of gene subsets when meprin α was located on cell membranes or in the intestinal lumen or when meprin α was totally absent.

In summary, the human meprins form disulfide-linked heterodimers when co-expressed, which leads to a plasma membrane localization of meprin α and changes in posttranslational modifications (Figure 26G). Furthermore, meprin α can be activated on the cell surface but was not able to cleave known meprin β substrates. However, the meprin enzyme complex exhibited enhanced stability and increased activity of each meprin monomer. Additionally, transcriptome analyses revealed changes in gene subsets depending on localization of meprin α, demonstrating the physiological relevance of the meprin enzyme complex (this was published in (Peters et al., *in press*) and is attached as appendix 4).

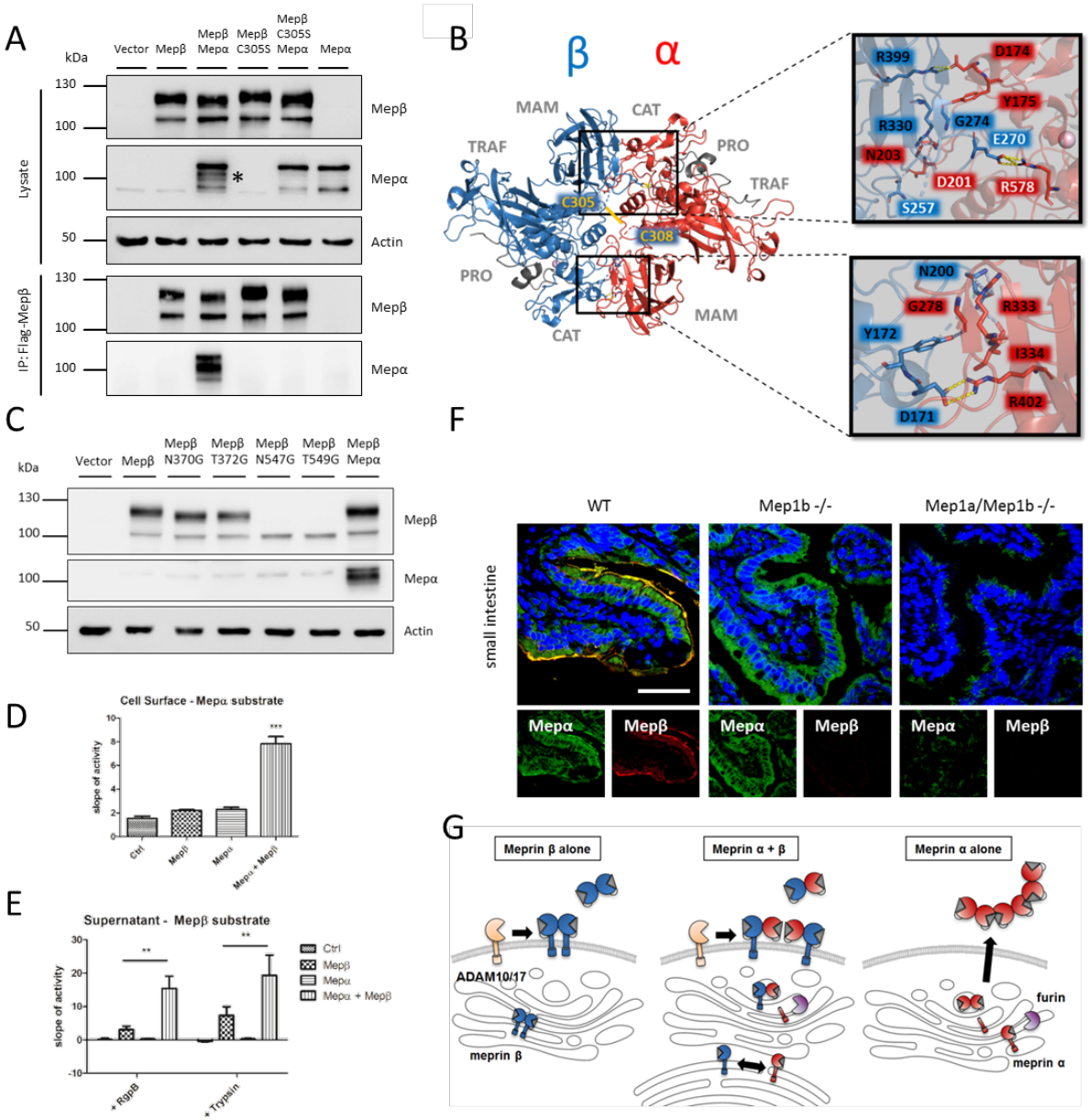

Figure 26: Meprin α and meprin β form an enzyme complex that tethers meprin α to the cell membrane and alters gene expression.

(A) Co-immunoprecipitation of transfected meprin α with meprin β or meprin β C305S in HeLa cells revealed disulfide linkage and altered posttranslational modifications of both proteases. (B) Homology model of the meprin enzyme complex with interacting amino acid residues. The approximate position of the intermolecular disulfide bond between C305 and C308 of the heterodimer is highlighted via a yellow line. (C) Mutation of glycosylation site N547 in meprin β led to inappropriate folding and ER retention of the protease. (D) Membrane bound meprin α could be activated by RgpB within the meprin enzyme complex on the cell surface (n = 3). (E) Shed meprin β showed significantly increased activity within the meprin enzyme complex in cell supernatants (n = 3). (F) Co-immunofluorescence staining for meprin α (green) and meprin β (red) in small intestine sections of wildtype, meprin β knock-out and meprin double knock-out mice. Surface staining of meprin α in endothelial cells was not obtained in meprin β deficient mice. (G) Meprin β is shed by ADAM10/17 on the plasma membrane in single transfection and in the meprin enzyme complex. Meprin α is processed by furin on the secretory pathway and secreted into the extracellular space. Tethered to meprin β in the heterodimer, meprin α requires shedding of meprin β. Adapted from (Peters et al., *in press*) appendix 4.

4. Discussion

4.1 Expression and localization of meprins regulate ECM turnover and cell migration

Since discovery of meprin metalloproteases in different species, ongoing identification of substrates *in vitro* and *in vivo* sheds light on their role within the proteolytic web in various tissues. A well suitable model for understanding the biological function of a protein is the generation of knock-out mice. For example, if a target protein is involved in embryonic development, its absence may cause defects in organogenesis or could result in prenatal lethality. In case of meprin α and meprin β, knock-out mice are viable and show no obvious phenotype compared to wildtype mice (Banerjee et al., 2009; Norman et al., 2003). However, dermal thickness in skin is reduced and showed less tensile strength, less collagen deposition and an Ehlers-Danlos syndrome-like phenotype (Broder et al., 2013). A more important role for meprins emerged through pathology-associated mouse models. DSS-treated meprin α knock-out mice were more susceptible to inflammation and intestinal injury compared to littermates (Banerjee et al., 2009). In line with this, reduced mRNA expression of meprin α was observed in inflamed mucosa of patients suffering from Crohn's disease (CD) or ulcerative colitis (UC), highlighting a possible protective role of meprin α for the onset of disease (Banerjee et al., 2009; Häsler et al., 2017). An anti-inflammatory function of meprin α was further shown in human pulmonary artery endothelial cells (hPAEC), where binding of meprin α to heparan sulphate prevented infiltration of inflammatory cells (Biasin et al., 2018). However, in contrast to the protective role in IBD, meprin α impaired the integrity of the endothelial monolayer of hPAECs, which could also coincide for meprin α being located at the plasma membrane in an enzyme complex with meprin β. Since meprin β can be shed by ADAM proteases from the cell surface (Herzog et al., 2014; Wichert et al., 2017), the release of meprin α from endothelial cells in an enzyme complex would be a regulated process by limited proteolysis that could restore barrier integrity in IBD. Interestingly, meprin β knock-out mice were rather protected from injury after DSS-induced colitis, indicating that expression of meprin α might prevent IBD progression, when the enzyme is not tethered to the epithelium (Banerjee et al., 2011). Both, the anti-inflammatory function and the impairment of the endothelial layer by meprin α, point towards a tightly regulated mechanism in which substrate availability, different cell types and localization of the enzyme have a crucial impact on the enzymes function. This could be further strengthened by another contrary observation, which was made in a scratch wound healing assay in the present study, where inhibition of endogenous meprin α by actinonin as well as addition of recombinant active meprin α decelerated cell migration.

Migration and metastasis of cancer cells require ECM remodeling and cleavage of adhesion molecules by proteases. Actinonin treatment of human breast carcinoma cells and silencing of meprin α in liver cancer cells HepG2 and Huh7 decreased migration and invasiveness *in vitro*, while over-expression or recombinant active meprin α promoted migration (Breig et al., 2017; Matters et al., 2005). In contrast to epithelial expressed meprin α, observations in human colorectal adenocarcinoma cells (CaCo-2)

revealed secretion of meprin α also to the basolateral site, thereby leading to an accumulation in tumor stroma for ECM remodeling (Minder et al., 2012). Mechanistically, cleavage of EGFR by meprin α and subsequent ERK1/2/MAPK phosphorylation could result in the accelerated migration, while meprin α itself could be activated by Reptin, a protein that contributes to tumor malignancy (Breig et al., 2017; Ren et al., 2013). Besides meprin α, meprin β expression was also identified in cancer cell lines like HeLa cells or HT29 colon adenocarcinoma cells, where meprin β could promote cancer cell migration through cleavage of adhesion molecules (Dietrich et al., 1996). The adhesion molecule CD99 is a hallmark of Ewing Sarcoma and was identified as potential meprin β substrate in a proteomics approach (Ambros et al., 1991; Fellinger et al., 1991; Jefferson et al., 2013). Further characterization of the meprin β cleavage of CD99 revealed enhanced transendothelial migration of Lewis lung carcinoma cells (Bedau et al., 2017a). Moreover, cancer-associated mutations within the meprin β cleavage site in CD99 did not prevent but rather increased cell migration (Bedau et al., 2017b). Interestingly, meprin β over-expression in HeLa cells was shown to increase phosphorylation of Src kinase, which could promote anchorage-independent growth, survival and spreading of cancer cells. Potential inductors of meprin β expression are retinoic acid or phorbol myristal actetate, that further activate the transcription factor complex AP-1 (Dietrich et al., 1996; Matters and Bond, 1999; Sharma and Richards, 2000). Interestingly, transcribed meprin β mRNA in cancer cells differs from the mRNA expressed in kidney and intestine by alternative splicing and altered promoter binding usage (Dietrich et al., 1996; Jiang et al., 2000; Matters and Bond, 1999). Indeed, AP-1 and PEA3 binding elements were identified upstream of the meprin β gene, that could be used besides the tissue specific promoter sites for kidney and intestinal epithelial cells. The alternative splicing in murine cancer cells lead to an elongated meprin β' with differences in signal peptide and pro-peptide compared to meprin β in kidney (Jiang et al., 2000). In contrast, human meprin β' mRNA differs solely in the 5' untranslated region. This indicates variances in stability or expression rather on RNA level than on protein level, which might be beneficial for cancer cells. The induction of meprin β' by the AP-1 transcription factor complex could be further strengthened by the Fra2 transgenic mouse model (Eferl et al., 2008). As part of AP-1, Fra2 over-expression in mice led to fibrosis of the lung and an early death of the mice. Here, meprin β was identified as most highly upregulated gene in these lungs promoting ECM deposition and fibrosis (Biasin et al., 2014). Indeed, transcription of meprin β' mRNA was observed in fibrotic skin of Fra2 tg mice, confirming the pathology-associated regulation of meprin β' by AP-1, as described in cancer cells. Biasin and colleagues further identified TGFβ as another possible activator of AP-1 and meprin β in pulmonary lung arteries (Biasin et al., 2014). The growth factor TGFβ influences cell migration, differentiation and tissue regeneration and plays a major role in wound healing processes (Frank et al., 1996; Massagué, 2012). Since meprin knock-out mice show reduced collagen deposition in the dermis, where meprins maturate proteins of the ECM (Broder et al., 2013; Kronenberg et al., 2010), their role in wound healing should be elucidated. Interestingly, loss of the meprin related astacin proteases BMP-1 and Tll1 resulted in delayed wound

healing and markedly thinned and fragile skin (Muir et al., 2016). In the present study, meprin double knock-out mice revealed reduced re-epithelialization by migrating keratinocytes. Further, an *in vitro* assay regarding keratinocyte migration showed decreased migration of actinonin-treated HaCaT keratinocytes on the one hand and slightly increased wound healing of isolated meprin double knock-out keratinocytes on the other hand. These opposing results might arise due to the case that the HaCaT cell line consists of immortal cells differing in gene expression to primary keratinocytes. Moreover, platelets and inflammatory cells also contribute to wound healing in various stages and supply diverse cytokines like TGFβ and PDGF, growth- and angiogenic factors, which are missing in cell culture (Martin and Leibovich, 2005). Previous studies further reported expression of meprins on CD45+ leukocytes in the lamina propria of human inflamed bowel and mesenteric lymph node where loss of meprin β by gene knock-out decreased the ability of leukocytes to migrate through matrigel (Crisman et al., 2004; Lottaz et al., 1999). Comparable to this, less infiltration of inflammatory cells was observed in an air pouch acute inflammation model with meprin β deficient mice and wildtype littermates (Bedau et al., 2017b, 2017a). Here, cell migration probably functions via cleavage of CD99 by meprin β or reduced ECM remodeling. Therefore, analysis of inflammatory cells in wounds of meprin deficient mice should be performed in order to elucidate the role of meprins for inflammatory cell infiltration in wound healing.

Another possibility for the unaltered wound healing in meprin single knock-out mice could be compensatory expression of other enzymes replacing meprin activity. Both meprin α and meprin β have a preference for acidic amino acid residues and an overlapping substrate spectrum (Becker-Pauly et al., 2011; Jefferson et al., 2013). Therefore, loss of one meprin might be compensated by the other meprin enzyme. In normal murine skin homeostasis, no increased expression of the remaining meprin or other astacin family members was observed in knock-out mice. However, a compensatory effect during wound healing remains to be elucidated. Obviously, loss of both meprins reduced re-epithelialization in wound healing studies, while presence of only one meprin was sufficient for normal re-epithelialization. The meprin related proteases BMP-1 and Tll1 were also found to be expressed in murine skin, likewise preferring acidic amino acid residues and cleaving similar substrates like meprins (Becker-Pauly et al., 2011; Hopkins et al., 2007). Interestingly, loss of both BMP-1 and Tll1 (BTPs) in skin of conditional knock-out mice reduced wound closure, wound thickness and re-epithelialization, indicating that meprins and BTPs have diverse functions in wound healing like different substrates or are expressed in other cells and/or other stages of the healing process (Muir et al., 2016).

4.2 The role of meprin β in the onset of skin diseases

Since identification of meprin expression in skin (Becker-Pauly et al., 2007), research has focused on maturation of potential substrates that play a role in ECM constitution. First, procollagen III was shown to be maturated both at the N- and the C-terminus by meprin α and meprin β (Kronenberg et al.,

2010). To that time, collagen maturation was known to be performed by different proteases cleaving only the C-terminus (tolloid proteases and BMP-1) or the N-terminus (ADAMTS-2, 3 and 14) leading to collagen fibril formation (Hopkins et al., 2007). Consistent with the other astacin-like proteinase family members BMP-1 and Tll1, equal processing of procollagen by meprins could be observed with the exception that meprins were not dependent on the procollagen C-proteinase enhancer-1 (PCPE-1) (Kronenberg et al., 2010). A following study focused on meprin cleavage of another fibrillary collagen in skin, collagen I (Broder et al., 2013). As shown for procollagen III, N- and C-terminal processing of procollagen I was performed by meprins *in vivo* and *in vitro*, leading to spontaneous fibril formation of recombinant procollagen I. Furthermore, less tightly packed collagen fibrils were observed in meprin knock-out mice reducing overall tensile strength of the skin. In addition to the identification of meprins in skin, their expression in different skin diseases and keratinization disorders was studied. An altered distribution of meprins was observed within hyperproliferation of the epidermis in Netherton syndrome and psoriasis vulgaris (Becker-Pauly et al., 2007). Meprin α was not only observed in the basal layer but also in the uppermost layers of the epidermis, while meprin β showed also signals in the cornified layer. Moreover, in keloid dermis, meprins showed increased expression, most likely supporting the enhanced deposition of ECM (Kronenberg et al., 2010). Altogether, these observations emphasized meprins as potential target in the onset of skin disorders like fibrosis or psoriasis.

Mouse models can be used for the study and understanding of disease developments like fibrosis in an organism since *in vitro* models are limited in time and tissue/cell interplay. Therefore, several genetic mouse models have been established, for example targeting the TGFβ activation pathway or the connective tissue protein fibrillin (Smith and Chan, 2010). Also, chemical agents such as bleomycin can be used to induce dermal fibrosis, accumulation of myofibroblasts and ECM deposition via TGFβ activation (Yamamoto et al., 1999). Bleomycin-treatment of meprin knock-out mice was performed in order to elucidate the role of meprins in developing lung fibrosis (Biasin et al., 2017). Meprin β deficient mice had decreased collagen deposition and tissue density, again proving its role in ECM development. However, no changes in lung function or infiltration of immune cells could be observed. Furthermore, meprin double deficient mice did not show alterations compared to wildtype mice, indicating possible compensation by other collagen maturating enzymes. The role of meprin β in lung fibrosis was also highlighted in the genetic model of Fra2 over-expressing mice. Transgenic mice developed lung fibrosis and pulmonary hypertension that led to an early death (Eferl et al., 2008). Here, Fra2 was identified as transcription factor of meprin β, that was the most highly upregulated gene in the fibrotic lungs and might contribute to the excess collagen deposition (Biasin et al., 2014). Not only the lungs were affected by fibrosis, also the skin showed thickening of the dermis and increased collagen densities from week 12 to 16 (Maurer et al., 2009; Reich et al., 2010). A thickening of dermis and epidermis could be confirmed in this study, with additional increase in fibrosis marker genes ACTA2, Col1a2 and TGFβ1. Interestingly, meprin β was also highly upregulated with high variation between the individual mice. In this mouse model, the role of meprin β in the developing

lung or skin fibrosis needs further investigation. On the one hand, meprin β knock-out mice could be crossed to Fra2 transgenic mice to exclude influence of meprin β in any cell type and tissue. However, the meprin β gene and the introduced Fra2 transgene are both located close together on chromosome 18, complicating breeding or combination of both alleles on one chromosome by homologous recombination. To overcome this problem, the Mep1b gene could be disrupted in Fra2 transgenic mice using the novel technique CRISPR/Cas9. Here, possible off-target effects have to be considered and excluded (Zhang et al., 2015). On the other hand, meprin β activity could be blocked by treatment of Fra2 mice with a specific meprin β inhibitor. This method requires some pharmacological aspects like toxicity and stability of the inhibitor. Furthermore, the amount and time interval of the applied inhibitor as well as its specificity for meprin β have to be tested. These approaches could prove the role of meprin β in developing fibrosis. However, the Fra2 mouse model is limited for studying ongoing skin fibrosis as mice die from lung failure shortly after onset of disease. Nevertheless, it is a valuable model to study systemic fibrotic disease and relevant participating proteins like meprin β.

A more comprehensive mouse model for studying the impact of meprin β contribution to skin diseases is the direct over-expression of the enzyme in specific cells. Therefore, a Cre recombinase inducible meprin β over-expressing mouse model was generated. To target the major collagen expressing cells in skin, meprin β over-expressing mice were crossed to Col1a2-Cre mice, leading to meprin β expression in fibroblasts that transcribe the α2 chain of type I collagen (Zheng et al., 2002). 12 weeks old mice did not develop an obvious phenotype after tamoxifen induction and type I collagen maturation and deposition in the dermis appeared unaltered compared to control littermates. Since Fra2 tg mice start to develop fibrotic skin from week 12, meprin β over-expression in fibroblasts should be further investigated at higher age. Although meprin β expression was observed in the dermis, it is likely that no endogenous activators of meprin β were present in dermal fibroblasts. Reported skin expressed meprin β activators are kallikrein-related peptidases KLK4, 5 and 8 (Ohler et al., 2010). However, these enzymes are only expressed in the upper parts of the epidermis and thought to be essential for desquamation and skin barrier function (Brattsand and Egelrud, 1999; Komatsu et al., 2003, 2005). The other meprin β activator trypsin was identified in basal keratinocytes, vascular endothelial cells and macrophages (Becker et al., 2003; Koshikawa et al., 1997, 1998). Interestingly, aberrant trypsin expression was linked to pathological processes like inflammation and tumor invasion. The only known membrane bound meprin β activator matriptase-2 was not identified to be expressed in skin so far (Jäckle et al., 2015). It might be possible that fibroblasts express not yet identified meprin β activators or that known activators are produced by infiltrating cells in skin diseases linked to inflammation. Furthermore, increased meprin β expression must not necessarily lead to increased expression of ECM components that require maturation by meprin β. In skin of meprin β deficient mice, no change in expression of fibrosis related genes ACTA2, TGFb1 and Col1a2 has been observed in a fibrosis PCR array (Broder et al., 2013). This is in line with protein level of full length and maturated collagen I, which appeared unaltered in the over-expressing mice. Also no increased α-

SMA could be observed, which is a well-established marker for myofibroblasts. During tissue injury, fibroblasts differentiate to myofibroblasts that are contractile and deposit ECM like collagens for tissue repair. Persistence of myofibroblasts after wound closure is thought to be significant for propagation of fibrosis (Hinz et al., 2007). Little to no co-localization of meprin β and α-SMA was observed in immunofluorescence staining in skin, indicating meprin β expression on quiescent skin fibroblasts. Therefore, over-expression of meprin β in dermal fibroblasts does not promote development of skin fibrosis in 12 week old Col1a2-Cre MB-KI mice. Probably, other fibrosis stimulating factors or cell types are needed to promote onset of skin fibrosis and meprin β expression might occur from a downstream mechanism.

Other skin diseases that involve altered meprin expression like psoriasis vulgaris and Netherton syndrome target the epidermis (Becker-Pauly et al., 2007). Hence, induction of meprin β over-expression in the epidermis was performed using tamoxifen inducible Cre recombinase via cytokeratin 5 promoter in basal keratinocytes. Interestingly, affected mice developed a reticulate pigmentation phenotype during tamoxifen treatment that was present in ears, tails and dorsal skin. Furthermore, mice suffered from hair loss and showed thickening of the epidermis. A comparison of the symptoms with known human diseases and syndromes pointed towards phenotypes as described for Dermatopathia Pigmentosa Reticularis (DPR) or Epidermolysis bullosa simplex with mottled pigmentation and noncicatricial alopecia (MP-EBS) (Belligni et al., 2011; Nagai et al., 2016). In both rare syndromes, patients were described suffering from reticulate pigmentation spread over their body and non-scarring hair loss. The trigger for the developing syndrome was identified by sequencing analyses of patients that revealed dominant mutations in KRT5 or KRT14, which lead to a loss of function of cytokeratins to form heterodimeric fibrils in keratinocytes (Lee et al., 2012). Since these mutations are not present in the meprin β over-expressing mouse model, a more complex molecular mechanism should be considered that promotes these phenotype. Decreased expression of one of the cytokeratins was supposed, which could prevent proper fibril formation. Interestingly, even increased transcription of cytokeratin 14 and 5 could be observed in the meprin β over-expressing mouse model. For cytokeratin 14, a 20 kDa C-terminal fragment occurred predominantly in meprin β over-expressing skin lysates in Western blot analyses. This fragment might correlate to the overall increased cytokeratin 14 level or be indicative of fibril cleavage and depletion. Nevertheless, direct cleavage of intracellular cytokeratin 14 by meprin β appeared unlikely because the enzyme is located on the outer plasma membrane. Keratin fibrils are connected to the plasma membrane via protein components of the desmosomes and hemidesmosomes that are located within the outer membrane (Fuchs and Raghavan, 2002). Loss of this connection by meprin β cleavage would disrupt the cytoskeleton of keratinocytes and probably mimic loss of proper keratin fibril formation and induce cell stress. Of note, desmogleins were described as candidate substrates for meprin β in an *in vitro* proteomics approach (Jefferson et al., 2013). Therefore, expression of desmosomal molecules desmoglein 1 and 3 was investigated in meprin β over-expressing mice. Interestingly, full length

desmoglein 1 signals were only obtained in control mice skin in Western blot analysis but expression was unchanged on mRNA level. For desmoglein 3, no full length form could be observed but a cleavage fragment of 20 kDa appeared mainly in meprin β over-expressing mice while mRNA levels were significantly increased. Cleavage of desmogleins 1 and 3 by meprin β could disrupt adhesion capability of keratinocytes and lead to the hair loss phenotype as described for desmoglein 3 -/- mice (Koch et al., 1997). Hence, desmoglein 1 and 3 might represent novel *in vivo* substrates for meprin β or they are cleaved by a downstream protease. Kallikreins were shown to interact with meprin β and cleave corneodesmosomal proteins leading to desquamation of keratinocytes (Caubet et al., 2004; Ohler et al., 2010). However, desmoglein 1 was only cleaved by KLK5, a meprin β activator, and not by KLK7, which can be activated by meprin β. Furthermore, other adhesion molecules were considered as potential meprin β substrates in the epidermis. E-cadherin mediates intercellular adhesion junctions of keratinocytes and hair follicles and loss of E-cadherin promotes hair loss and alters differentiation of epidermal keratinocytes (Young et al., 2003). Moreover, E-cadherin was described to be cleaved by meprin β, thereby generating a 100 kDa fragment (Huguenin et al., 2008). Interestingly, cleavage fragments were obtained in all genotypes but showed increased signals in meprin β over-expressing mice. For β1 integrin, on the other hand, whose loss in mice leads also to hair loss and hyperthickening of the epidermis (Brakebusch et al., 2000), less cleavage fragments and stabilization of the full length protein was observed in presence of meprin β. Summarizing, there are hints that point out cleavage of adhesion molecules by meprin β in the epidermis. Loss of adhesion could promote early desquamation of keratinocytes, mechanical cell stress and induce hyperproliferation of keratinocytes in order to compensate tissue fragility (Kottke et al., 2006). However, identification of particular epidermis related substrates for meprin β remains elusive and might resolved by an overall proteomics screen using mass spectrometry.

Chronic skin inflammation and hyperproliferation are also hallmarks of psoriasis. Expression of meprin β was widely associated with inflammation and the release of pro-inflammatory cytokines like IL6, IL1β and IL18 by macrophages (Li et al., 2014). Interestingly, keratinocytes itself are also able to express interleukins that act in an autocrine or paracrine fashion to themselves or other skin cells (Baliwag et al., 2015). Therefore, expression of pro-inflammatory cytokines in skin of meprin β over-expressing mice was investigated. Indeed, upregulation of IL6, Il1β and IL18 was present in comparison to control mice as well as higher expression of the Langerhans cell marker CD207 and macrophage marker Adgre1 that could indicate an inflammatory condition and subsequent pigmentation of the skin. The unusual dermal pigmentation, which was seen in the mouse tails, points towards a pigmentary incontinence, a process that follows inflammation and cell damage and that was described in DPR patients (Belligni et al., 2011; Masu and Seiji, 1983). In normal skin homeostasis, melanin is transported as melanosomes from melanocytes to keratinocytes in order to protect the nucleus from UV radiation and DNA damage (Yamaguchi et al., 2007). Upon cell damage, free melanosomes are taken up by dermal macrophages, also called melanophages, that persist within the

dermis (Masu and Seiji, 1983). An increased amount of melanocytes was not observed in meprin β over-expressing mice, but overall melanin production showed an increase which can be also observed during inflammatory processes. Upon inflammatory cytokine secretion or UV radiation, keratinocytes produce prostaglandins, e.g. α-MSH (α-melanocyte-stimulating hormone), that stimulate the melanin production (Brenner and Hearing, 2008). Excessive melanosomes and pigment are then taken up by melanophages and stored within in the dermis, a process that is also used for inlaying tattoo pigment (Baranska et al., 2018; Collin, 2018). Therefore, the pigmentation phenotype could be a secondary effect of meprin β over-expression, which might resulted from skin inflammation and cellular stress by loss of adhesion of keratinocytes within the cellular network. Interestingly, upon UV radiation and tanning of human skin, total amount of melanocytes was shown to remain unchanged as seen in the meprin β over-expressing mouse model (Tadokoro et al., 2005). Furthermore, Tadokoro and colleagues reported distribution of melanin to the upper layers of the epidermis as a long term result after UV radiation. This distribution to the upper part was also observed in meprin β expressing regions in ear and dorsal skin. Therefore, over-expression of meprin β in the epidermis might activate similar mechanisms as UV damage that also result in thickening of epidermis and inflammation (D'Orazio et al., 2013). However, additional research is needed for understanding the exact underlying mechanism.

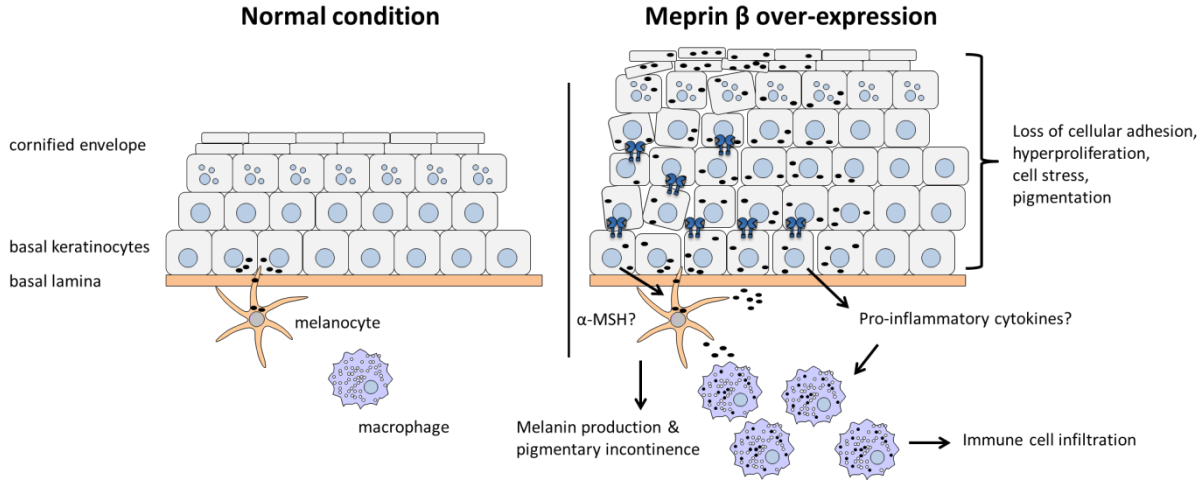

Figure 27: Phenotypic changes of epidermis by meprin β over-expression.

Meprin β over-expression in basal keratinocytes might lead to cleavage of adhesion molecules in desmosomes and hemidesmosomes, which induces cellular stress. Mechanical problems of the epidermis are compensated by hyperproliferation of keratinocytes. In order to protect affected keratinocytes, α-MSH (α-melanocyte-stimulating hormone) secretion leads to melanin production in melanocytes, which is transported to keratinocytes. Excessive melanin in the dermis is taken up by melanophages and stored (pigmentary incontinence). Furthermore, secretion of pro-inflammatory cytokines induces inflammation, resulting in immune cell infiltration and a psoriasis like phenotype.

Conclusively, over-expressing meprin β in the epidermis might result in induction of cell stress, inflammation and development of a psoriasis like phenotype. Hence, increased meprin β expression in psoriatic skin diseases with pigmentation could be considered as hallmark for development and

progression of disease. Establishment of the meprin β over-expressing mouse model could also be used for generation and investigation of other inflammatory disease models where meprin β activity could play a role. As proof of concept, investigation on inhibition of meprin β in these mouse models could prove functionality of meprin β inhibitors *in vivo* and display a therapeutic target for inflammatory disorders. Moreover, generation of a meprin α over-expressing mouse model could be used for identification of novel *in vivo* substrates and strengthen the role of meprin α in the onset of pathological conditions.

5. **References**

Adair-Kirk, T.L., and Senior, R.M. (2008). Fragments of extracellular matrix as mediators of inflammation. Int. J. Biochem. Cell Biol. *40*, 1101–1110.

Ambros, I.M., Ambros, P.F., Strehl, S., Kovar, H., Gadner, H., and Salzer-Kuntschik, M. (1991). MIC2 is a specific marker for ewing's sarcoma and peripheral primitive neuroectodermal tumors. Evidence for a common histogenesis of ewing's sarcoma and peripheral primitive neuroectodermal tumors from MIC2 expression and specific chromosome aberration. Cancer *67*, 1886–1893.

Angel, P., Szabowski, a, and Schorpp-Kistner, M. (2001). Function and regulation of AP-1 subunits in skin physiology and pathology. Oncogene *20*, 2413–2423.

Arnold, P., Otte, A., and Becker-Pauly, C. (2017). Meprin metalloproteases: Molecular regulation and function in inflammation and fibrosis. Biochim. Biophys. Acta - Mol. Cell Res. *1864*, 2096–2104.

Arolas, J.L., Broder, C., Jefferson, T., Guevara, T., Sterchi, E.E., Bode, W., Stocker, W., Becker-Pauly, C., and Gomis-Ruth, F.X. (2012). Structural basis for the sheddase function of human meprin β metalloproteinase at the plasma membrane. Proc. Natl. Acad. Sci. *109*, 16131–16136.

Baliwag, J., Barnes, D.H., and Johnston, A. (2015). Cytokines in psoriasis. Cytokine *73*, 342–350.

Banerjee, S., Oneda, B., Yap, L.M., Jewell, D.P., Matters, G.L., Fitzpatrick, L.R., Seibold, F., Sterchi, E.E., Ahmad, T., Lottaz, D., et al. (2009). MEP1A allele for meprin A metalloprotease is a susceptibility gene for inflammatory bowel disease. Mucosal Immunol. *2*, 220–231.

Banerjee, S., Jin, G., Bradley, S.G., Matters, G.L., Gailey, R.D., Crisman, J.M., Bond, J.S., Banerjee, S., Jin, G., Bradley, S.G., et al. (2011). Balance of meprin A and B in mice affects the progression of experimental inflammatory bowel disease. Am. J. Physiol. Gastrointest. Liver Physiol. *300*, 273–282.

Baranska, A., Shawket, A., Jouve, M., Baratin, M., Malosse, C., Voluzan, O., Vu Manh, T.-P., Fiore, F., Bajénoff, M., Benaroch, P., et al. (2018). Unveiling skin macrophage dynamics explains both tattoo persistence and strenuous removal. J. Exp. Med. *215*, 1115–1133.

Becker-Pauly, C., Höwel, M., Walker, T., Vlad, A., Aufenvenne, K., Oji, V., Lottaz, D., Sterchi, E.E., Debela, M., Magdolen, V., et al. (2007). The alpha and beta subunits of the metalloprotease meprin are expressed in separate layers of human epidermis, revealing different functions in keratinocyte proliferation and differentiation. J. Invest. Dermatol. *127*, 1115–1125.

Becker-Pauly, C., Barré, O., Schilling, O., Auf dem Keller, U., Ohler, A., Broder, C., Schütte, A., Kappelhoff, R., Stöcker, W., and Overall, C.M. (2011). Proteomic analyses reveal an acidic prime side specificity for the astacin metalloprotease family reflected by physiological substrates. Mol. Cell. Proteomics *10*, M111.009233.

Becker, C., Kruse, M.N., Slotty, K. a, Kohler, D., Harris, J.R., Rosmann, S., Sterchi, E.E., and Stocker, W. (2003). Differences in the activation mechanism between the alpha and beta subunits of human meprin. Biol Chem *384*, 825–831.

Bedau, T., Peters, F., Prox, J., Arnold, P., Schmidt, F., Finkernagel, M., Köllmann, S., Wichert, R., Otte, A., Ohler, A., et al. (2017a). Ectodomain shedding of CD99 within highly conserved regions is mediated by the metalloprotease meprin β and promotes transendothelial cell migration. FASEB J. *31*, 1226–1237.

Bedau, T., Schumacher, N., Peters, F., Prox, J., Arnold, P., Koudelka, T., Helm, O., Schmidt, F., Rabe, B., Jentzsch, M., et al. (2017b). Cancer-associated mutations in the canonical cleavage site do not influence CD99 shedding by the metalloprotease meprin β but alter cell migration in vitro. Oncotarget *8*, 54873–54888.

Belligni, E.F., Dokal, I., and Hennekam, R.C.M. (2011). Prenatal and postnatal growth retardation, microcephaly, developmental delay, and pigmentation abnormalities: Naegeli syndrome, dyskeratosis

congenita, poikiloderma Clericuzio type, or separate entity? Eur. J. Med. Genet. *54*, 231–235.

Bertenshaw, G.P., Norcum, M.T., and Bond, J.S. (2003). Structure of homo- and hetero-oligomeric meprin metalloproteases: Dimers, tetramers, and high molecular mass multimers. J. Biol. Chem. *278*, 2522–2532.

Beynon, R.J., Shannon, J.D., and Bond, J.S. (1981). Purification and characterization of a metallo-endoproteinase from mouse kidney. Biochem. J. *199*, 591–598.

Biasin, V., Marsh, L.M., Egemnazarov, B., Wilhelm, J., Ghanim, B., Klepetko, W., Wygrecka, M., Olschewski, H., Eferl, R., Olschewski, A., et al. (2014). Meprin β, a novel mediator of vascular remodelling underlying pulmonary hypertension. J. Pathol. *233*, 7–17.

Biasin, V., Wygrecka, M., Marsh, L.M., Becker-Pauly, C., Brcic, L., Ghanim, B., Klepetko, W., Olschewski, A., and Kwapiszewska, G. (2017). Meprin β contributes to collagen deposition in lung fibrosis. Sci. Rep. *7*, 39969.

Biasin, V., Wygrecka, M., Bärnthaler, T., Jandl, K., Jain, P.P., Bálint, Z., Kovacs, G., Leitinger, G., Kolb-Lenz, D., Kornmueller, K., et al. (2018). Docking of Meprin α to Heparan Sulphate Protects the Endothelium from Inflammatory Cell Extravasation. Thromb. Haemost. *118*, 1790–1802.

Boehncke, W.-H., and Schön, M.P. (2015). Psoriasis. Lancet *386*, 983–994.

Brakebusch, C., Grose, R., Quondamatteo, F., Ramirez, A., Jorcano, J.L., Pirro, A., Svensson, M., Herken, R., Sasaki, T., Timpl, R., et al. (2000). Skin and hair follicle integrity is crucially dependent on beta 1 integrin expression on keratinocytes. EMBO J. *19*, 3990–4003.

Brattsand, M., and Egelrud, T. (1999). Purification, Molecular Cloning, and Expression of a Human Stratum Corneum Trypsin-like Serine Protease with Possible Function in Desquamation. J. Biol. Chem. *274*, 30033–30040.

Breig, O., Yates, M., Neaud, V., Couchy, G., Grigoletto, A., Lucchesi, C., Prox, J., Zucman-Rossi, J., Becker-Pauly, C., and Rosenbaum, J. (2017). Metalloproteinase meprin α regulates migration and invasion of human hepatocarcinoma cells and is a mediator of the oncoprotein Reptin. Oncotarget *8*, 7839–7851.

Brenner, M., and Hearing, V.J. (2008). Modifying skin pigmentation - approaches through intrinsic biochemistry and exogenous agents. Drug Discov. Today. Dis. Mech. *5*, e189–e199.

Broder, C., Arnold, P., Vadon-Le Goff, S., Konerding, M. a, Bahr, K., Müller, S., Overall, C.M., Bond, J.S., Koudelka, T., Tholey, A., et al. (2013). Metalloproteases meprin α and meprin β are C- and N-procollagen proteinases important for collagen assembly and tensile strength. Proc. Natl. Acad. Sci. U. S. A. *110*, 14219–14224.

Bylander, J., Li, Q., Ramesh, G., Zhang, B., Reeves, W.B., and Bond, J.S. (2008). Targeted disruption of the meprin metalloproteinase beta gene protects against renal ischemia-reperfusion injury in mice. Am. J. Physiol. Renal Physiol. *294*, F480–F490.

Carr, J.C., Sherman, S.K., Wang, D., Dahdaleh, F.S., Bellizzi, A.M., O'Dorisio, M.S., O'Dorisio, T.M., and Howe, J.R. (2013). Overexpression of Membrane Proteins in Primary and Metastatic Gastrointestinal Neuroendocrine Tumors. Ann. Surg. Oncol. *20*, 739–746.

Caubet, C., Jonca, N., Brattsand, M., Guerrin, M., Bernard, D., Schmidt, R., Egelrud, T., Simon, M., and Serre, G. (2004). Degradation of corneodesmosome proteins by two serine proteases of the kallikrein family, SCTE/KLK5/hK5 and SCCE/KLK7/hK7. J. Invest. Dermatol. *122*, 1235–1244.

Chung, K.Y., Agarwal, A., Uitto, J., and Mauviel, A. (1996). An AP-1 binding sequence is essential for regulation of the human α2(I) collagen (COL1A2) promoter activity by transforming growth factor-β. J. Biol. Chem. *271*, 3272–3278.

Collin, M. (2018). Death, eaters, and dark marks. J. Exp. Med. *215*, 1005–1006.

Crisman, J.M., Zhang, B., Norman, L.P., and Bond, J.S. (2004). Deletion of the mouse meprin beta metalloprotease gene diminishes the ability of leukocytes to disseminate through extracellular matrix. J. Immunol. *172*, 4510–4519.

D'Orazio, J., Jarrett, S., Amaro-Ortiz, A., and Scott, T. (2013). UV radiation and the skin. Int. J. Mol. Sci. *14*, 12222–12248.

Dietrich, J.M., Jiang, W., and Bond, J.S. (1996). A novel meprin beta' mRNA in mouse embryonal and human colon carcinoma cells. J. Biol. Chem. *271*, 2271–2278.

Dumermuth, E., Sterchi, E., Jiang, W., Wolz, R., Bond, J., Flannery, A., and Beynon, R. (1991). The astacin family of metalloendopeptidases. J. Biol. Chem. *266*, 21381–21385.

Eferl, R., Hasselblatt, P., Rath, M., Popper, H., Zenz, R., Komnenovic, V., Idarraga, M.-H., Kenner, L., and Wagner, E.F. (2008). Development of pulmonary fibrosis through a pathway involving the transcription factor Fra-2/AP-1. Proc. Natl. Acad. Sci. U. S. A. *105*, 10525–10530.

Fellinger, E.J., Garin-Chesa, P., Triche, T.J., Huvos, A.G., and Rettig, W.J. (1991). Immunohistochemical analysis of Ewing's sarcoma cell surface antigen p30/32MIC2. Am. J. Pathol. *139*, 317–325.

Frank, S., Madlener, M., and Werner, S. (1996). Transforming Growth Factors 1, 2, and 3 and Their Receptors Are Differentially Regulated during Normal and Impaired Wound Healing. J. Biol. Chem. *271*, 10188–10193.

Fuchs, E., and Raghavan, S. (2002). Getting under the skin of epidermal morphogenesis. Nat. Rev. Genet. *3*, 199–209.

Gao, P., and Si, L.-Y. (2010). Meprin-alpha metalloproteases enhance lipopolysaccharide-stimulated production of tumour necrosis factor-alpha and interleukin-1beta in peripheral blood mononuclear cells via activation of NF-kappaB. Regul. Pept. *160*, 99–105.

Goliger, J.A., and Paul, D.L. (1995). Wounding alters epidermal connexin expression and gap junction-mediated intercellular communication. Mol. Biol. Cell *6*, 1491–1501.

Gomis-Rüth, F.X., Trillo-Muyo, S., and Stöcker, W. (2012). Functional and structural insights into astacin metallopeptidases. Biol. Chem. *393*, 1027–1041.

Gorbea, C.M., Marchand, P., Jiang, W., Copeland, N.G., Gilbert, D.J., Jenkins, N. a, and Bond, J.S. (1993). Cloning, expression, and chromosomal localization of the mouse meprin beta subunit. J. Biol. Chem. *268*, 21035–21043.

Grünberg, J., Dumermuth, E., Eldering, J.A., and Sterchi, E.E. (1993). Expression of the alpha subunit of PABA peptide hydrolase (EC 3.4.24.18) in MDCK cells. FEBS Lett. *335*, 376–379.

Häsler, R., Sheibani-Tezerji, R., Sinha, A., Barann, M., Rehman, A., Esser, D., Aden, K., Knecht, C., Brandt, B., Nikolaus, S., et al. (2017). Uncoupling of mucosal gene regulation, mRNA splicing and adherent microbiota signatures in inflammatory bowel disease. Gut *66*, 2087–2097.

Herzog, C., Seth, R., Shah, S. V., and Kaushal, G.P. (2007). Role of meprin A in renal tubular epithelial cell injury. Kidney Int. *71*, 1009–1018.

Herzog, C., Haun, R.S., Kaushal, V., Mayeux, P.R., Shah, S. V, and Kaushal, G.P. (2009). Meprin A and meprin alpha generate biologically functional IL-1beta from pro-IL-1beta. Biochem. Biophys. Res. Commun. *379*, 904–908.

Herzog, C., Haun, R.S., Ludwig, A., Shah, S. V., and Kaushal, G.P. (2014). ADAM10 is the major sheddase responsible for the release of membrane-Associated meprin A. J. Biol. Chem. *289*, 13308–13322.

Herzog, C., Marisiddaiah, R., Haun, R.S., and Kaushal, G.P. (2015). Basement membrane protein nidogen-1 is a target of meprin β in cisplatin nephrotoxicity. Toxicol. Lett. *236*, 110–116.

Hinz, B., Phan, S.H., Thannickal, V.J., Galli, A., Bochaton-Piallat, M.-L., and Gabbiani, G. (2007). The myofibroblast: one function, multiple origins. Am. J. Pathol. *170*, 1807–1816.

Hopkins, D.R., Keles, S., and Greenspan, D.S. (2007). The bone morphogenetic protein 1/Tolloid-like metalloproteinases. Matrix Biol. *26*, 508–523.

Hübner, G., Brauchle, M., Smola, H., Madlener, M., Fässler, R., and Werner, S. (1996). Differential regulation of pro-inflammatory cytokines during wound healing in normal and glucocorticoid-treated mice. Cytokine *8*, 548–556.

Huguenin, M., Müller, E.J., Trachsel-Rösmann, S., Oneda, B., Ambort, D., Sterchi, E.E., and Lottaz, D. (2008). The metalloprotease meprinβ processes E-cadherin and weakens intercellular adhesion. PLoS One *3*.

Jäckle, F., Schmidt, F., Wichert, R., Arnold, P., Prox, J., Mangold, M., Ohler, A., Pietrzik, C.U., Koudelka, T., Tholey, A., et al. (2015). Metalloprotease meprin β is activated by transmembrane serine protease matriptase-2 at the cell surface thereby enhancing APP shedding. Biochem. J. *470*, 91–103.

Jefferson, T., Auf Dem Keller, U., Bellac, C., Metz, V. V., Broder, C., Hedrich, J., Ohler, A., Maier, W., Magdolen, V., Sterchi, E., et al. (2013). The substrate degradome of meprin metalloproteases reveals an unexpected proteolytic link between meprin β and ADAM10. Cell. Mol. Life Sci. *70*, 309–333.

Jiang, W., Sadler, P.M., Jenkinsfl, N.A., Gilbert, D.J., Copeland, N.G., and Bond, J.S. (1993). Tissue-specific expression and chromosomal localization of the alpha subunit of mouse meprin A. J Biol Chem. *268*, 10380–10385.

Jiang, W., Kumar, J.M., Matters, G.L., and Bond, J.S. (2000). Structure of the mouse metalloprotease meprin β gene (Mep1b): Alternative splicing in cancer cells. Gene *248*, 77–87.

Johnson, G.D., and Bond, J.S. (1997). Activation mechanism of meprins, members of the astacin metalloendopeptidase family. J. Biol. Chem. *272*, 28126–28132.

Johnson, G.D., and Hersh, L.B. (1992). Cloning a rat meprin cDNA reveals the enzyme is a heterodimer. J. Biol. Chem. *267*, 13505–13512.

Karimova, M., Baker, O., Camgoz, A., Naumann, R., Buchholz, F., and Anastassiadis, K. (2018). A single reporter mouse line for Vika, Flp, Dre, and Cre-recombination. Sci. Rep. *8*, 14453.

Kaushal, G.P., Walker, P.D., and Shah, S. V. (1994). An old enzyme with a new function: purification and characterization of a distinct matrix-degrading metalloproteinase in rat kidney cortex and its identification as meprin. J. Cell Biol. *126*, 1319–1327.

Keiffer, T.R., and Bond, J.S. (2014). Meprin metalloproteases inactivate interleukin 6. J. Biol. Chem. *289*, 7580–7588.

Kentsis, A., Shulman, A., Ahmed, S., Brennan, E., Monuteaux, M.C., Lee, Y.-H., Lipsett, S., Paulo, J.A., Dedeoglu, F., Fuhlbrigge, R., et al. (2013). Urine proteomics for discovery of improved diagnostic markers of Kawasaki disease. EMBO Mol. Med. *5*, 210–220.

Kessler, E., Takahara, K., Biniaminov, L., Brusel, M., and Greenspan, D.S. (1996). Bone morphogenetic protein-1: the type I procollagen C-proteinase. Science *271*, 360–362.

Koch, P.J., Mahoney, M.G., Ishikawa, H., Pulkkinen, L., Uitto, J., Shultz, L., Murphy, G.F., Whitaker-Menezes, D., and Stanley, J.R. (1997). Targeted disruption of the pemphigus vulgaris antigen (desmoglein 3) gene in mice causes loss of keratinocyte cell adhesion with a phenotype similar to pemphigus vulgaris. J. Cell Biol. *137*, 1091–1102.

Komatsu, N., Takata, M., Otsuki, N., Toyama, T., Ohka, R., Takehara, K., and Saijoh, K. (2003). Expression and Localization of Tissue Kallikrein mRNAs in Human Epidermis and Appendages. J.

Invest. Dermatol. *121*, 542–549.

Komatsu, N., Saijoh, K., Toyama, T., Ohka, R., Otsuki, N., Hussack, G., Takehara, K., and Diamandis, E.P. (2005). Multiple tissue kallikrein mRNA and protein expression in normal skin and skin diseases. Br. J. Dermatol. *153*, 274–281.

Koshikawa, N., Nagashima, Y., Miyagi, Y., Mizushima, H., Yanoma, S., Yasumitsu, H., and Miyazaki, K. (1997). Expression of trypsin in vascular endothelial cells. FEBS Lett. *409*, 442–448.

Koshikawa, N., Hasegawa, S., Nagashima, Y., Mitsuhashi, K., Tsubota, Y., Miyata, S., Miyagi, Y., Yasumitsu, H., and Miyazaki, K. (1998). Expression of trypsin by epithelial cells of various tissues, leukocytes, and neurons in human and mouse. Am. J. Pathol. *153*, 937–944.

Kottke, M.D., Delva, E., and Kowalczyk, A.P. (2006). The desmosome: cell science lessons from human diseases. J. Cell Sci. *119*, 797–806.

Kronenberg, D., Bruns, B.C., Moali, C., Vadon-Le Goff, S., Sterchi, E.E., Traupe, H., Böhm, M., Hulmes, D.J.S., Stöcker, W., and Becker-Pauly, C. (2010). Processing of procollagen III by meprins: new players in extracellular matrix assembly? J. Invest. Dermatol. *130*, 2727–2735.

Lee, C.-H., Kim, M.-S., Chung, B.M., Leahy, D.J., and Coulombe, P.A. (2012). Structural basis for heteromeric assembly and perinuclear organization of keratin filaments. Nat. Struct. Mol. Biol. *19*, 707–715.

Li, S.-W., Arita, M., Fertala, A., Bao, Y., Kopen, G.C., Långsjö, T.K., Hyttinen, M.M., Helminen, H.J., and Prockop, D.J. (2001). Transgenic mice with inactive alleles for procollagen N-proteinase (ADAMTS-2) develop fragile skin and male sterility. Biochem. J. *355*, 271–278.

Li, S.W., Sieron, A.L., Fertala, A., Hojima, Y., Arnold, W. V., and Prockop, D.J. (1996). The C-proteinase that processes procollagens to fibrillar collagens is identical to the protein previously identified as bone morphogenic protein-1. Proc. Natl. Acad. Sci. *93*, 5127–5130.

Li, Y.-J., Fan, Y.-H., Tang, J., Li, J.-B., and Yu, C.-H. (2014). Meprin-β regulates production of pro-inflammatory factors via a disintegrin and metalloproteinase-10 (ADAM-10) dependent pathway in macrophages. Int. Immunopharmacol. *18*, 77–84.

Lottaz, D., Hahn, D., Müller, S., Müller, C., and Sterchi, E.E. (1999). Secretion of human meprin from intestinal epithelial cells depends on differential expression of the alpha and beta subunits. Eur. J. Biochem. *259*, 496–504.

Maitra, A., Hansel, D.E., Argani, P., Ashfaq, R., Rahman, A., Naji, A., Deng, S., Geradts, J., Hawthorne, L., House, M.G., et al. (2003). Global expression analysis of well-differentiated pancreatic endocrine neoplasms using oligonucleotide microarrays. Clin. Cancer Res. *9*, 5988–5995.

Marchand, P., Tang, J., Johnson, G.D., and Bond, J.S. (1995). COOH-terminal Proteolytic Processing of Secreted and Membrane Forms of the alpha Subunit of the Metalloprotease Meprin A. J. Biol. Chem. *270*, 5449–5456.

Martin, P., and Leibovich, S.J. (2005). Inflammatory cells during wound repair: The good, the bad and the ugly. Trends Cell Biol. *15*, 599–607.

Massagué, J. (2012). TGFβ signalling in context. Nat. Rev. Mol. Cell Biol. *13*, 616–630.

Masu, S., and Seiji, M. (1983). Pigmentary incontinence in fixed drug eruptions. Histologic and electron microscopic findings. J. Am. Acad. Dermatol. *8*, 525–532.

Matters, G.L., and Bond, J.S. (1999). Expression and regulation of the meprin beta gene in human cancer cells. Mol. Carcinog. *25*, 169–178.

Matters, G.L., Manni, A., and Bond, J.S. (2005). Inhibitors of Polyamine Biosynthesis Decrease the Expression of the Metalloproteases Meprin α and MMP-7 in Hormone-independent Human Breast Cancer Cells. Clin. Exp. Metastasis *22*, 331–339.

Maurer, B., Busch, N., Jüngel, A., Pileckyte, M., Gay, R.E., Michel, B.A., Schett, G., Gay, S., Distler, J., and Distler, O. (2009). Transcription factor fos-related antigen-2 induces progressive peripheral vasculopathy in mice closely resembling human systemic sclerosis. Circulation *120*, 2367–2376.

Mezentsev, A., Nikolaev, A., and Bruskin, S. (2014). Matrix metalloproteinases and their role in psoriasis. Gene *540*, 1–10.

Minder, P., Bayha, E., Becker-Pauly, C., and Sterchi, E.E. (2012). Meprinα Transactivates the Epidermal Growth Factor Receptor (EGFR) via Ligand Shedding, thereby Enhancing Colorectal Cancer Cell Proliferation and Migration. J. Biol. Chem. *287*, 35201–35211.

Mittelstadt, M.L., and Patel, R.C. (2012). AP-1 Mediated Transcriptional Repression of Matrix Metalloproteinase-9 by Recruitment of Histone Deacetylase 1 in Response to Interferon β. PLoS One *7*, e42152.

Moulin, V., Lawny, F., Barritault, D., and Caruelle, J.P. (1998). Platelet releasate treatment improves skin healing in diabetic rats through endogenous growth factor secretion. Cell. Mol. Biol. (Noisy-Le-Grand). *44*, 961–971.

Muir, A.M., Massoudi, D., Nguyen, N., Keene, D.R., Lee, S.-J., Birk, D.E., Davidson, J.M., Marinkovich, M.P., and Greenspan, D.S. (2016). BMP1-like proteinases are essential to the structure and wound healing of skin. Matrix Biol. 1–18.

Nagai, H., Oiso, N., Tomida, S., Sakai, K., Fujiwara, S., Nakamachi, Y., Kawano, S., Kawada, A., Nishio, K., and Nishigori, C. (2016). Epidermolysis bullosa simplex with mottled pigmentation with noncicatricial alopecia: identification of a recurrent p.P25L mutation in KRT5 in four affected family members. Br. J. Dermatol. *174*, 633–635.

Nickoloff, B.J., Bonish, B.K., Marble, D.J., Schriedel, K.A., DiPietro, L.A., Gordon, K.B., and Lingen, M.W. (2006). Lessons Learned from Psoriatic Plaques Concerning Mechanisms of Tissue Repair, Remodeling, and Inflammation. J. Investig. Dermatology Symp. Proc. *11*, 16–29.

Nickoloff, B.J., Qin, J.-Z., and Nestle, F.O. (2007). Immunopathogenesis of Psoriasis. Clin. Rev. Allergy Immunol. *33*, 45–56.

Norman, L.P., Jiang, W., Han, X., Thomas, L., Bond, J.S., and Saunders, T.L. (2003). Targeted Disruption of the Meprin β Gene in Mice Leads to Underrepresentation of Knockout Mice and Changes in Renal Gene Expression Profiles. Mol. Cell. Biol. *23*, 1221–1230.

Nwomeh, B.C., Liang, H.X., Diegelmann, R.F., Cohen, I.K., and Yager, D.R. (1998). Dynamics of the matrix metalloproteinases MMP-1 and MMP-8 in acute open human dermal wounds. Wound Repair Regen. *6*, 127–134.

Ohler, A., Debela, M., Wagner, S., Magdolen, V., and Becker-Pauly, C. (2010). Analyzing the protease web in skin: meprin metalloproteases are activated specifically by KLK4, 5 and 8 vice versa leading to processing of proKLK7 thereby triggering its activation. Biol. Chem. *391*, 455–460.

Okuno, Y., Nakamura-Ishizu, A., Kishi, K., Suda, T., and Kubota, Y. (2011). Bone marrow-derived cells serve as proangiogenic macrophages but not endothelial cells in wound healing. Blood *117*, 5264–5272.

Oneda, B., Lods, N., Lottaz, D., Becker-Pauly, C., Stöcker, W., Pippin, J., Huguenin, M., Ambort, D., Marti, H.-P., and Sterchi, E.E. (2008). Metalloprotease meprin beta in rat kidney: glomerular localization and differential expression in glomerulonephritis. PLoS One *3*, e2278.

Pasparakis, M., Haase, I., and Nestle, F.O. (2014). Mechanisms regulating skin immunity and inflammation. Nat. Rev. Immunol. *14*, 289–301.

Prox, J., Arnold, P., and Becker-Pauly, C. (2015). Meprin α and meprin β: Procollagen proteinases in health and disease. Matrix Biol. *44–46*, 7–13.

Reich, N., Maurer, B., Akhmetshina, A., Venalis, P., Dees, C., Zerr, P., Palumbo, K., Zwerina, J., Nevskaya, T., Gay, S., et al. (2010). The transcription factor Fra-2 regulates the production of extracellular matrix in systemic sclerosis. Arthritis Rheum. *62*, 280–290.

Ren, J., Li, W., Liu, H., Yan, L., Jiao, W., Li, D., Tang, Y., Gu, G., and Xu, Z. (2013). Overexpression of reptin in renal cell carcinoma contributes to tumor malignancies and its inhibition triggers senescence of cancer cells. Urol. Oncol. *31*, 1358–1366.

Schütte, A., Ermund, A., Becker-Pauly, C., Johansson, M.E. V, Rodriguez-Pineiro, A.M., Bäckhed, F., Müller, S., Lottaz, D., Bond, J.S., and Hansson, G.C. (2014). Microbial-induced meprin β cleavage in MUC2 mucin and a functional CFTR channel are required to release anchored small intestinal mucus. Proc. Natl. Acad. Sci. U. S. A. *111*, 12396–12401.

Scotlandi, K., Zuntini, M., Manara, M.C., Sciandra, M., Rocchi, A., Benini, S., Nicoletti, G., Bernard, G., Nanni, P., Lollini, P.-L., et al. (2007). CD99 isoforms dictate opposite functions in tumour malignancy and metastases by activating or repressing c-Src kinase activity. Oncogene *26*, 6604–6618.

Sharma, S.C., and Richards, J.S. (2000). Regulation of AP1 (Jun/Fos) Factor Expression and Activation in Ovarian Granulosa Cells. J. Biol. Chem. *275*, 33718–33728.

Shechter, R., and Schwartz, M. (2013). CNS sterile injury: just another wound healing? Trends Mol. Med. *19*, 135–143.

Smith, G.P., and Chan, E.S.L. (2010). Molecular pathogenesis of skin fibrosis: Insight from animal models. Curr. Rheumatol. Rep. *12*, 26–33.

Sterchi, E.E., Green, J.R., and Lentze, M.J. (1982). Non-pancreatic hydrolysis of N-benzoyl-l-tyrosyl-p-aminobenzoic acid (PABA-peptide) in the human small intestine. Clin. Sci. (Lond). *62*, 557–560.

Tadokoro, T., Yamaguchi, Y., Batzer, J., Coelho, S.G., Zmudzka, B.Z., Miller, S.A., Wolber, R., Beer, J.Z., and Hearing, V.J. (2005). Mechanisms of skin tanning in different racial/ethnic groups in response to ultraviolet radiation. J. Invest. Dermatol. *124*, 1326–1332.

Tomasek, J.J., Gabbiani, G., Hinz, B., Chaponnier, C., and Brown, R.A. (2002). Myofibroblasts and mechano-regulation of connective tissue remodelling. Nat. Rev. Mol. Cell Biol. *3*, 349–363.

Trachtman, H., Valderrama, E., Dietrich, J.M., and Bond, J.S. (1995). The Role of Meprin A in the Pathogenesis of Acute Renal Failure. Biochem. Biophys. Res. Commun. *208*, 498–505.

Tredget, E.E., Nedelec, B., Scott, P.G., and Ghahary, A. (1997). Hypertrophic scars, keloids, and contractures. The cellular and molecular basis for therapy. Surg. Clin. North Am. *77*, 701–730.

Walker, P.D., Kaushal, G.P., and Shah, S. V. (1998). Meprin A, the major matrix degrading enzyme in renal tubules, produces a novel nidogen fragmentin vitro andin vivo. Kidney Int. *53*, 1673–1680.

Wang, Y.-G., Kim, S.-J., Baek, J.-H., Lee, H.-W., Jeong, S.-Y., and Chun, K.-H. (2012). Galectin-3 increases the motility of mouse melanoma cells by regulating matrix metalloproteinase-1 expression. Exp. Mol. Med. *44*, 387.

Wichert, R., Ermund, A., Schmidt, S., Schweinlin, M., Ksiazek, M., Arnold, P., Knittler, K., Wilkens, F., Potempa, B., Rabe, B., et al. (2017). Mucus Detachment by Host Metalloprotease Meprin β Requires Shedding of Its Inactive Pro-form, which Is Abrogated by the Pathogenic Protease RgpB. Cell Rep. *21*, 2090–2103.

Xue, M., and Jackson, C.J. (2015). Extracellular Matrix Reorganization During Wound Healing and Its Impact on Abnormal Scarring. Adv. Wound Care *4*, 119–136.

Yamaguchi, Y., Brenner, M., and Hearing, V.J. (2007). The regulation of skin pigmentation. J. Biol. Chem. *282*, 27557–27561.

Yamamoto, T., Takagawa, S., Katayama, I., Yamazaki, K., Hamazaki, Y., Shinkai, H., and Nishioka,

K. (1999). Animal model of sclerotic skin. I: Local injections of bleomycin induce sclerotic skin mimicking scleroderma. J. Invest. Dermatol. *112*, 456–462.

Young, P., Boussadia, O., Halfter, H., Grose, R., Berger, P., Leone, D.P., Robenek, H., Charnay, P., Kemler, R., and Suter, U. (2003). E-cadherin controls adherens junctions in the epidermis and the renewal of hair follicles. EMBO J. *22*, 5723–5733.

Zhang, X.-H., Tee, L.Y., Wang, X.-G., Huang, Q.-S., and Yang, S.-H. (2015). Off-target Effects in CRISPR/Cas9-mediated Genome Engineering. Mol. Ther. - Nucleic Acids *4*, e264.

Zheng, B., Zhang, Z., Black, C.M., de Crombrugghe, B., and Denton, C.P. (2002). Ligand-dependent genetic recombination in fibroblasts : a potentially powerful technique for investigating gene function in fibrosis. Am. J. Pathol. *160*, 1609–1617.

Eidesstattliche Erklärung

Hiermit erkläre ich, dass die Abhandlung nach Inhalt und Form die eigene Arbeit ist und keine anderen als die angegebenen Quellen und Hilfsmittel verwendet wurden. Weiterhin versichere ich, dass diese Arbeit unter Einhaltung der Regeln guter wissenschaftlicher Praxis der Deutschen Forschungsgemeinschaft entstanden ist und noch nicht als Abschlussarbeit an anderer Stelle vorgelegen hat. Mir wurde des Weiteren kein akademischer Grad entzogen.

Kiel, _____ _____

(Datum) (Florian Peters)

Danksagung

Mein Dank gilt…

…Christoph für die Möglichkeit in seiner Arbeitsgruppe promovieren zu dürfen sowie die langjährige Unterstützung und Förderung seit meiner Bachelorarbeit. Außerdem danke ich für viele lustige Tagungen und Bierclub-Sitzungen sowie auch wissenschaftliche Diskussionen.

…Herrn Prof. Dr. Thomas Roeder für die Übernahme des Zweitgutachtens dieser Arbeit.

…allen aktuellen und ehemaligen Kollegen meiner Arbeitsgruppe für die tolle Zeit während der Arbeit, auf Tagungen und in der Freizeit. Da wären zu nennen: Franka, Fred, Anna, Lui, Cynthia, Lennard, Martin, Luisa, Friederike, Anne, Ingrid, Inez, Philipp, Rielana und Frederike. Insbesondere möchte ich Lennard für die Hilfe bei unzähligen Färbungen und Genotypisierungen danken, was mich sehr unterstützt hat.

…allen weiteren Mitarbeitern des Biochemischen Institutes sowie des Anatomischen Institutes für Hilfsbereitschaft und Unterstützung bei verschiedensten Experimenten.

…meinen Studienfreunden Philipp, Sascha, Johanna und Vivian („Backstreet Boys“-Gruppe), die mit mir gemeinsam die Hochs und Tiefs der Promotion erlebt haben.

…meiner Familie für die stetige Unterstützung in allen Lebenslagen sowie Luka für zahlreiche wissenschaftliche Diskussionen, Coachings und das gemeinsame Entdecken der Welt.

Appendix

I Abbreviations

ADAM(TS)	a disintegrin and metalloprotease (with thrombospondin motifs)
Adgre	adhesion G protein-coupled receptor E2
α-MSH	α-melanocyte-stimulating hormone
AP-1	activator protein 1
APP	amyloid precursor protein
α-SMA	α-smooth muscle actin
b	bases
BCA	bicinchoninic acid
BMP-1	bone morphogenetic protein 1
BTP	BMP-1 and Tll1 proteases
CCL	C-C motif chemokine
CD	Crohn's disease
CD(99)	cluster of differentiation 99
cDNA	complementary DNA
CFSE	carboxyfluorescein succinimidyl ester
CHO	Chinese Hamster Ovary
Col1a2	collagen alpha-2(I) chain
C-pro	C-pro-peptide
CRISPR/Cas9	Clustered Regularly Interspaced Short Palindromic Repeats/CRISPR-associated9
C-telo	C-telopeptide
CTF	C-terminal fragment
Da	Dalton
DAPI	4′,6-Diamidin-2-phenylindol
ddH_2O	double distilled water
DMEM	Dulbecco Minimal Essential Medium
DMSO	dimethyl sulfoxide
DNA	desoxyribonucleic acid
Dnp	2,4-Dinitrophenyl
dNTP	deoxynucleotide
DPR	Dermatopathia Pigmentosa Reticularis
DSS	dextran sulfate sodium
DTT	dithiothreitole
ECM	extracellular matrix
EGF(R)	epidermal growth factor (receptor)
EMT	epithelial–mesenchymal transition
ER	endoplasmic reticulum
ERK	extracellular signal–regulated kinases

FCS	fetal calf serum
Fra2	Fos-related antigen 2
GAG	glycosaminoglycan
GAPDH	glyceraldehyde-3-phosphate dehydrogenase
H&E	hematoxylin and eosin
HaCaT	human adult low calcium high temperature keratinocytes
HA-Tag	human influenza hemagglutinin-Tag
hPAEC	human pulmonary artery endothelial cells
HRP	horseradish peroxidase
IBD	inflammatory bowel disease
IL	interleukin
IPAH	idiopathic pulmonary arterial hypertension
KI	knock-in
KLK	kallikrein
KO	knock-out
KRT	cytokeratin
LLC	Lewis lung carcinoma cells
LPS	lipopolysaccharides
MAM	meprin A5 protein, receptor tyrosine phosphatase μ
MAPK	mitogen-activated protein kinase
MB	meprin β
Mca	7-Methyloxycoumarin-4-yl) acetyl
MEF	mouse embryonic fibroblasts
MeOH	methanol
Mep	meprin
Meprin	metalloprotease from renal tissue
MMP	matrix metalloprotease
MP-EBS	Epidermolysis bullosa simplex with mottled pigmentation and noncicatricial alopecia
mRNA	messenger RNA
mTLD	mammalian tolloid
ND	normal diet
Neg	negative
NTC	non template control
PAGE	polyacrylamide gel electrophoresis
PBS	phosphate buffered saline
PCPE-1	procollagen 1 C-proteinase enhancer
PCR	polymerase chain reaction
PDGF	platelet-derived growth factor
PEA3	polyoma enhancer activator 3
PFA	paraformaldehyde
PMA	phorbol myristal acetate

Pos	positive
qPCR	quantitative RT-PCR
Rpm	rotations per minute
RgpB	Arg-gingipain
RT-PCR	reverse transcription polymerase chain reaction
SDS	sodium dodecyl sulfate
SI	small intestine
TAE	Tris base, acetic acid and EDTA
TAILS	terminal amine isotopic labeling of substrates
TAM	tamoxifen
TBS	Tris buffered saline
TEM	transendothelial migration
TGFβ	transforming growth factor β
Tll	tolloid
TNFα	tumor necrosis factor α
TRAF	tumor-necrosis-factor-receptor associated factor
UC	ulcerative colitis
UV	ultraviolet
wt	wildtype

II Publications

1. **Ectodomain shedding of CD99 within highly conserved regions is mediated by the metalloprotease meprin β and promotes transendothelial cell migration.**
   Bedau T*, **Peters F***, Prox J*, Arnold P, Schmidt F, Finkernagel M, Köllmann S, Wichert R, Otte A, Ohler A, Stirnberg M, Lucius R, Koudelka T, Tholey A, Biasin V, Pietrzik CU, Kwapiszewska G, Becker-Pauly C.
   FASEB J. 2017 Mar;31(3):1226-1237
   *These authors contributed equally to the work.

2. **Cancer-associated mutations in the canonical cleavage site do not influence CD99 shedding by the metalloprotease meprin β but alter cell migration in vitro.**
   Bedau T, Schumacher N, **Peters F**, Prox J, Arnold P, Koudelka T, Helm O, Schmidt F, Rabe B, Jenzsch M, Rosenstiel P, Sebens S, Tholey A, Rose-John S, Becker-Pauly C.
   Oncotarget. 2017 Jul 4;8(33):54873-54888

3. **Docking of Meprin α to Heparan Sulphate Protects the Endothelium from Inflammatory Cell Extravasation.**
   Biasin V, Wygrecka M, Bärnthaler T, Jandl K, Jain PP, Bálint Z, Kovacs G, Leitinger G, Kolb-Lenz D, Kornmueller K, **Peters F**, Sinn K, Klepetko W, Heinemann A, Olschewski A, Becker-Pauly C, Kwapiszewska G.
   Thromb Haemost. 2018 Oct;118(10):1790-1802

4. **Tethering soluble meprin α in an enzyme complex to the cell surface affects IBD associated genes.**
   Peters F, Scharfenberg F, Colmorgen C, Armbrust F, Wichert R, Arnold P, Potempa B, Potempa J, Pietrzik CU, Häsler R, Rosenstiel P, Becker-Pauly C.
   FASEB J.; *in press*